

Full-Depth Recycling Study: Test Track Construction and First Level Analysis of Phase 1 HVS and Laboratory Testing

Authors:

D. Jones, R. Wu, and S. Louw

Partnered Pavement Research Center (PPRC) Contract Strategic Plan Element 4.36:
Recycling of Rubberized HMA in RAP and FDR Projects

PREPARED FOR:

California Department of Transportation
Division of Research, Innovation, and System Information
Office of Materials and Infrastructure Roadway Research

PREPARED BY:

University of California
Pavement Research Center
UC Davis, UC Berkeley



DOCUMENT RETRIEVAL PAGE		Research Report: UCPRC-RR-2014-03			
Title: Full-Depth Recycling Study: Test Track Construction and First Level Analysis of Phase 1 HVS and Laboratory Testing					
Authors: D. Jones, R. Wu, and S. Louw					
Caltrans Technical Leads: A. Fong and D. Maskey					
Prepared for: Caltrans	FHWA No.: CA152374A	Work submitted: 8/20/2014		Date June 2014	
Strategic Plan Element No: 4.36		Status: Final		Version No.: 1	
<p>Abstract: This first-level report describes the first phase of a study comparing the performance of four different full-depth pavement reclamation strategies, namely pulverization with no stabilization (FDR-NS), stabilization with foamed asphalt and portland cement (FDR-FA), stabilization with portland cement only (FDR-PC), and stabilization with engineered asphalt emulsion (FDR-EE). A literature review, the test track layout and design, stabilization and asphalt concrete mix designs, and test track construction are discussed, as well as results of Heavy Vehicle Simulator (HVS) and laboratory testing.</p> <p>A number of problems were experienced during construction of the FDR-PC and FDR-EE lanes on the test track and consequently only the FDR-NS and FDR-FA lanes and one section of the FDR-PC lane (5 percent measured cement content) were considered satisfactorily uniform for the purposes of accelerated pavement testing. The FDR-FA and FDR-PC sections performed very well and testing on both was terminated long before the terminal rut of 0.5 in. (12.5 mm) or average crack density of 0.8 ft/ft² (2.5 m/m²) were reached (no cracks were observed on either section). The two FDR-NS sections performed acceptably, with the section with the thicker asphalt surfacing (120 mm) outperforming the section with the thinner asphalt surfacing (60 mm), as expected. Terminal rut was reached on both sections, but no cracking was observed. The FDR-EE sections performed poorly, with terminal rut and terminal cracking both reached after a limited number of load repetitions. This poor performance was attributed to problems associated with construction, and consequently no conclusions can be drawn from the test results regarding this stabilization strategy. The advantages of using foamed asphalt with cement and cement only recycling strategies over recycling strategies with no stabilization are clearly evident from the results.</p> <p>A second phase of accelerated pavement testing, full-scale field testing, and additional laboratory testing are planned to collect sufficient data for the development of mechanistic-empirical design criteria (and revised gravel factors) for full-depth reclaimed pavements. However, there is sufficient evidence to show that pavements that are rehabilitated using full-depth reclamation strategies will satisfactorily withstand design traffic levels common in California. Rehabilitation using this approach is quick, has minimal disruption to traffic, reuses all materials, does not require removal of material from the site, and effectively replaces weak base layers, thus preventing reflective cracking that is common in more traditional overlay projects. Based on these conclusions, it is recommended that full-depth reclamation be promoted as an appropriate rehabilitation strategy in California. Future research on partial- and full-depth reclamation should be coordinated to facilitate consistent design and specification documentation, and to facilitate the preparation of a comprehensive guide covering all forms of pavement recycling.</p>					
<p>Keywords: Full-depth reclamation; Full-depth recycling; FDR; foamed asphalt, foamed bitumen, portland cement</p>					
<p>Proposals for implementation: Full-depth reclamation should be considered as an alternative to mill and overlay rehabilitation strategies on severely cracked or rutted pavements.</p>					
<p>Related documents: UCPRC-GL-2008-01, UCPRC-RR-2008-07</p>					
Signatures:					
D. Jones 1st Author	J.T. Harvey Technical Review	D. Spinner Editor	J.T. Harvey Principal Investigator	A. Fong Caltrans Technical Lead	T.J. Holland Caltrans Contract Manager

DISCLAIMER STATEMENT

This document is disseminated in the interest of information exchange. The contents of this report reflect the views of the authors who are responsible for the facts and accuracy of the data presented herein. The contents do not necessarily reflect the official views or policies of the State of California or the Federal Highway Administration. This publication does not constitute a standard, specification or regulation. This report does not constitute an endorsement by the Department of any product described herein.

For individuals with sensory disabilities, this document is available in alternate formats. For information, call (916) 654-8899, TTY 711, or write to California Department of Transportation, Division of Research, Innovation and System Information, MS-83, P.O. Box 942873, Sacramento, CA 94273-0001.

PROJECT OBJECTIVES

The objective of the Caltrans/UCPRC full-depth recycling study is to develop comprehensive guidelines for the rehabilitation design of pavements using full-depth reclamation techniques. This will be achieved in two phase through the following tasks:

1. A literature review on research related to the topic (*Completed in Phase 1*).
2. Monitoring of existing and new field experiments (*To be undertaken in Phase 2*).
3. Full-depth reclamation of an existing gap-graded rubberized warm-mix asphalt test track using pulverization with no stabilization, with portland cement stabilization, with foamed asphalt plus cement stabilization, and with asphalt emulsion stabilization (*Completed in Phase 1*).
4. Accelerated load testing to compare the four different full-depth reclamation strategies. (*Testing under dry conditions completed in Phase 1. Testing under wet conditions to be completed in Phase 2*).
5. Laboratory testing to refine mix-design procedures and identify suitable criteria for mechanistic-empirical design procedures and performance models. (*Standard materials characterization completed in Phase 1. Testing to assess mechanistic properties to be undertaken in Phase 2*).
6. Preparation of project selection and mechanistic-empirical design guidelines for full-depth reclamation in California (*To be undertaken in Phase 2*).
7. Preparation of reports documenting the study and study results.

This report covers the first phase of the study, which was limited to some of the tasks assessing full-depth reclamation. Initial work on Tasks 1, 3, 4, 5, and 7 is discussed. The remainder of the work on all tasks will be completed in Phase 2.

ACKNOWLEDGEMENTS

The University of California Pavement Research Center acknowledges the following individuals and organizations who contributed to the project:

- Mr. Paul Burdick, Mr. Deepak Maskey, Ms. Amy Fong, and Dr. T. Joseph Holland, Caltrans
- Mr. Richard Haro and Mr. Donatas Greb, formerly of HSI Engineering, Inc.
- Mr. John Jordan, Mr. Tim Robben, and the staff of Western Stabilization
- Mr. Robert Durham and the staff of Durham Construction, Inc.
- Mr. Marco Estrada of Pavement Recycling Systems, Inc.
- Ms. Sara Alzate, Ms. Lisa Wolf, and Mr. Al Palmer of Road Science
- Mr. Jeff Wykoff of the California Nevada Cement Association
- Mr. Chris Barkley, Mr. Bill Clarkson, and the paving crew, Teichert Construction
- The UCPRC Heavy Vehicle Simulator crew and UCPRC laboratory staff

Blank page

EXECUTIVE SUMMARY

The first phase of a comprehensive study into pavement rehabilitation using in-place recycling strategies has been completed for the California Department of Transportation (Caltrans) by the University of California Pavement Research Center (UCPRC). This phase of the study, which focused on full-depth reclamation (FDR), was based on a workplan approved by Caltrans and included a literature review of research undertaken on the topic, the design and construction of a test track, accelerated pavement testing using a Heavy Vehicle Simulator (HVS), and a series of laboratory tests on specimens sampled from the test track to assess rutting and fatigue cracking performance of the asphalt concrete. Four different FDR strategies were investigated, namely pulverization with no stabilization, stabilization with foamed asphalt and portland cement, stabilization with portland cement only, and stabilization with engineered asphalt emulsion. The objective of the study is to develop comprehensive guidelines for the rehabilitation and capital maintenance (CAPM) design of pavements using partial- or full-depth reclamation techniques.

A comprehensive literature review found that although considerable research has been undertaken on both full-depth reclamation (FDR [recycling of the surfacing and base materials]) and partial-depth reclamation (PDR [recycling of the upper layers of the surfacing only]), in the laboratory and in full-scale field experiments, most of the findings and conclusions published are either project-specific or very general in detail. Limited guidance on how to select and design FDR and PDR projects using the different stabilization strategies has been published, and no work appears to have been published on the development of parameters for the mechanistic-empirical rehabilitation design of highways using FDR or PDR strategies.

The test track is located at the University of California Pavement Research Center (UCPRC) in Davis, California, and was originally constructed to assess the performance of seven different warm-mix asphalt technologies in a gap-graded rubberized asphalt mix. The design and construction of the test track was a cooperative effort between Caltrans, the UCPRC, and industry. The test track is 360 ft. by 53 ft. (110 m by 16 m) divided into four lanes. The top 10 in. (250 mm) of the pavement structure (4.7 in. [120 mm] of asphalt concrete and 5.3 in. [130 mm] of the original aggregate base) was recycled. The mix designs for the portland cement and engineered asphalt emulsion stabilized lanes were developed in conjunction with industry partners. The mix design for the foamed asphalt plus portland cement stabilized lane was completed by UCPRC based on earlier research. Recycling and the subsequent placement of the asphalt surfacing, were undertaken using conventional equipment and techniques. Accelerated pavement testing was undertaken with two Heavy Vehicle Simulators.

Observations made during construction of the test track include the following:

- Based on the results of testing of rubberized warm-mix asphalt in a previous study on the UCPRC North Track, it was concluded that preparation of the subgrade and construction of the original base during that study resulted in a generally consistent subgrade and base platform for the FDR study.
- Recycling of the test track was completed with mixed success:
 - + Conventional FDR construction procedures were followed on the lane where no stabilizer was added (FDR-NS). Recycling depth was well controlled and the pulverized material had a consistent grading and uniform moisture content. No problems were observed with recycling the relatively new asphalt concrete surface (i.e., limited aging), although some smoke was observed as the cutting teeth milled through the rubberized layer. Satisfactory compaction and a satisfactory surface finish were achieved on the recycled layer.
 - + Numerous problems were encountered during construction of the engineered asphalt emulsion stabilized lane (FDR-EE), including the addition of too much water and blocked nozzles that lead to uneven and under- or over-application of asphalt emulsion, all of which resulted in uneven compaction.
 - + Construction of the foamed asphalt plus cement stabilized lane (FDR-FA) followed conventional procedures and no problems were observed. The cement was evenly distributed at the correct application rate and good mixing of the foamed asphalt and cement was achieved. The recycled material had a consistent grading and uniform moisture content. Satisfactory compaction and a satisfactory surface finish were achieved.
 - + On the lane stabilized with portland cement (FDR-PC), the spread rate of the cement was not well controlled, and this led to the application of excess stabilizer. Problems with mixing resulted from this excess cement. Only part of one lane was considered suitable for HVS testing.
 - + Gradations for the pulverized material on all four lanes were well within the specified limits.
 - + Densities after compaction met or exceeded the specification on the FDR-NS and FDR-FA lanes, but were slightly lower than specification on the FDR-PC and FDR-EE lanes. The lower than specification densities were attributed to the construction problems on both lanes and, on the FDR-PC lane, to the generalization of the laboratory reference density, given that reference densities were not determined for the range of cement contents actually applied on the day of construction.
- Placement of the hot-mix asphalt followed conventional procedures. Thickness and compaction appeared to be consistent across the test track.
- The FDR-NS and FDR-FA lanes and one section of the FDR-PC lane (5 percent measured cement content) were considered satisfactorily uniform for the purposes of accelerated pavement testing. The FDR-EE and the remainder of the FDR-PC sections were not considered representative of typical FDR construction with these stabilization strategies. However, HVS testing on the FDR-EE section was undertaken to quantify the effects of these construction issues on the performance of the pavement structure and to justify any recommendations with regard to construction specification language for FDR-EE projects.

Key findings from the study include the following:

- The FDR-FA and FDR-PC sections performed very well and testing on both was terminated long before the terminal rut of 0.5 in. (12.5 mm) or average crack density of 0.8 ft/ft² (2.5 m/m²) was reached (no cracks were observed on either section). The two FDR-NS sections performed acceptably, with the section with the thicker asphalt surfacing (120 mm) outperforming the section with the thinner asphalt surfacing (60 mm), as expected. Terminal rut was reached on both of these sections, but no cracking was observed. The FDR-EE sections performed poorly, with terminal rut and terminal cracking both reached after a limited number of load repetitions. This poor performance was attributed to problems associated with construction, and consequently no conclusions can be drawn from the test results regarding this stabilization strategy.
- Key observations from the HVS testing include these:
 - + Terminal rut depths were recorded on the thinner (60 mm) FDR-NS section after approximately 490,000 equivalent standard axle loads (ESALs) had been applied, and on the thicker (120 mm) FDR-NS section after more than 21.4 million ESALs had been applied. The thicker surfacing layer therefore had a significant influence on the performance of the structure.
 - + On the FDR-FA section, only 4 mm of rutting was measured after more than 17.7 million ESALs, while on the FDR-PC section, only 2.1 mm of rutting was measured after more than 44 million ESALs. Testing was halted on the FDR-FA and FDR-PC sections at these loading points due to time and project-funding constraints. Permanent deformation in the recycled layers was consistent with the surface measurements, with considerable deformation recorded in the FDR-NS layers, but very little deformation recorded in the stabilized layers.
 - + Measured and backcalculated stiffnesses were significantly higher on the FDR-FA and FDR-PC sections compared to the two FDR-NS sections, as expected. Although the stiffnesses dropped considerably in the recycled layers on the FDR-FA and FDR-PC sections after trafficking, they were still orders of magnitude higher than those recorded on the FDR-NS sections, despite their having been subjected to millions more equivalent standard axle loads. The presence of the recycled asphalt concrete material, the presence of rubber in this material, and the fact that the recycled asphalt was relatively unaged did not appear to affect the stiffness of the layer. Recycled aged asphalt would typically result in slightly higher stiffnesses in the recycled layer compared to recycled unaged asphalt.
 - + Elastic deflection at the bottom of the FDR-FA and FDR-PC layers after completion of testing (17.7 and 44.0 million ESALs, respectively) was approximately the same as that at the bottom of the FDR-NS layers after 490,000 and 21.4 million ESALs, respectively. The rate of change in deflection was, however, slightly higher on the FDR-FA and FDR-PC sections, which is consistent with stabilized layers containing cement.
- The advantages of using foamed asphalt with cement and cement only recycling strategies over recycling strategies with no stabilization are clearly evident from the results.

Although a second phase of accelerated pavement testing, full-scale field testing, and additional laboratory testing still needs to be undertaken to collect sufficient data for the development of mechanistic-empirical design criteria (and revised gravel factors) for full-depth reclaimed pavements, there is sufficient evidence to show that pavements that are rehabilitated using full-depth reclamation strategies will satisfactorily withstand design traffic levels common in California. Rehabilitation using

this approach is quick, has minimal disruption to traffic, reuses all materials, does not require removal of material from the site, and effectively replaces weak base layers, thus preventing the reflective cracking that is common in more traditional overlay projects.

Based on the above conclusions, it is recommended that full-depth reclamation be promoted as an appropriate rehabilitation strategy in California. Although partial-depth reclamation was not investigated in this study, future research on partial- and full-depth reclamation should be coordinated to facilitate consistent design and specification documentation, and to facilitate the preparation of a comprehensive guide covering all forms of pavement recycling.

TABLE OF CONTENTS

EXECUTIVE SUMMARY	v
LIST OF TABLES	xii
LIST OF FIGURES	xiii
LIST OF ABBREVIATIONS	xvi
CONVERSION FACTORS	xvii
1. INTRODUCTION	1
1.1 Background to Pavement Recycling in California	1
1.2 Terminology	2
1.3 Problem Statements	2
1.4 Project Objectives	5
1.5 Measurement Units	6
2. LITERATURE REVIEW	7
3. TEST TRACK LOCATION, DESIGN, AND CONSTRUCTION	9
3.1 Test Track Location	9
3.2 Test Track Layout	9
3.3 Pavement Design	11
3.3.1 Subgrade and Base Course Properties (Original Pavement)	12
3.3.2 Subgrade Preparation for the Original Pavement	12
3.3.3 Base Course Construction for the Original Pavement	13
3.3.4 Asphalt Surfacing on Original Pavement: Bottom Lift	15
3.3.5 Asphalt Surfacing on Original Pavement: Rubberized Asphalt Concrete	17
3.4 Full-Depth Reclamation Mix Designs	18
3.4.1 Material Sampling Prior to Recycling	18
3.4.2 Mix Design for FDR-EE Section	18
3.4.3 Mix Design for FDR-FA Section	18
3.4.4 Mix Design for FDR-PC Sections	19
3.5 Full-Depth Reclamation	19
3.5.1 Lane 1: No Stabilizer (FDR-NS)	19
3.5.2 Lane 2: Engineered Emulsion (FDR-EE)	21
3.5.3 Lane 3: Foamed Asphalt with Portland Cement (FDR-FA)	24
3.5.4 Lane 4: Portland Cement (FDR-PC)	25
3.5.5 Construction Quality Control	27
3.6 Asphalt Concrete Surfacing	30
3.6.1 Material Properties	30
3.6.2 Prime Coat Application	30
3.6.3 Asphalt Concrete Placement	32
3.6.4 Construction Quality Control	33
3.6.5 As-Built Layer Thicknesses	34
3.7 Material Sampling	37
3.8 Construction Summary	37
4. TRACK LAYOUT, INSTRUMENTATION, AND TEST CRITERIA	39
4.1 Testing Protocols	39
4.2 Test Track Layout	39
4.3 HVS Test Section Layout	40
4.4 Test Section Instrumentation	40
4.5 Test Section Measurements	42
4.5.1 Temperature	42
4.5.2 Surface Profile	42
4.5.3 Strain	42
4.5.4 Pressure	44
4.5.5 Elastic Vertical Deflection	44

4.6	Phase 1 HVS Test Criteria.....	45
4.6.1	Test Section Failure Criteria	45
4.6.2	Phase 1 Environmental Conditions	45
4.6.3	Phase 1 Test Duration	46
4.6.4	Phase 1 Loading Program	46
5.	PHASE 1 HVS TEST DATA SUMMARY	49
5.1	Introduction	49
5.2	Rainfall	49
5.3	Section 672HB: No Stabilizer with 60 mm Surfacing (FDR-NS [60 mm]).....	50
5.3.1	Test Summary	50
5.3.2	Air Temperatures	50
5.3.3	Pavement Temperatures	52
5.3.4	Permanent Deformation on the Surface (Rutting).....	52
5.3.5	Permanent Deformation in the Underlying Layers	54
5.3.6	Tensile Strain at the Bottom of the Asphalt Concrete Layer	55
5.3.7	Vertical Pressure at the Top of the Recycled Layer.....	56
5.3.8	Deflection on the Surface (Road Surface Deflectometer).....	57
5.3.9	Deflection in the Underlying Layers (Multi-Depth Deflectometer)	57
5.3.10	Deflection in the Pavement Structure (Falling Weight Deflectometer).....	57
5.3.11	Visual Assessment	59
5.4	Section 677HC: No Stabilizer with 120 mm Surfacing (FDR-NS [120 mm]).....	59
5.4.1	Test Summary	59
5.4.2	Air Temperatures	61
5.4.3	Pavement Temperatures	62
5.4.4	Permanent Deformation on the Surface (Rutting).....	63
5.4.5	Permanent Deformation in the Underlying Layers	65
5.4.6	Tensile Strain at the Bottom of the Asphalt Concrete Layer	66
5.4.7	Vertical Pressure at the Top of the Recycled Layer.....	67
5.4.8	Deflection on the Surface (Road Surface Deflectometer).....	67
5.4.9	Deflection in the Underlying Layers (Multi-Depth Deflectometer)	68
5.4.10	Deflection in the Pavement Structure (Falling Weight Deflectometer).....	68
5.4.11	Visual Assessment	70
5.5	Section 673HB: Foamed Asphalt with Portland Cement (FDR-FA)	70
5.5.1	Test Summary	70
5.5.2	Air Temperatures	72
5.5.3	Pavement Temperatures	73
5.5.4	Permanent Deformation on the Surface (Rutting).....	74
5.5.5	Permanent Deformation in the Underlying Layers	76
5.5.6	Tensile Strain at the Bottom of the Asphalt Concrete Layer	77
5.5.7	Vertical Pressure at the Top of the Recycled Layer.....	78
5.5.8	Deflection on the Surface (Road Surface Deflectometer).....	79
5.5.9	Deflection in the Underlying Layers (Multi-Depth Deflectometer)	79
5.5.10	Deflection in the Pavement Structure (Falling Weight Deflectometer).....	80
5.5.11	Visual Assessment	81
5.6	Section 674HB: Portland Cement (FDR-PC).....	82
5.6.1	Test Summary	82
5.6.2	Air Temperatures	83
5.6.3	Pavement Temperatures	84
5.6.4	Permanent Deformation on the Surface (Rutting).....	85
5.6.5	Permanent Deformation in the Underlying Layers	87
5.6.6	Tensile Strain at the Bottom of the Asphalt Concrete Layer	88
5.6.7	Vertical Pressure at the Top of the Recycled Layer.....	89
5.6.8	Deflection on the Surface (Road Surface Deflectometer).....	90

5.6.9	Deflection in the Underlying Layers (Multi-Depth Deflectometer)	90
5.6.10	Deflection in the Pavement Structure (Falling Weight Deflectometer)	91
5.6.11	Visual Assessment	92
5.7	Section 675HC: Engineered Emulsion (FDR-EE #1)	93
5.7.1	Test Summary	93
5.7.2	Air Temperatures	94
5.7.3	Pavement Temperatures	95
5.7.4	Permanent Deformation on the Surface (Rutting).....	96
5.7.5	Permanent Deformation in the Underlying Layers	98
5.7.6	Tensile Strain at the Bottom of the Asphalt Concrete Layer	99
5.7.7	Vertical Pressure at the Top of the Recycled Layer.....	100
5.7.8	Deflection on the Surface (Road Surface Deflectometer).....	100
5.7.9	Deflection in the Underlying Layers (Multi-Depth Deflectometer)	100
5.7.10	Deflection in the Pavement Structure (Falling Weight Deflectometer).....	101
5.7.11	Visual Assessment	102
5.8	Section 676HC: Engineered Emulsion (FDR-EE #2)	104
5.8.1	Test Summary	104
5.8.2	Air Temperatures	105
5.8.3	Pavement Temperatures	106
5.8.4	Permanent Deformation on the Surface (Rutting).....	107
5.8.5	Permanent Deformation in the Underlying Layers	109
5.8.6	Tensile Strain at the Bottom of the Asphalt Concrete Layer	110
5.8.7	Vertical Pressure at the Top of the Recycled Layer.....	110
5.8.8	Deflection on the Surface (Road Surface Deflectometer).....	110
5.8.9	Deflection in the Underlying Layers (Multi-Depth Deflectometer)	111
5.8.10	Deflection in the Pavement Structure (Falling Weight Deflectometer).....	112
5.8.11	Visual Assessment	113
5.9	HVS Test Summary.....	115
5.10	Phase 2 HVS Testing.....	117
6.	PHASE 1 LABORATORY TEST DATA SUMMARY.....	119
6.1	Introduction	119
6.2	Characterization of Unstabilized Recycled Material and Asphalt Concrete Surfacing.....	119
6.3	Mechanistic Properties of the Asphalt Concrete Surfacing	119
6.3.1	Experiment Design.....	119
6.3.2	Shear Testing Results.....	121
6.3.3	Fatigue Cracking Test Results	122
6.4	Frequency Sweep Test Results.....	122
6.5	Phase 2 Laboratory Testing	123
7.	MECHANISTIC ANALYSIS	125
8.	CONCLUSIONS AND INTERIM RECOMMENDATIONS.....	127
8.1	Summary and Conclusions	127
8.2	Recommendations	129
	REFERENCES.....	131

LIST OF TABLES

Table 1.1: Suggested Acronyms for Partial- and Full-Depth Stabilizer Combinations	3
Table 3.1: Summary of DCP Survey on Subgrade Material	12
Table 3.2: Summary of Subgrade Density Measurements (47,48).....	13
Table 3.3: Base Course Material Properties (47,48)	14
Table 3.4: Summary of Nuclear Gauge Density Measurements on Base Course Layer (47,48)	15
Table 3.5: Summary of DCP Survey on Base and Subgrade Material (47,48)	15
Table 3.6: Key Bottom Lift HMA Mix Design Parameters (47,48).....	16
Table 3.7: Quality Control of Mix After Production (47,48).....	17
Table 3.8: Mix Design: FDR-EE.....	18
Table 3.9: Mix Design: FDR-FA	19
Table 3.10: Mix Design: FDR-PC.....	19
Table 3.11: Recycled Layer Material Properties.....	28
Table 3.12: Summary of Nuclear Gauge Density Measurements on Recycled Layer	28
Table 3.13: Recalculated Dry Density Measurements using Gravimetric Moisture Content	29
Table 3.14: Result of Quality Control Strength Tests	30
Table 3.15: Key HMA Mix Design Parameters	30
Table 3.16: Summary of Asphalt Concrete Density Measurements	33
Table 3.17: As-Built HMA Layer Thicknesses.....	34
Table 4.1: Test Duration for Phase 1 HVS Rutting Tests	46
Table 4.2: Summary of Phase 1 HVS Loading Program.....	46
Table 5.1: 672HB: Temperature Summary for Air and Pavement.....	52
Table 5.2: 672HB: Deformation in Each Layer	55
Table 5.3: 677HC: Temperature Summary for Air and Pavement.....	62
Table 5.4: 677HC: Deformation in Each Layer	66
Table 5.5: 673HB: Temperature Summary for Air and Pavement.....	73
Table 5.6: 673HB: Deformation in Each Layer	77
Table 5.7: 674HB: Temperature Summary for Air and Pavement.....	85
Table 5.8: 674HB: Deformation in Each Layer	88
Table 5.9: 675HC: Temperature Summary for Air and Pavement.....	96
Table 5.10: 675HC: Deformation in Each Layer	99
Table 5.11: 676HC: Temperature Summary for Air and Pavement.....	106
Table 5.12: 676HC: Deformation in Each Layer	109
Table 6.1: Shear Test Results	121
Table 6.2: Fatigue Cracking Test Results.....	122
Table 6.3: Frequency Sweep Test Results.....	122

LIST OF FIGURES

Figure 3.1: Aerial view of the UCPRC research facility.....	9
Figure 3.2: Planned test track layout.....	10
Figure 3.3: Original pavement structure for the rubberized warm-mix asphalt test sections.....	11
Figure 3.4: Pavement structure for the FDR study test sections.....	11
Figure 3.5: FDR-NS: Test track recycling.....	20
Figure 3.6: FDR-NS: Chunks at start of test pulverization.....	20
Figure 3.7: FDR-NS: Smoke during pulverization.....	20
Figure 3.8: FDR-NS: Pulverized material.....	20
Figure 3.9: FDR-NS: Initial compaction with padfoot roller.....	20
Figure 3.10: FDR-NS: Compaction with smooth drum roller.....	21
Figure 3.11: FDR-NS: Surface leveling with a grader.....	21
Figure 3.12: FDR-NS: Compaction with rubber-tired roller.....	21
Figure 3.13: FDR-NS: Completed recycled layer surface.....	21
Figure 3.14: FDR-EE: Recycling train.....	22
Figure 3.15: FDR-EE: Inconsistent emulsion application across width of test track.....	22
Figure 3.16: FDR-EE: Excess emulsion applied during recycling.....	22
Figure 3.17: FDR-EE: Compaction with padfoot roller.....	23
Figure 3.18: FDR-EE: Excess fluid during and after compaction with smooth drum roller.....	23
Figure 3.19: FDR-EE: Puddled water on surface after compaction.....	24
Figure 3.20: FDR-EE: Excavation showing wet recycled layer.....	24
Figure 3.21: FDR-FA: Spreading cement on old asphalt surface.....	25
Figure 3.22: FDR-FA: Recycling train.....	25
Figure 3.23: FDR-FA: Uniform mix behind recycler.....	25
Figure 3.24: FDR-FA: Padfoot roller compaction on uniform mix.....	25
Figure 3.25: FDR-FA: Steel wheel compaction showing tightly bound surface.....	25
Figure 3.26: FDR-FA: Final compaction showing tightly bound surface.....	25
Figure 3.27: FDR-PC: Excess cement on Cell #7.....	26
Figure 3.28: FDR-PC: Removing excess cement on Cell #8.....	26
Figure 3.29: FDR-PC: Uniform mixing after first pulverization pass with no water.....	27
Figure 3.30: FDR-PC: Water spray prior to second mixing pass.....	27
Figure 3.31: FDR-PC: Second mixing pass with water.....	27
Figure 3.32: FDR-PC: Uniform mix after second recycling pass.....	27
Figure 3.33: FDR-PC: Inconsistent mix on high cement content cells.....	27
Figure 3.34: Broomed surface of FDR-NS layer.....	31
Figure 3.35: Broomed surface of FDR-EE layer showing dark, moist surface.....	31
Figure 3.36: Prime coat application.....	31
Figure 3.37: Asphalt concrete placement.....	32
Figure 3.38: First lift of asphalt concrete after compaction.....	33
Figure 3.39: Second lift of asphalt concrete showing shearing over instrumentation cables.....	33
Figure 3.40: Thermal image of test track during construction.....	34
Figure 3.41: Unbound layer DCP penetration curves for unstabilized sections.....	35
Figure 3.42: Unbound layer DCP penetration curves for stabilized sections.....	36
Figure 3.43: Sampling location for laboratory specimens.....	37
Figure 4.1: Test track layout.....	39
Figure 4.2: Schematic of an HVS test section.....	40
Figure 4.3: Strain gauge installation.....	41
Figure 4.4: Pressure cell installation.....	41
Figure 4.5: A model multi-depth deflectometer (MDD), showing five modules.....	42
Figure 4.6: Illustration of maximum rut depth and deformation for a leveled profile.....	43

Figure 4.7: Example strain reading and definition of summary quantities.....	44
Figure 4.8: Example pressure cell reading and definition of summary quantities.	44
Figure 4.9: Example elastic vertical deflection measured with MDD.	45
Figure 5.1: Measured rainfall during Phase 1 HVS testing.....	49
Figure 5.2: 672HB: HVS loading history.....	50
Figure 5.3: 672HB: Daily average air temperatures outside the environmental chamber.....	51
Figure 5.4: 672HB: Daily average air temperatures inside the environmental chamber.....	51
Figure 5.5: 672HB: Daily average pavement temperatures.	52
Figure 5.6: 672HB: Profilometer cross section at various load repetitions.....	53
Figure 5.7: 672HB: Average maximum total rut and average deformation.....	53
Figure 5.8: 672HB: Contour plots of permanent surface deformation.....	54
Figure 5.9: 672HB: Permanent deformation in the underlying layers.	55
Figure 5.10: 672HB: Tensile strain at the bottom of the asphalt concrete layer.	56
Figure 5.11: 672HB: Vertical pressure at the top of the recycled layer.	56
Figure 5.12: 672HB: Surface deflection (RSD).	57
Figure 5.13: 672HB: Elastic deflection in the underlying layers.	58
Figure 5.14: 672HB: Surface deflection (FWD).	58
Figure 5.15: 672HB: Backcalculated stiffness of recycled layer (FWD).....	59
Figure 5.16: 672HB: Test section photographs.....	60
Figure 5.17: 677HC: HVS loading history.....	61
Figure 5.18: 677HC: Daily average air temperatures outside the environmental chamber.....	61
Figure 5.19: 677HC: Daily average air temperatures inside the environmental chamber.....	62
Figure 5.20: 677HC: Daily average pavement temperatures.	63
Figure 5.21: 677HC: Profilometer cross section at various load repetitions.....	64
Figure 5.22: 677HC: Average maximum total rut and average deformation.....	64
Figure 5.23: 677HC: Contour plots of permanent surface deformation.....	65
Figure 5.24: 677HC: Permanent deformation in the underlying layers.	65
Figure 5.25: 677HC: Tensile strain at the bottom of the asphalt concrete layer.	66
Figure 5.26: 677HC: Vertical pressure at the top of the recycled layer.	67
Figure 5.27: 677HC: Surface deflection (RSD).	68
Figure 5.28: 677HC: Elastic deflection in the underlying layers.	69
Figure 5.29: 677HC: Surface deflection (FWD).	69
Figure 5.30: 677HC: Backcalculated stiffness of recycled layer (FWD).....	70
Figure 5.31: 677HC: Test section photographs.....	71
Figure 5.32: 673HB: HVS loading history.....	72
Figure 5.33: 673HB: Daily average air temperatures outside the environmental chamber.....	72
Figure 5.34: 673HB: Daily average air temperatures inside the environmental chamber.....	73
Figure 5.35: 673HB: Daily average pavement temperatures.	74
Figure 5.36: 673HB: Profilometer cross section at various load repetitions.....	74
Figure 5.37: 673HB: Average maximum total rut and average deformation.....	75
Figure 5.38: 673HB: Contour plots of permanent surface deformation.....	76
Figure 5.39: 673HB: Permanent deformation in the underlying layers.	76
Figure 5.40: 673HB: Tensile strain at the bottom of the asphalt concrete layer.	78
Figure 5.41: 673HB: Vertical pressure at the top of the recycled layer.	78
Figure 5.42: 673HB: Surface deflection (RSD).	79
Figure 5.43: 673HB: Elastic deflection in the underlying layers.	80
Figure 5.44: 673HB: Surface deflection (FWD).	80
Figure 5.45: 673HB: Backcalculated stiffness of recycled layer (FWD).....	81
Figure 5.46: 673HB: Test section photographs.....	82
Figure 5.47: 674HB: HVS loading history.....	83
Figure 5.48: 674HB: Daily average air temperatures outside the environmental chamber.....	84
Figure 5.49: 674HB: Daily average air temperatures inside the environmental chamber.....	84
Figure 5.50: 674HB: Daily average pavement temperatures.	85

Figure 5.51: 674HB: Profilometer cross section at various load repetitions.....	86
Figure 5.52: 674HB: Average maximum total rut and average deformation.....	86
Figure 5.53: 674HB: Contour plots of permanent surface deformation.....	87
Figure 5.54: 674HB: Permanent deformation in the underlying layers.	87
Figure 5.55: 674HB: Tensile strain at the bottom of the asphalt concrete layer.	88
Figure 5.56: 674HB: Vertical pressure at the top of the recycled layer.	89
Figure 5.57: 674HB: Surface deflection (RSD).	90
Figure 5.58: 674HB: Elastic deflection in the underlying layers.	91
Figure 5.59: 674HB: Surface deflection (FWD).	91
Figure 5.60: 674HB: Backcalculated stiffness of recycled layer (FWD).....	92
Figure 5.61: 674HB: Test section photographs.....	93
Figure 5.62: 675HC: HVS loading history.....	94
Figure 5.63: 675HC: Daily average air temperatures outside the environmental chamber.....	95
Figure 5.64: 675HC: Daily average air temperatures inside the environmental chamber.....	95
Figure 5.65: 675HC: Daily average pavement temperatures.	96
Figure 5.66: 675HC: Profilometer cross section at various load repetitions.....	97
Figure 5.67: 675HC: Average maximum total rut and average deformation.....	97
Figure 5.68: 675HC: Contour plots of permanent surface deformation.....	98
Figure 5.69: 675HC: Permanent deformation in the underlying layers.	98
Figure 5.70: 675HC: Tensile strain at the bottom of the asphalt concrete layer.	99
Figure 5.71: 675HC: Vertical pressure at the top of the recycled layer.	100
Figure 5.72: 675HC: Surface deflection (RSD).	101
Figure 5.73: 675HC: Elastic deflection in the underlying layers.	101
Figure 5.74: 675HC: Surface deflection (FWD).	102
Figure 5.75: 675HC: Backcalculated stiffness of recycled layer (FWD).....	102
Figure 5.76: 675HC: Crack location and pattern.....	103
Figure 5.77: 675HC: Test section photographs.....	103
Figure 5.78: 675HC: Test section photographs (<i>continued</i>).....	104
Figure 5.79: 676HC: HVS loading history.....	105
Figure 5.80: 676HC: Daily average air temperatures outside the environmental chamber.....	105
Figure 5.81: 676HC: Daily average air temperatures inside the environmental chamber.....	106
Figure 5.82: 676HC: Daily average pavement temperatures.	107
Figure 5.83: 676HC: Profilometer cross section at various load repetitions.....	107
Figure 5.84: 676HC: Average maximum total rut and average deformation.....	108
Figure 5.85: 676HC: Contour plots of permanent surface deformation.....	108
Figure 5.86: 676HC: Permanent deformation in the underlying layers.	109
Figure 5.87: 676HC: Tensile strain at the bottom of the asphalt concrete layer.	110
Figure 5.88: 676HC: Vertical pressure at the top of the recycled layer.	111
Figure 5.89: 676HC: Surface deflection (RSD).	111
Figure 5.90: 676HC: Elastic deflection in the underlying layers.	112
Figure 5.91: 676HC: Surface deflection (FWD).	112
Figure 5.92: 676HC: Backcalculated stiffness of recycled layer (FWD).....	113
Figure 5.93: 676HC: Crack location and pattern.....	113
Figure 5.94: 676HC: Test section photographs.....	114
Figure 5.95: Comparison of average maximum rut.....	115
Figure 5.96: Comparison of backcalculated stiffness before and after testing.....	116
Figure 6.1: Master curve.	123

LIST OF ABBREVIATIONS

AADT	Annual average daily traffic
AASHTO	American Association of State Highway and Transportation Officials
AMPT	Asphalt mix performance tester
APT	Accelerated pavement testing
ARRA	Asphalt Recycling and Reclaiming Association
ASTM	American Society for Testing and Materials
C_e	Calibration coefficient
Caltrans	California Department of Transportation
CAPM	Capital maintenance
CFR	Cold foam recycling
CIR	Cold in-place recycling
DCP	Dynamic cone penetrometer
DISR	Deep in situ recycling or deep in situ reclaiming
ESAL	Equivalent standard axle load
FDR	Full-depth reclamation or full-depth recycling
FDR-AE	Full-depth reclamation stabilized with asphalt emulsion
FDR-EE	Full-depth reclamation stabilized with engineered asphalt emulsion
FDR-FA	Full-depth reclamation stabilized with foamed asphalt and cement
FDR-NS	Full-depth reclamation with no stabilizer
FDR-PC	Full-depth reclamation stabilized with portland cement
FWD	Falling weight deflectometer
GF	Gauge factor
HIR	Hot in-place reclamation of hot in-place recycling
HMA	Hot mix asphalt
H-PDR	Hot partial depth reclamation
HVS	Heavy Vehicle Simulator
ITS	Indirect tensile strength
LVDT	Linear variable differential transformer
MDD	Multi-depth deflectometer
M-E	Mechanistic empirical
PDR	Partial depth reclamation or partial depth recycling
RAP	Recycled asphalt pavement
RHMA-G	Gap-graded rubberized hot-mix asphalt
RSD	Road surface deflectometer
RWMA-G	Gap-graded rubberized warm-mix asphalt
UCPRC	University of California Pavement Research Center
V_r	Voltage ratio

CONVERSION FACTORS

SI* (MODERN METRIC) CONVERSION FACTORS				
APPROXIMATE CONVERSIONS TO SI UNITS				
Symbol	When You Know	Multiply By	To Find	Symbol
LENGTH				
in	inches	25.4	Millimeters	mm
ft	feet	0.305	Meters	m
yd	yards	0.914	Meters	m
mi	miles	1.61	Kilometers	Km
AREA				
in ²	square inches	645.2	Square millimeters	mm ²
ft ²	square feet	0.093	Square meters	m ²
yd ²	square yard	0.836	Square meters	m ²
ac	acres	0.405	Hectares	ha
mi ²	square miles	2.59	Square kilometers	km ²
VOLUME				
fl oz	fluid ounces	29.57	Milliliters	mL
gal	gallons	3.785	Liters	L
ft ³	cubic feet	0.028	cubic meters	m ³
yd ³	cubic yards	0.765	cubic meters	m ³
NOTE: volumes greater than 1000 L shall be shown in m ³				
MASS				
oz	ounces	28.35	Grams	g
lb	pounds	0.454	Kilograms	kg
T	short tons (2000 lb)	0.907	megagrams (or "metric ton")	Mg (or "t")
TEMPERATURE (exact degrees)				
°F	Fahrenheit	5 (F-32)/9 or (F-32)/1.8	Celsius	°C
ILLUMINATION				
fc	foot-candles	10.76	Lux	lx
fl	foot-Lamberts	3.426	candela/m ²	cd/m ²
FORCE and PRESSURE or STRESS				
lbf	poundforce	4.45	Newtons	N
lbf/in ²	poundforce per square inch	6.89	Kilopascals	kPa
APPROXIMATE CONVERSIONS FROM SI UNITS				
Symbol	When You Know	Multiply By	To Find	Symbol
LENGTH				
mm	millimeters	0.039	Inches	in
m	meters	3.28	Feet	ft
m	meters	1.09	Yards	yd
km	kilometers	0.621	Miles	mi
AREA				
mm ²	square millimeters	0.0016	square inches	in ²
m ²	square meters	10.764	square feet	ft ²
m ²	square meters	1.195	square yards	yd ²
ha	Hectares	2.47	Acres	ac
km ²	square kilometers	0.386	square miles	mi ²
VOLUME				
mL	Milliliters	0.034	fluid ounces	fl oz
L	liters	0.264	Gallons	gal
m ³	cubic meters	35.314	cubic feet	ft ³
m ³	cubic meters	1.307	cubic yards	yd ³
MASS				
g	grams	0.035	Ounces	oz
kg	kilograms	2.202	Pounds	lb
Mg (or "t")	megagrams (or "metric ton")	1.103	short tons (2000 lb)	T
TEMPERATURE (exact degrees)				
°C	Celsius	1.8C+32	Fahrenheit	°F
ILLUMINATION				
lx	lux	0.0929	foot-candles	fc
cd/m ²	candela/m ²	0.2919	foot-Lamberts	fl
FORCE and PRESSURE or STRESS				
N	newtons	0.225	Poundforce	lbf
kPa	kilopascals	0.145	poundforce per square inch	lbf/in ²

*SI is the symbol for the International System of Units. Appropriate rounding should be made to comply with Section 4 of ASTM E380 (Revised March 2003)

Blank page

1. INTRODUCTION

1.1 Background to Pavement Recycling in California

The California Department of Transportation (Caltrans) has been using full-depth reclamation (FDR) as a rehabilitation strategy since 2001, following its introduction at a Caltrans/UCPRC workshop in 2000. Most FDR projects built since that time have used a combination of foamed asphalt and portland cement as the stabilizing agent. A number of FDR projects have also been completed where no stabilizing agent was used, a rehabilitation strategy referred to as “pulverization,” and a limited number of projects have been reported where only portland cement or foamed asphalt was used. When the project discussed in this report started, there was no record of the use of asphalt emulsion as a stabilizing agent on any Caltrans FDR project, except for a pilot project in District 4 in the mid-1990s that did not use conventional FDR equipment for recycling the asphalt pavement.

In 2009, the University of California Pavement Research Center (UCPRC) prepared detailed guidelines for FDR with foamed asphalt (1). The content of this guideline was based on a comprehensive study that included regular monitoring of a number of pilot projects and a multiphase laboratory testing study on materials sampled from these projects (2).

Cold in-place recycling (CIR) of asphalt surfacing layers, has been used as a rehabilitation or capital maintenance strategy on Caltrans projects on a limited scale since 2009 (approximately 27 projects were documented at the beginning of the study covered in this report). Among these CIR projects, a combination of asphalt emulsion and either cement or lime has been the most common stabilization strategy used, although a combination of foamed asphalt and either cement or lime is also an appropriate strategy (3,4) that has been used in a number of local government projects in California. Typical recycling depths are around 4.0 in. (100 mm). No comprehensive research on CIR has been undertaken in California, no project selection and mix design guidelines have been prepared, and there is no published information on the effects of recycled rubberized asphalt pavement on CIR performance.

A limited number of hot in-place recycling (HIR) projects have also been undertaken. Hot binder with and without the addition of lime has been used in these projects. Typical recycling depths are around 2.0 in. (50 mm). No comprehensive research on HIR has been undertaken in California, no project selection and mix design guidelines have been prepared, nor have the effects of the presence of rubberized binders been assessed.

In all the FDR projects recorded to date, no mention has been made of whether any of the recycled asphalt layers contained asphalt rubber. Nor has any published research been undertaken to determine whether the presence of tire rubber in the existing asphalt layers could influence the performance of the pavement using FDR or PDR rehabilitation strategies.

1.2 Terminology

A number of different terms are used to describe full- and partial-depth reclamation, which can lead to confusion when developing guideline documentation or rehabilitation designs, writing general and project specifications, preparing bid documents, etc. For example, full-depth reclamation (FDR) is also called full-depth-recycling, deep in situ recycling (DISR), cold in-place recycling (CIR), or cold-foam recycling (CFR, when referring to the use of foamed asphalt, even though the foamed asphalt temperature is typically around 350°F [175°C]), with the term “cold” referring to the pavement not being heated during the milling process). Partial-depth reclamation (PDR) is also called partial-depth recycling, cold in-place recycling (CIR, contradicting with CIR used as an alternative to FDR), or cold in-place reclamation. The term “cold” again refers to the pavement not being heated during the milling process. These terms generally do not include the stabilizer type or only include the primary stabilizer (e.g., FDR-FA is commonly used to describe both foamed asphalt only, and a combination of foamed asphalt and cement). Further confusion can arise if both hot in-place and cold in-place recycling techniques are being considered in partial depth reclamation projects.

The use of more consistent and descriptive terminology is therefore proposed to prevent any misunderstandings as the use of these technologies increases. Suggested terminology and associated acronyms are listed in Table 1.1 and are used in this document. Note that partial-depth reclamation can be further differentiated between cold and hot techniques.

1.3 Problem Statements

The FDR studies completed by the UCPRC for Caltrans to date have assessed pulverized unstabilized layers and layers stabilized with foamed asphalt/cement. Partial-depth recycling, the full-depth recycling of rubberized asphalt layers, and the use of other stabilizers including cement only, lime, modified cementitious additives, asphalt emulsion, and synthetic polymer emulsions needs to be assessed and the guideline documentation updated. Personal experience of the authors combined with a limited literature review on the topic has revealed that the earlier UCPRC FDR project is the only comprehensive documented study (1,2) on in-place recycling undertaken in the U.S. and that no similar comprehensive, documented studies have been undertaken on other FDR strategies. The *Wirtgen Cold Recycling*

Technology Manual (3), which is based on research mostly undertaken in Europe and South Africa, provides comprehensive guidance on all aspects of full- and partial-depth recycling, but it caters to a broad international audience, and includes topics and approaches that are not necessarily applicable to Caltrans projects. The Asphalt Recycling and Reclaiming Association’s (ARRA) *Basic Asphalt Recycling Manual (4)* provides a valuable overview of full- and partial- depth reclamation, based on the experience of contractors, but it does not provide sufficiently specific guidelines for project selection, mix design, and construction of these types of projects in California.

Table 1.1: Suggested Acronyms for Partial- and Full-Depth Stabilizer Combinations

Process	Depth	Primary Stabilizer	Secondary Stabilizer	Suggested Acronym	
Cold	Partial	Foamed asphalt	None	PDR-FA	
			Cement	PDR-FA-C	
	Asphalt emulsion/ Engineered emulsion	None	Lime	PDR-FA-L	
			Fly ash	PDR-FA-F	
	Full	No stabilizer	None	PDR-AE/PDR-EE	
			Cement	PDR-AE-C	
			Lime	PDR-AE-L	
			Fly ash	PDR-AE-F	
			Foamed asphalt	None	FDR-NS
				Cement	FDR-FA
Lime				FDR-FA-C	
Asphalt emulsion	Fly ash	FDR-FA-L			
	Kiln dust	FDR-FA-F			
	None	FDR-FA-K			
	Cement	FDR-AE			
Portland cement	None	Lime	FDR-AE-C		
		Fly ash	FDR-AE-L		
		Kiln dust	FDR-AE-F		
Lime	None	Kiln dust	FDR-AE-K		
		Asphalt emulsion	FDR-PC		
Synthetic polymer	None	Foamed asphalt	FDR-PC-AE		
			FDR-PC-FA		
Hot	Partial	Asphalt (hot)	None	H-PDR-A	
			Lime	H-PDR-A-L	

The following FDR and PDR problem statements have been identified and require additional research or refinement/calibration for California conditions:

- No comprehensive guidelines exist to guide engineers on how to choose between partial depth rehabilitation (PDR, or cold-in-place [CIR]/hot-in-place recycling [HIR]) and FDR, or on how to choose the most appropriate stabilizer or stabilizer combination in each of the strategies. Convention implies that PDR is more suited to the rehabilitation of pavements where distress is limited to the upper layers of asphalt concrete (i.e., rutting, top-down cracking, and/or moisture damage), whereas FDR is more suited to pavements where distress originates in the base layer or bottom of the asphalt layers (i.e., base failure and/or fatigue cracking). However, other criteria will also influence the decision on which strategy will be most appropriate for a specific project.

- No studies comparing any of the recycling strategies have been documented to support the writing of comprehensive guidelines for selecting the most appropriate recycling strategy for a particular project.
- No comprehensive monitoring of the long-term field performance of FDR with asphalt emulsion (FDR-AE) and FDR with only portland cement (FDR-PC) or any type of PDR projects has been documented. Consequently, there is limited information available for these pavement types regarding the following:
 - + Initial stiffness and changes in stiffness over time with regard to temperature, seasonal moisture fluctuations, and increasing age. This issue is important as these are fundamental properties that influence the performance of the pavement over time and which are used in mechanistic design of pavements.
 - + Fatigue and reflective cracking behavior. This issue is particularly important as it is probably a primary criterion for deciding on whether to use PDR or FDR.
 - + Thermal cracking behavior. This issue is important as it will dictate any climatic limitations for where these strategies can be used.
 - + Shrinkage cracking and subsequent reflection cracking behavior on FDR-PC pavements. This issue is important as they will be contributing factors to stabilizer selection, determination of the thickness of the overlay, and modeling of the long-term performance and maintenance requirements.
 - + Rutting behavior. This issue is important because PDR layers typically have relatively high air-void contents that may be susceptible to densification (rutting) if they are covered by thin overlays (i.e., < 2 in. [50 mm]).
 - + Moisture sensitivity. This issue is important because layers with high air-void contents are more susceptible to stripping, which leads to rutting, raveling, and cracking.
 - + Freeze-thaw cycling. This issue is important for the same reason cited above with high air-void pavements often being potentially more susceptible to moisture ingress and potential frost-heave during freeze periods. This problem may limit the use of PDR in high-altitude areas of the state.
 - + Effects of heavy truck traffic. Most literature refers to use of PDR on relatively light traffic roads (typically less than 10,000 AADT).
 - + Effects of early trafficking (i.e., same day as construction) on FDR-PC and FDR-AE pavements. This is important because most Caltrans FDR projects are completed in lane closures with traffic detoured using pilot cars, and the projects are required to be opened to traffic before nightfall of each day. The effects of placing the overlay on the FDR layer before it cures sufficiently to allow the cement or asphalt emulsion to gain strength have also not been quantified.
- No documentation exists on the collection of data for the development of mechanistic-empirical design and performance models for FDR, beyond the initial parameters developed for the California mechanistic-empirical pavement design procedure (*CalME*) by UCPRC for FDR-FA, FDR-AE and FDR-NS (no stabilizer) based on a limited number of projects. Also, no documentation exists on the actual development, calibration, and use of these models in pavement design and pavement management.
- In California, PDR projects are usually funded through Capital Maintenance (CAPM) funds, whereas FDR projects are usually funded through rehabilitation funds. Consequently, the project investigation for FDR is considerably more thorough than that for PDR and the less-comprehensive PDR project investigation might overlook some of the issues that render PDR an inappropriate strategy. The implications of this less intensive project investigation have not been evaluated in terms of risk to Caltrans.
- No studies have been undertaken to assess the influence of recycled rubberized asphalt on FDR performance.

1.4 Project Objectives

The objective of the Caltrans/UCPRC full-depth recycling study is to ultimately develop a comprehensive guideline document for the rehabilitation and Capital Maintenance (CAPM) design of pavements using partial- or full-depth reclamation techniques. This will be achieved through the following tasks, which will be undertaken in a number of phases:

1. A literature review on research related to the topic, with special emphasis on project selection, identifying the most suitable recycling strategy, identifying the most suitable stabilizer or stabilizer combination, mix design, empirical and mechanistic-empirical pavement design, equipment, construction guidelines, construction specifications, and accelerated and long-term performance, with special emphasis on change in stiffness over time, cracking behavior, rutting/densification, freeze-thaw, and moisture sensitivity. The potential effects of the presence of rubberized asphalt layers in the pavement being recycled will also be investigated. *This task was completed in Phase 1 and the findings are summarized in Chapter 2 of this report. New research findings published in the literature will continue to be monitored throughout the remainder of the study.*
2. Monitoring of existing and new field experiments to assess construction issues, stiffness, cracking (reflective, fatigue, longitudinal, transverse, thermal, and/or shrinkage depending on the strategy) rutting/densification, freeze-thaw, moisture sensitivity, and other observed distresses, as well as any possible effects of the presence of recycled rubberized asphalt. *This task was not included in Phase 1 due to a change in the funding for the study. Potential sites were and continue to be identified, and will be included in Phase 2.*
3. Full-depth reclamation of an existing gap-graded rubberized warm-mix asphalt test track using pulverization with no stabilization, with portland cement stabilization, with foamed asphalt plus cement stabilization, and with asphalt emulsion stabilization. *This task was completed in Phase 1 and is discussed in Chapter 3 of this report.*
4. Accelerated load testing to compare the four different full-depth reclamation strategies. If a suitable site can be located, partial depth recycling will also be assessed. *FDR testing under dry conditions was completed in Phase 1 and is discussed in Chapters 4 and 5. Additional FDR testing under wet conditions is planned for Phase 2 to assess moisture sensitivity of the recycled layers. No accelerated pavement testing on PDR projects is planned at this time.*
5. Laboratory testing to refine mix-design procedures and identify suitable criteria for mechanistic-empirical design procedures and performance models. *Basic characterization of the recycled material from the FDR test track and testing of the asphalt concrete surfacing material used on the test track was completed in Phase 1 and is discussed in Chapter 6. Additional testing of the stabilized materials is planned for Phase 2. No laboratory testing of PDR materials is planned at this time.*
6. Preparation of project selection and mechanistic-empirical design guidelines for partial- and full-depth recycling in California. *No work was completed on this task in Phase 1.*
7. Preparation of reports documenting the study and study results. *This report summarizes the work completed in Phase 1.*

This report covers the first phase of the study, which was limited to some of the tasks assessing full-depth reclamation. Initial work on Tasks 1, 3, 4, 5, and 7 is discussed.

1.5 Measurement Units

Although Caltrans recently returned to the use of U.S. standard measurement units, metric units have always been used by the UCPRC in the design and layout of HVS test tracks, and for laboratory, HVS, and field measurements and data storage. In this report, both English and metric units (provided in parentheses after the English units) are provided in general discussion. In keeping with convention, metric units are used in HVS and laboratory data analyses and reporting. A conversion table is provided on page xvii at the beginning of this report.

2. LITERATURE REVIEW

A literature review of research undertaken on full- and partial-depth reclamation since the completion of the earlier UCPRC study (1,2) was carried out. The review covered documentation from state departments of transportation, Transportation Research Board publications, and national and international journals covering pavement engineering. The revised Asphalt Recycling and Reclaiming Association's (ARRA) *Basic Asphalt Recycling Manual* was not available for review at the time of this report's preparation.

Although numerous publications on the topic were located (5-46), they mostly documented project level field and/or laboratory tests and did not directly address the problem statements listed in Section 1.3 or the objectives listed in Section 1.4. Although some documents in the search implied guidance (44), the information listed was based on the results of department of transportation surveys, and no actual guidance was provided. Some useful approaches to mechanistic-empirical design of FDR pavements are covered in the revised *Wirtgen Cold Recycling Technology Manual* (3). The literature review did not locate any publications on accelerated load testing of FDR or PDR projects, or on the monitoring of FDR or PDR field sections with different design parameters.

Blank page

3. TEST TRACK LOCATION, DESIGN, AND CONSTRUCTION

3.1 Test Track Location

The full-depth reclamation experiment is located on the North Test Track at the University of California Pavement Research Center facility in Davis, California. An aerial view of the site is shown in Figure 3.1. The track was first constructed as part of the third phase of a Caltrans/UCPRC warm-mix asphalt study, and it was used to investigate and compare differences in the performance of seven different warm-mix asphalt technologies in gap-graded rubberized asphalt mixes against that of two gap-graded rubberized hot-mix asphalt control sections (47,48). The FDR study described in this report is the second research project undertaken on this test track.



Figure 3.1: Aerial view of the UCPRC research facility.

3.2 Test Track Layout

The North Test Track is 361 ft (110 m) long and 52.5 ft (16 m) wide. It has a two percent crossfall in the north-south direction. The original test track (warm-mix asphalt study) was constructed as three lanes, but was recycled as four lanes to accommodate the four recycling strategies investigated (no stabilizer, asphalt emulsion, foamed asphalt with portland cement, and portland cement only) and to standardize the lane width for conventional construction equipment.

The planned FDR test track layout is shown in Figure 3.2. All test track measurements and locations discussed in this report are based on this layout.

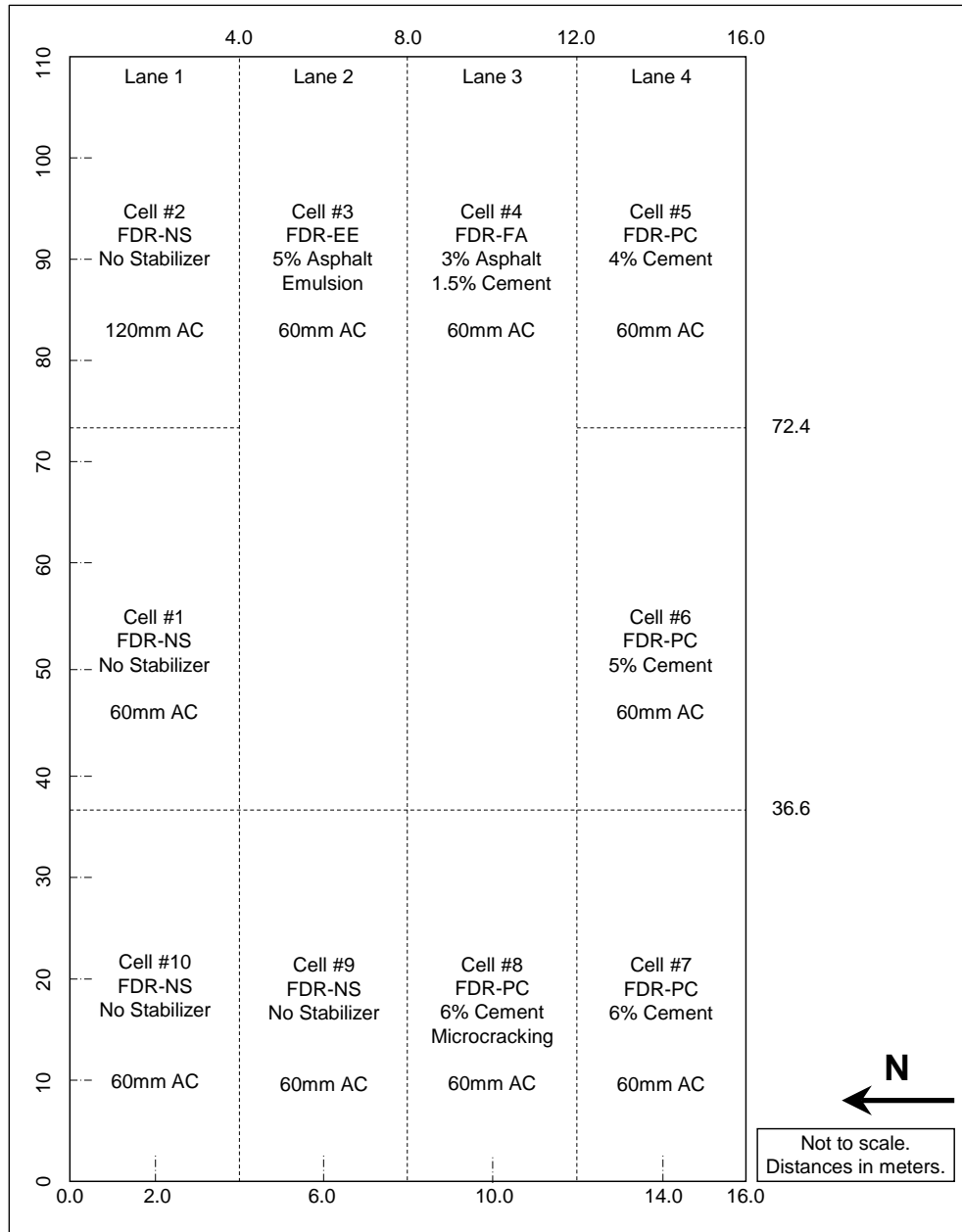


Figure 3.2: Planned test track layout.

The warm-mix asphalt test track was recycled in place using the following four different full-depth reclamation strategies (note that Cells #9 and #10 were included in the test track for a different study):

- Lane 1: No stabilizer (FDR-NS)
 - + Cell #1 surfaced with 60 mm asphalt concrete
 - + Cell #2 surfaced with 120 mm asphalt concrete
- Lane 2: Engineered asphalt emulsion (FDR-EE), surfaced with 60 mm asphalt concrete
 - + Cell #3 with 5.0 percent asphalt emulsion (3.0 percent residual asphalt content).
- Lane 3: Foamed asphalt with cement (FDR-FA), surfaced with 60 mm asphalt concrete
 - + Cell #4 with 3.0 percent foamed asphalt and 1.5 percent cement

- + Cell #8 with 6 percent cement. Cemented base microcracked with a vibrating steel drum roller 48 hours after final compaction.
- Lane 4: Portland cement (FDR-PC), surfaced with 60 mm asphalt concrete
 - + Cell #5 with 4 percent cement
 - + Cell #6 with 5 percent cement
 - + Cell #7 with 6 percent cement

3.3 Pavement Design

Pavement design for the FDR study was based on typical Caltrans practice. Recycle depth was set at 0.83 ft (250 mm), resulting in a new recycled base layer consisting of 0.4 ft (120 mm) of recycled asphalt concrete and 0.43 ft (130 mm) of the existing base. Given that the study was dedicated to understanding the behavior and performance of the recycled base, a relatively thin (0.2 ft [60 mm]) asphalt concrete surfacing was used in the design. However, Cell #2 of the FDR-NS lane was surfaced with 0.4 ft (120 mm) of asphalt concrete to compare performance of FDR-NS with two surfacing thicknesses. The pavement designs for the original and recycled test track are shown in Figure 3.3 and Figure 3.4. Details for the original pavement are provided in Section 3.3.1 through Section 3.3.5 (47,48).

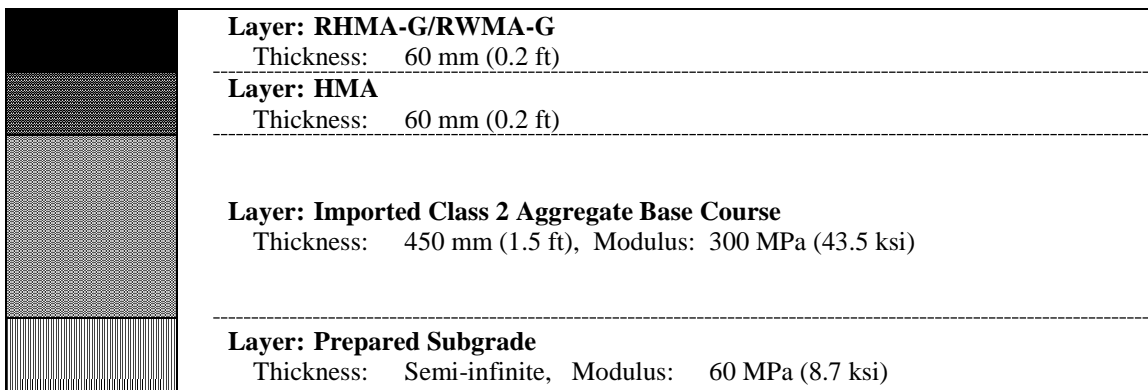


Figure 3.3: Original pavement structure for the rubberized warm-mix asphalt test sections.

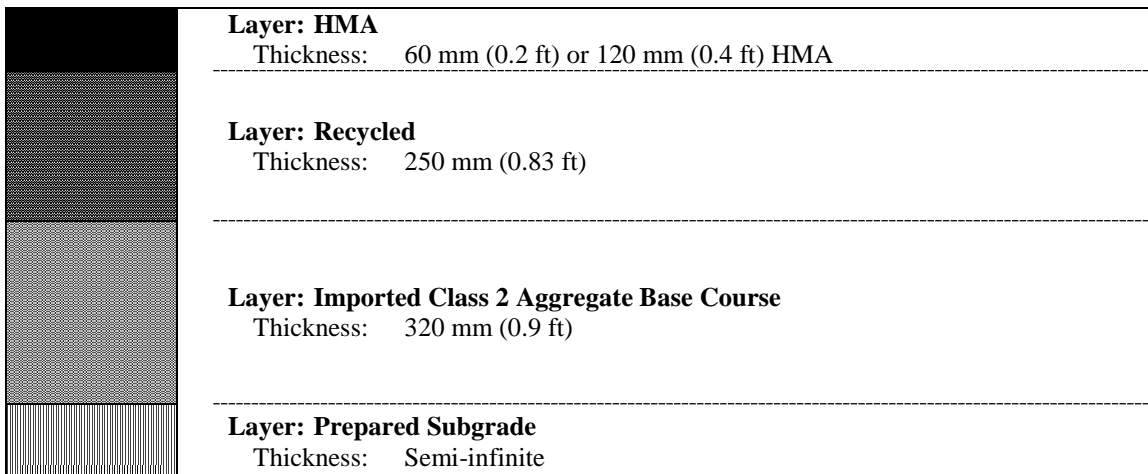


Figure 3.4: Pavement structure for the FDR study test sections.

3.3.1 Subgrade and Base Course Properties (Original Pavement)

Dynamic cone penetrometer (DCP) tests were performed along the center lines of each the original three lanes over the length and width of the test track prior to original construction to obtain an indication of the in situ subgrade strength. The results are summarized in Table 3.1. Penetration rates varied between 11 mm per blow and 30 mm per blow, with the weakest areas in the middle of the track. Variation was attributed to the degree of soil mixing, to temporary stockpiling of the lime-treated soils used during construction of the adjacent building pad (lime treatment was used to dry the soil in some areas of the site), to compaction from equipment during construction of the adjacent facility, and to varying subgrade moisture contents (47,48).

Table 3.1: Summary of DCP Survey on Subgrade Material

Test Location ¹ (m)	Penetration Rate (mm/blow)			Estimated California Bearing Ratio ²			Estimated Stiffness (MPa) ²		
	Lane #1	Lane #2	Lane #3	Lane #1	Lane #2	Lane #3	Lane #1	Lane #2	Lane #3
10	17	21	19	11	9	9	56	41	44
20	16	18	15	12	10	13	60	46	63
30	14	16	13	14	12	15	66	60	71
40	13	22	16	15	8	12	71	40	60
50	13	26	15	15	6	13	71	36	63
60	12	25	16	17	6	12	77	37	60
70	15	30	15	13	5	13	63	30	63
80	14	28	15	14	5	13	66	34	63
90	12	26	14	17	6	14	77	36	66
100	11	20	15	19	9	13	85	42	63

¹ Measured from southwest corner of the track. ² Estimated from DCP analysis software tool.

3.3.2 Subgrade Preparation for the Original Pavement

Subgrade preparation included vegetation removal, preliminary leveling, ripping, watering and mixing, compaction, and final leveling to include a two percent north–south crossfall as follows (47,48):

- Removing vegetation with a grader, windrowing of the deleterious material toward the center of the track, collecting this material with a scraper and dumping it in a temporary stockpile for removal
- Preliminary leveling with a grader followed by watering
- Ripping to a depth of 12 in. (300 mm)
- Watering and mixing using both the scraper and grader. Pockets of high clay content soils were observed during this process, which required additional working with the grader and scraper to break up the clods.
- Initial compaction with a padfoot roller. Despite extensive mixing, some clay pockets were still observed after completion of the initial compaction, with padfoot impressions clearly visible. Clay pockets appeared to predominate on the eastern half of the track.
- Final compaction with a vibrating smooth drum roller
- Final leveling with a grader
- Density checks on the finished surface with a nuclear density gauge

Quality control of the subgrade preparation was limited to density checks with a nuclear gauge following California Test (CT) 231 and comparison of the results against a laboratory maximum wet density of 134.2 lb/ft³ (2,150 kg/m³) determined according to CT 216. Nuclear gauge measurements were taken at 10 different locations selected according to a nonbiased plan. Samples for laboratory density determination were taken at the first three locations. Results are summarized in Table 3.2 and indicate that the subgrade density was generally consistent across the test track. Relative compaction varied between 95.4 percent and 99.2 percent with an average of 97.0 percent, two percent above the Caltrans-specified minimum density of 95 percent for subgrade compaction. No location had a relative compaction lower than this minimum.

Table 3.2: Summary of Subgrade Density Measurements (47,48)

Location	Wet Density		Relative Compaction	Moisture Content	Dry Density	
	(lb/ft ³)	(kg/m ³)			(lb/ft ³)	(kg/m ³)
1	130.5	2,091	97.3	15.6	112.6	1,804
2	132.6	2,124	98.8	17.3	113.1	1,811
3	131.3	2,103	97.8	16.8	112.4	1,801
4	130.2	2,086	97.0	16.2	112.1	1,796
5	133.2	2,133	99.2	15.2	115.6	1,852
6	128.9	2,065	96.0	17.8	109.5	1,754
7	132.2	2,117	98.5	17.9	112.1	1,795
8	128.1	2,052	95.4	18.7	107.9	1,728
9	132.3	2,120	98.6	16.5	113.6	1,820
10	128.7	2,062	95.9	15.0	111.9	1,793
Average	130.8	2,095	97.0	17.0	112.1	1,795
Std. Dev.	1.8	29	1.3	1.2	2.1	34

3.3.3 Base Course Construction for the Original Pavement

Base course aggregates were sourced from the Teichert Cache Creek quarry near Woodland, California. Key material properties are summarized in Table 3.3. The material met Caltrans specifications, except for the percent passing the #200 sieve, which exceeded the specification operating range by 3.0 percent, and just met the contract compliance limits.

The warm-mix asphalt test track base course was constructed two days after the subgrade preparation. The construction process included aggregate spreading, watering, compaction, and final leveling to include a two percent north–south crossfall as follows (47,48):

- Transporting crushed base course material (alluvial) that complied with Caltrans Class 2 aggregate base course specifications from the Teichert Cache Creek aggregate source to the test track with a fleet of bottom-dump trucks and trailers
- Dumping the aggregate in windrows
- Spreading the aggregate with a grader to a thickness of approximately 4.0 in. (100 mm)
- Adding water to bring the aggregate to the optimum moisture content and re-mixing with the grader to ensure even distribution of the moisture throughout the material

- Initial compaction of the spread material with a vibrating steel wheel roller
- Repeating the process until the design thickness of 1.5 ft (450 mm) was achieved
- Applying water generously followed by compaction to pump fines to the surface to provide good aggregate interlock (slushing)
- Final leveling with a grader. Final levels were checked with a total station to ensure that a consistent base course thickness had been achieved.
- Removal of excess material with a scraper, followed by final compaction
- Density checks on the finished surface with a nuclear density gauge

Table 3.3: Base Course Material Properties (47,48)

Property	Result	Operating Range	Contract Compliance
Grading: 1" (25 mm)	100	100	100
3/4" (19 mm)	99.1	90 – 100	87 – 100
1/2" (12.5 mm)	90.1	–	–
3/8" (9.5 mm)	83.5	–	–
#4 (4.75 mm)	63.3	35 – 60	30 – 65
#8 (2.36 mm)	48.8	–	–
#16 (1.18 mm)	39.2	–	–
#30 (600 µm)	30.8	10 – 30	5 – 35
#50 (300 µm)	21.6	–	–
#100 (150 µm)	15.6	–	–
#200 (75 µm)	12.3	2 – 9	0 – 12
Liquid Limit		–	–
Plastic Limit	Non-plastic	–	–
Plasticity Index		–	–
Maximum Dry Density (lb/ft ³)(kg/m ³)	140.6 (2,252)	–	–
Optimum Moisture Content	6.0	–	–
R-Value	79	–	>78
Sand equivalent	30	25	>22
Durability index – course	78	–	>35
Durability index – fine	52	–	>35

Quality control of the base course construction was limited to density checks with a nuclear gauge following CT 231 and comparison of the results against a laboratory maximum wet density of 150.5 lb/ft³ (2,410 kg/m³) determined according to CT 216. Nuclear gauge measurements were taken at 10 different locations selected according to a nonbiased plan. A sample for laboratory density determination was taken at the first location. Results are summarized in Table 3.4 and indicate that the base course density properties were generally consistent across the test track, but that the material was relatively wet compared to the laboratory-determined optimum moisture content. Relative compaction varied between 96.7 percent and 99.4 percent with an average of 98.0 percent, three percent above the Caltrans-specified minimum density of 95 percent for base compaction. No location had a relative compaction lower than this minimum.

Follow-up dynamic cone penetrometer (DCP) measurements were also undertaken on the base at the same locations as the original subgrade DCP survey. The results are summarized in Table 3.5 and indicate that although average penetration rates (mm/blow) were consistent across the track, there was considerable

difference in the average calculated stiffness of the base from the redefined layers based on actual penetration. Consequently, the contractor was requested to recompact the track with a static steel drum roller prior to priming to consolidate the base layer and accelerate movement of any infiltrated water to the surface. A significant improvement in subgrade stiffness attributed to the subgrade preparation and confinement by the base was also noted.

Table 3.4: Summary of Nuclear Gauge Density Measurements on Base Course Layer (47,48)

Location	Wet Density		Relative Compaction (%)	Moisture Content (%)	Dry Density	
	(lb/ft ³)	(kg/m ³)			(lb/ft ³)	(kg/m ³)
1	146.5	2,346	97.3	6.6	137.4	2,201
2	148.5	2,379	98.7	7.0	138.8	2,223
3	148.0	2,371	98.4	8.0	137.0	2,195
4	147.1	2,356	97.8	7.8	136.5	2,186
5	148.7	2,382	98.8	6.3	139.9	2,241
6	145.5	2,330	96.7	6.8	136.2	2,182
7	149.0	2,387	99.0	8.2	137.7	2,206
8	145.6	2,332	96.8	7.7	135.2	2,165
9	149.5	2,395	99.4	6.9	139.8	2,240
10	145.7	2,334	96.8	7.8	135.2	2,165
Average	147.4	2,361	98.0	7.3	137.3	2,200
Std. Dev.	1.5	25	1.0	0.7	1.7	27.6

Table 3.5: Summary of DCP Survey on Base and Subgrade Material (47,48)

Test Location (m) ¹	Penetration Rate (mm/blow)						Estimated Stiffness (MPa [ksi]) ²					
	Base			Subgrade			Base			Subgrade		
	Lane			Lane			Lane			Lane		
	#1	#2	#3	#1	#2	#3	#1	#2	#3	#1	#2	#3
10	3	-	-	9	-	-	430 (62)	-	-	111 (16)	-	-
20	-	3	-	-	8	-	-	395 (57)	-	-	119 (17)	-
30	-	-	3	-	-	7	-	-	320 (46)	-	-	139 (20)
40	4	-	-	9	-	-	332 (48)	-	-	114 (17)	-	-
50	-	4	-	-	9	-	-	299 (43)	-	-	107 (16)	-
60	-	-	4	-	-	9	-	-	279 (41)	-	-	137 (20)
70	4	-	-	10	-	-	255 (37)	-	-	99 (14)	-	-
80	-	4	-	-	10	-	-	260 (38)	-	-	105 (15)	-
90	-	-	4	-	-	7	-	-	273 (40)	-	-	148 (22)
100	4	-	-	11	-	-	259 (38)	-	-	116 (17)	-	-

¹ Measured from southwest corner of the track. ² Estimated from DCP analysis software tool (*WinDCP Ver 5.0, [49]*).

3.3.4 Asphalt Surfacing on Original Pavement: Bottom Lift

Material Properties

Dense-graded asphalt concrete for the bottom lift was sourced from Teichert’s Woodland Asphalt Plant. Key material properties are summarized in Table 3.6. The material met Caltrans specifications.

Prime Coat Application

On the day before the prime coat application, the test track was compacted with a twin-drum steel roller (no vibration) to consolidate the base layer and accelerate movement of infiltrated water to the surface. An

SS-1 asphalt emulsion prime coat was applied to the surface at a rate of 0.25 gal./yd² (1.0 L/m²). The time of application was 1:00 p.m., ambient temperature was 88°F (35°C), and relative humidity was 28 percent. A consistent application was achieved; however, differential penetration was observed, which was attributed to patches of near-surface moisture.

Table 3.6: Key Bottom Lift HMA Mix Design Parameters (47,48)

Parameter	Specification	Actual
Grading: 1" (25 mm)	100	100
3/4" (19 mm)	100	98
1/2" (12.5 mm)	90 – 100	84
3/8" (9.5 mm)	77 – 89	75
#4 (4.75 mm)	33 – 47	52
#8 (2.36 mm)	18 – 28	34
#16 (1.18 mm)	–	22
#30 (600 µm)	–	15
#50 (300 µm)	–	9
#100 (150 µm)	–	6
#200 (75 µm)	3 – 7	4
Asphalt binder grade	–	PG 64-16
Asphalt binder content (% by aggregate mass)	–	5.0
Hveem stability at optimum bitumen content	>37	41.0
Air-void content (%)	2 – 6	4.0
Dust proportion	0.6 – 1.3	0.9
Voids in mineral aggregate (LP-2) (%)	>13	13.0
Voids filled with asphalt (LP-3) (%)	65 – 75	69.0
Crushed particles (1 face) (%)	>90	92
Sand equivalent (%)	>47	71.0
Fine aggregate angularity (%)	>47	54.0
Los Angeles Abrasion at 100 repetitions (%)	<12	5.0
Los Angeles Abrasion at 500 repetitions (%)	<45	21.3

Asphalt Placement

The bottom lift of asphalt concrete was placed on October 30, 2009. Construction started at approximately 8:30 a.m. Ambient air temperature was 50°F (10°C) and the relative humidity was 45 percent. Construction was completed at approximately 11:00 a.m. when ambient temperature was 61°F (16°C) and the relative humidity was 40 percent.

Mix was transported using bottom-dump trucks and placed in a windrow on the surface. During placement, a pickup machine connected to the paver collected the material and fed it into the paver hopper. Paving followed conventional procedures. A breakdown roller (dual steel drum) closely followed the paver, applying about four passes. A single pass was made with an intermediate rubber-tired roller, followed by another four passes with a finish roller (dual steel drum).

3.3.5 Asphalt Surfacing on Original Pavement: Rubberized Asphalt Concrete

Material Properties

Rubberized asphalt concrete was sourced from two different asphalt plants (Granite Construction Bradshaw Plant in Sacramento and George Reed Construction Marysville Plant) to accommodate the seven different warm-mix asphalt technologies, which included two plant-specific mechanical foaming technologies. Hot-mix controls were produced at both plants for performance comparisons. Mix designs were prepared by the two plants and both met the Caltrans specifications for 1/2 in. (12.5 mm) gap-graded rubberized hot-mix asphalt (RHMA-G). Control mix properties for the two plants are summarized in Table 3.7. Conventional construction procedures were followed (47,48).

Table 3.7: Quality Control of Mix After Production (47,48)

Parameter	Granite		George Reed	
	Specification/ Target	Actual (Control) ¹	Specification/ Target	Actual (Control)
Grading ¹				
3/4" (19 mm)	100	100	100	100
1/2" (12.5 mm)	90 – 100	99	90 – 100	98
3/8" (9.5 mm)	78 – 88	78	78 – 88	87
#4 (4.75 mm)	32 – 42	<u>31</u>	32 – 42	39
#8 (2.36 mm)	17 – 25	19	17 – 25	20
#16 (1.18 mm)	–	13	–	12
#30 (0.6 mm)	7 – 15	10	7 – 15	8
#50 (0.3 mm)	–	7	–	6
#100 (0.15 mm)	–	6	–	4
#200 (0.075 mm)	2 – 7	4	2 – 7	3
Sand equivalent ²	47	68	>47	73
AC binder content (%) ³	7.3	<u>7.73</u>	8.3	7.7
Hveem stability	>23	31	>23	43
RICE specific gravity ⁴	–	2,452	–	2,505
Unit weight	–	2,482	–	2,388
Moisture (before plant) (%)	–	Not tested	–	2.3
Moisture ⁶ (after silo) (%)	1.0	0.0	1.0	Not tested

¹ Underlined numbers indicate parameters that did not meet the specification

Tack Coat Application

The test track was broomed to remove dust and organic matter from the surface prior to any work being undertaken. A diluted SS-1 emulsion (70:30) was applied with a distributor at an application rate of approximately 0.08 gal./yd² (0.36 L/m²). Air and surface temperatures were 46°F (8°C) and 54°F (12°C), respectively. Relative humidity was 68 percent.

Asphalt Placement

The rubberized asphalt concrete mixes were produced and placed on April 7 and April 8, 2010. Construction started at approximately 10:00 a.m. Ambient air temperature was 54°F (13°C) and the relative humidity was 45 percent. Construction was completed at approximately 2:00 p.m. on both days when ambient temperature was 63°F (17°C) and the relative humidity was 40 percent.

Mix was transported using end-dump trucks and deposited directly into the paver hopper. Paving followed conventional procedures. The breakdown roller closely followed the paver, applying about seven passes with vibration followed by another five passes of finish rolling without vibration.

3.4 Full-Depth Reclamation Mix Designs

3.4.1 Material Sampling Prior to Recycling

Cores were removed from the original test track to aid in the design of the engineered emulsion mix. The designs for the cement and foamed asphalt mixes were completed using millings from another UCPRC project and from aggregate base sampled during the construction of the original test track. These materials were blended in equal proportions to mimic the test track design (i.e., 120 mm of recycled asphalt concrete [2 lifts of 60 mm] and 130 mm of recycled original base material). This mix was considered to be suitably representative of the recycled materials for purposes of mix design.

3.4.2 Mix Design for FDR-EE Section

The mix design for the FDR-EE section was conducted by Road Science, suppliers of the asphalt emulsion used to construct the test section. A design procedure similar to that proposed for use in the Caltrans specifications for FDR with asphalt emulsion was followed. A summary of the mix design is provided in Table 3.8. An emulsion content of 5.0 percent (3.0° percent residual asphalt content) was selected for the test track.

Table 3.8: Mix Design: FDR-EE

Parameter	Target	Results Per Emulsion Content (%)				
		3.5%	4.0%	4.5%	5.0%	5.5%
Percent water	–	3.0	3.0	3.0	3.0	3.0
Density (pcf [kg/m ³])	–	131 (2,096)	130 (2,089)	134 (2,143)	132 (2,119)	133 (2,137)
Max. specific gravity (G _{mm}) ¹	–	2.483	2.472	2.461	2.451	2.433
Bulk specific gravity (G _{mb}) ²	–	2.097	2.090	2.144	2.120	2.137
Percent air voids	–	15.5	15.5	12.9	13.5	12.2
Short-term strength (g/25mm) ³	≥175	102	110	127	158	187
ITS (psi [kPa]) ⁴	≥40 (276)	27 (186)	26 (179)	40 (276)	45 (310)	43 (296)
Percent vacuum saturated	≥55	61	60	60	62	61
Conditioned ITS (psi [kPa]) ⁴	≥25 (172)	15 (103)	23 (159)	21 (145)	27 (186)	26 (179)
Resilient modulus (ksi [MPa]) ⁵	≥150 (1,000)	–	–	–	156 (1,076)	–
Thermal cracking ITS (°C) ⁶	≤-7.0	–	–	–	-28.4	–

¹ ASTM D 2041 ² ASTM D 6752 ³ ASTM D 1560 ⁴ Indirect Tensile strength ASTM D 4867
⁵ ASTM D 4123 ⁶ AASHTO T322

3.4.3 Mix Design for FDR-FA Section

The properties of the blended materials were similar to one of the material blends tested as part of the earlier Caltrans/UCPRC research study on FDR with foamed asphalt (2). Consequently the mix design of 3.0 percent asphalt and 1.5 percent cement, determined for that earlier material blend by following the test

method described in the UCPRC FDR-FA guideline (1), was selected for use in the test track. The results are listed in Table 3.9.

Table 3.9: Mix Design: FDR-FA

Parameter	Target	Result ¹
		FA at 3.0%
Portland cement content (%)	–	1.5
Optimum moisture content (%)	–	6.0
Mixing moisture content (%)	–	4.8
Density (pcf [kg/m ³])	–	132.7 (2,125)
Expansion ratio	≥10	12
Half-life	≥12	16
Wet ITS, no cement (psi [kPa])	≥15 (100)	30.6 (211)
Dry ITS, no cement (psi [kPa])	–	49.0 (338)
Tensile strength retained	> 0.5	0.62

¹ Mix design according to UCPRC FDR-FA Guidelines (1)

3.4.4 Mix Design for FDR-PC Sections

The UCPRC and HSI Engineering both prepared mix designs for the cement-treated section (FDR-PC), following the procedure in the Caltrans *Maintenance Technical Advisory Guide* (Chapter 14, Full Depth Reclamation using Cement [50]). A summary of the mix design is provided in Table 3.10. Cement contents of 4.0, 5.0, and 6.0 percent were selected for the test track.

Table 3.10: Mix Design: FDR-PC

Parameter	Target	Cement Content (%)				
		2.0% ¹	4.0% ¹	5.0% ²	6.0% ¹	8.0% ¹
OMC (%)	–	6.0	6.0	6.0	7.0	8.0
Density (pcf [kg/m ³])	–	140.7 (2,254)	143.4 (2,297)	145.1 (2,325)	146.8 (2,351)	147.7 (2,366)
UCS (psi) ⁴	300 – 600	116	371	435	840	1,004
UCS (MPa) ⁴	2.0 – 4.0	0.8	2.6	3.0	5.8	6.9

¹ Prepared by UCPRC ² Prepared by HIS ³ Optimum moisture content
⁴ Unconfined compressive strength, ASTM D 1633 (compacted according to ASTM D 1557)

3.5 Full-Depth Reclamation

Full-depth reclamation of the test track took place on September 27, 2012. Construction started on Lane 2 (FDR-EE), followed by Lane 3 (FDR-FA), Lane 1 (FDR-NS), and then Lane 4 (FDR-PC). This order was requested by the contractor to facilitate matching of levels.

3.5.1 Lane 1: No Stabilizer (FDR-NS)

Conventional FDR construction procedures were followed on the FDR-NS lane. The recycler and connected water tanker made a single pass to pulverize and mix the material to optimum moisture content for compaction (Figure 3.5). Mixing moisture content settings were based on the moisture contents determined prior to recycling. As the recycler proceeded, some chunks of unpulverized asphalt concrete were noted at the start of the section (Figure 3.6), with occasional chunks appearing along the lane thereafter. Occasional smoke and heated rubber odors were noted as the recycler pulverized the asphalt

layers (Figure 3.7). This was attributed to the relatively unaged state of the rubberized asphalt surfacing. On completion of the recycling pass, the pulverized material appeared to have a consistent grading and uniform moisture content with very little oversized material (Figure 3.8). Recycling depth was well controlled, with an average depth of 8 in. (250 mm) maintained over the full length of the test section. Initial rolling was completed with a padfoot roller (Figure 3.9), followed by a vibrating smooth drum roller (Figure 3.10). Final levels were achieved with a grader after compaction with the smooth drum roller (Figure 3.11) and final compaction was completed with a rubber-tired roller (Figure 3.12).



Figure 3.5: FDR-NS: Test track recycling.



Figure 3.6: FDR-NS: Chunks at start of test pulverization.



Figure 3.7: FDR-NS: Smoke during pulverization.



Figure 3.8: FDR-NS: Pulverized material.



Figure 3.9: FDR-NS: Initial compaction with padfoot roller.



Figure 3.10: FDR-NS: Compaction with smooth drum roller.



Figure 3.11: FDR-NS: Surface leveling with a grader.



Figure 3.12: FDR-NS: Compaction with rubber-tired roller.



Figure 3.13: FDR-NS: Completed recycled layer surface.

3.5.2 Lane 2: Engineered Emulsion (FDR-EE)

The engineered emulsion lane was recycled in two passes. The first pass did not include any asphalt emulsion and was undertaken after consultation with the contractor and the emulsion supplier to assess the moisture content in the material being recycled. Although water metering was set to add water at a rate of 0.5 percent of the approximate mass of the dry aggregate during this first pass, the actual rates appeared to be higher than that in the first approximately 60 ft. (20 m), leading to the water flow being switched off. For the remainder of the first pass, the moisture content in the recycled material was variable, with some relatively dry areas and some relatively moist areas.

The second pass injected the asphalt emulsion through the recycler mixing system, fed from a tanker attached to the front of the equipment (Figure 3.14). A number of problems were noted. The initial binder application rate appeared to be too high and binder was only being sprayed in a 9 ft (3.0 m) wide strip on the right-hand side of the lane (viewed from behind the machine looking west) (Figure 3.15). As a result, the recycler was stopped at this point (approximately 90 ft [30 m] from the start of the section),

backed up to the start, and then a third pass was made to add binder to the untreated strip. Despite adjustments to the settings, the spray rate still appeared to be too high and there was some overlap with the previous application, resulting in excess emulsion being injected into the material (Figure 3.16). After completion of this third pass on the first 90 ft (30 m), the recycler was stopped and flow rates readjusted. After this change, the emulsion application rate appeared to be more consistent for the next approximately 90 ft (30 m), although more binder was still being applied on the right-hand side of the lane compared to the rest of the lane based on observations of the color and consistency of the recycled material, and on material adhering to the right rear tire of the recycler.



Figure 3.14: FDR-EE: Recycling train.



Figure 3.15: FDR-EE: Inconsistent emulsion application across width of test track.



Figure 3.16: FDR-EE: Excess emulsion applied during recycling.



Another adjustment was subsequently made; however, there was insufficient emulsion remaining to complete the injection of binder to the end of the lane (approximately 30 ft [10 m] was not injected with emulsion) or to reapply to the untreated strip on the left side of the lane. Although the correct quantity of emulsion, determined from the mix design, was delivered to the site to complete the project at the design

application rate, approximately 650 ft² (60 m²) of the lane was not stabilized, indicating that emulsion was injected at a rate considerably higher than the design in those parts of the lane that were treated.

The FDR-EE lane was compacted following the same sequence as that described for the FDR-NS lane. During compaction with the padfoot roller, the strip down the left side of the lane where no binder had been applied (Figure 3.17) was clearly visible. After completion of rolling with the smooth drum roller, the areas with excess fluid content in the recycled material in the first half of the lane was clearly visible in the form of puddles on the surface (Figure 3.18 and Figure 3.19). Excavation of the pulverized material in the adjacent FDR-FA lane clearly showed the high moisture content in the FDR-EE layer after compaction (Figure 3.20). Subsequent passes with the smooth drum roller caused additional water puddles to appear on the test track surface.



Figure 3.17: FDR-EE: Compaction with padfoot roller.
(Note untreated areas and emulsion adhering to tire).



Figure 3.18: FDR-EE: Excess fluid during and after compaction with smooth drum roller.



Figure 3.19: FDR-EE: Puddled water on surface after compaction.



Figure 3.20: FDR-EE: Excavation showing wet recycled layer.

3.5.3 Lane 3: Foamed Asphalt with Portland Cement (FDR-FA)

Given the problems experienced during construction of the FDR-EE lane, further adjustments were made to the recycler to ensure that similar problems were not experienced during construction of the FDR-FA lane.

Portland cement was first spread onto the asphalt surface with a mechanical spreader (Figure 3.21). Spread rates were checked with a tray placed in the middle of the lane. The average rate was 1.5 percent by approximate mass of dry aggregate, per the design. Before starting recycling, the expansion ratio and half-life of the foamed asphalt was checked using the spray nozzle on the side of the recycler. An expansion ratio of 12 and a half-life of 16 seconds were recorded, both of which were consistent with the mix design and exceeded the minimum specified requirements of 10 and 12, respectively (1). Asphalt temperature during recycling was approximately 340°F (170°C). The binder injection rate was set to an equivalent of 3.0 percent by approximate mass of dry aggregate, with a foaming water content of 3.0 percent. Mixing water content was set to achieve approximately 75 percent of the optimum moisture content of 6.0 percent, based on the testing prior to recycling (Section 3.4.1).

The lane was recycled in a single pass of the recycling train, which consisted of the asphalt binder and water tankers coupled to the front and rear of the recycler respectively (Figure 3.22). Foamed asphalt appeared to be evenly injected across the width of the test track and none of the problems experienced on the FDR-EE test section were observed. Recycling depth was consistent at 10 in. (250 mm) and the recycled material appeared to be uniformly mixed (Figure 3.23 and Figure 3.24). Compaction and leveling followed the same procedure as that used on the FDR-NS section (Figure 3.25 and Figure 3.26). Additional water was sprayed onto the surface prior to rolling with the rubber tired roller. The compacted surface was tightly bound and no wet spots were observed.



Figure 3.21: FDR-FA: Spreading cement on old asphalt surface.



Figure 3.22: FDR-FA: Recycling train.



Figure 3.23: FDR-FA: Uniform mix behind recycler.



Figure 3.24: FDR-FA: Padfoot roller compaction on uniform mix.



Figure 3.25: FDR-FA: Steel wheel compaction showing tightly bound surface.



Figure 3.26: FDR-FA: Final compaction showing tightly bound surface.

3.5.4 Lane 4: Portland Cement (FDR-PC)

The construction plan called for prepulverization of the existing test track lane to the design depth of 10 in. (250 mm). However, the contractor requested to recycle the FDR-PC lane in a single pass. Consequently, cement was spread directly onto the pavement surface with the mechanical spreader. Three

passes were made to achieve the three different cement contents of 4.0, 5.0, and 6.0 percent. Spread rates were checked with a tray placed in the middle of the lane. Cement contents were calculated to be 1.3 percent higher than the design on Cell #5 and Cell #6 (i.e., 5.3 and 6.3 percent, respectively). On Cell #7 and Cell #8, cement contents were in excess of 10 percent, indicating that there were problems with the feed rate on the mechanical spreader (Figure 3.27). Although an attempt was made to blade some of the cement off of these sections with the grader (Figure 3.28), a uniform spread could not be achieved.



Figure 3.27: FDR-PC: Excess cement on Cell #7.



Figure 3.28: FDR-PC: Removing excess cement on Cell #8.

Although a uniform cement spread rate was not achieved, construction continued. After spreading the cement, the recycler and attached water tanker started reclaiming the layer. However, the forward speed of the train was very slow and the consistency of the mixed material very poor due to the higher than design cement contents. It was therefore agreed with the contractor that the cement would first be mixed to the design depth of 10 in. (250 mm) without the addition of water. This was completed, but the equipment still appeared to experience difficulties with pulverizing the rubberized asphalt and uniformly mixing the higher contents of cement on Cell #6, Cell #7, and Cell #8. Mixing on Cell #5 (5.3 percent cement) appeared to be satisfactory (Figure 3.29). After this first pass with the recycler, water was sprayed onto the pulverized material with the water tanker (Figure 3.30). Thereafter, the recycler was recoupled to the water tanker and a second mixing pass made to add the required water to raise the moisture content to the optimum level for compaction (Figure 3.31). The mixed material appeared to be satisfactory on Cell #5 and Cell #6 (Figure 3.32), but inconsistent on the cells with the very high cement content (Cell #7 and Cell #8) (Figure 3.33). Compaction and leveling followed the same procedure as that used on the FDR-NS section. Additional water was sprayed onto the surface of all the cells as required during rolling with the smooth drum and rubber-tired rollers.



Figure 3.29: FDR-PC: Uniform mixing after first pulverization pass with no water.



Figure 3.30: FDR-PC: Water spray prior to second mixing pass.



Figure 3.31: FDR-PC: Second mixing pass with water.



Figure 3.32: FDR-PC: Uniform mix after second recycling pass.



Figure 3.33: FDR-PC: Inconsistent mix on high cement content cells.

3.5.5 Construction Quality Control

Samples of the recycled material were removed from the FDR-NS lane prior to compaction to determine the properties of the material. Material properties of the sampled material are summarized in Table 3.11. Material gradation was well within the specified limits. In-place density was measured with a nuclear gauge in each cell after compaction. Nuclear gauge compaction results are provided in Table 3.12.

Table 3.11: Recycled Layer Material Properties

Property	Result	Operating Range	Contract Compliance	Specification Compliance			
				FDR-NS	FDR-EE	FDR-FA	FDR-PC
Grading:							
3" (75 mm)	100	–	–	–	100	100	100
2" (50 mm)	100	–	–	100	95 – 100	95 – 100	95 – 100
1.5" (38 mm)	100	–	–	90 – 100	85 – 100	85 – 100	85 – 100
1" (25 mm)	100	100	100	–	–	–	–
3/4" (19 mm)	99	90 – 100	87 – 100	–	–	–	–
1/2" (12.5 mm)	91	–	–	–	–	–	–
3/8" (9.5 mm)	82	–	–	–	–	–	–
#4 (4.75 mm)	66	35 – 60	30 – 65	–	–	–	–
#8 (2.36 mm)	46	–	–	–	–	–	–
#16 (1.18 mm)	31	–	–	–	–	–	–
#30 (600 µm)	21	10 – 30	5 – 35	–	–	–	–
#40 (425 µm)	14	–	–	–	–	–	–
#50 (300 µm)	11	–	–	–	–	–	–
#100 (150 µm)	8	–	–	–	–	–	–
#200 (75 µm)	5	2 – 9	0 – 12	–	<20	–	–
Liquid Limit		–	–	–	–	–	–
Plastic Limit	Non-plastic	–	–	–	–	–	–
Plasticity Index		–	–	–	–	–	–
MDD ¹ (lb/ft ³)	135.5	–	–	–	–	–	–
MDD (kg/m ³)	2,171	–	–	–	–	–	–
OMC ² (%)	4.8	–	–	–	–	–	–

¹ Maximum dry density ² Optimum moisture content

Table 3.12: Summary of Nuclear Gauge Density Measurements on Recycled Layer

Cell		Wet Density ¹		Moisture Content ¹	Dry Density ¹		Relative Compaction ¹
		(lb/ft ³)	(kg/m ³)		(lb/ft ³)	(kg/m ³)	
1	FDR-NS	137.5	2,202	11.6	123.3	1,975	92
2	FDR-NS	137.1	2,195	12.4	122.0	1,954	92
3a	FDR-EE (E)	135.2	2,165	13.7	119.1	1,907	90
3b	FDR-EE (W)	137.7	2,205	12.2	122.8	1,967	93
4a	FDR-FA (E)	136.0	2,179	14.6	118.9	1,904	91
4b	FDR-FA (W)	136.8	2,204	8.2	126.5	2,026	92
5	FDR-PC	136.6	2,189	9.6	126.2	2,022	91
6	FDR-PC	135.7	2,174	8.6	124.9	2,001	90
7	FDR-PC	137.6	2,204	8.5	126.8	2,031	91
8	FDR-PC	137.6	2,204	7.9	127.6	2,043	92
9	FDR-NS	138.5	2,218	12.3	123.3	1,975	92
10	FDR-NS	136.2	2,182	9.6	124.3	1,991	93

¹ Average of two measurements per cell

The density measurements determined with a nuclear gauge showed some variability in the different cells and the relative compaction in all the cells was lower than the required specification. However, relative compaction (nuclear density gauge dry density on test track compared to maximum dry density determined in the laboratory [AASHTO T 180]) was generally consistent across all cells, with the unstabilized sections showing the highest relative compaction. Given the known inconsistencies with nuclear gauge moisture content measurements, especially when hydrocarbons are present (i.e., recycled

asphalt pavement and asphalt stabilizers in the recycled layer), dry densities were recalculated with gravimetric moisture contents that were determined from samples removed from behind the recycler during construction of the test track. The revised compaction measurements are summarized in Table 3.13. Recalculated relative compaction on each cell was higher and most cells, with the exception of the first half of the FDR-EE section and on all the FDR-PC sections, met or exceeded the Caltrans specification requirements (95 percent for FDR-NS, 97 percent for FDR-EE, and 98 percent for FDR-FA and FDR-PC). Low compaction on the FDR-EE section was attributed to the high moisture and asphalt emulsion contents discussed in Section 3.5.2. Low reported compaction on the FDR-PC sections was attributed to a combination of the construction problems discussed in Section 3.5.4 and to the generalization of the laboratory reference density, given that reference densities were not determined for the range of cement contents actually applied on the day of construction.

Table 3.13: Recalculated Dry Density Measurements using Gravimetric Moisture Content

Cell		Wet Density ¹		Gravimetric Moisture Content ¹	Dry Density ¹		Relative Compaction ¹
		(lb/ft ³)	(kg/m ³)		(%)	(lb/ft ³)	
1	FDR-NS	137.5	2,202	4.8	131.2	2,101	98
2	FDR-NS	137.1	2,195	4.2	131.6	2,107	99
3a	FDR-EE (E)	135.2	2,165	7.0	126.4	2,023	95
3b	FDR-EE (W)	137.7	2,205	6.2	129.7	2,076	98
4a	FDR-FA (E)	136.0	2,179	4.9	129.6	2,077	98
4b	FDR-FA (W)	136.8	2,204	4.8	130.5	2,103	99
5	FDR-PC	136.6	2,189	5.7	129.2	2,071	93
6	FDR-PC	135.7	2,174	5.8	128.3	2,055	92
7	FDR-PC	137.6	2,204	5.6	130.3	2,087	94
8	FDR-PC	137.6	2,204	5.4	130.6	2,091	94
9	FDR-NS	138.5	2,218	5.0	131.9	2,112	99
10	FDR-NS	136.2	2,182	5.0	129.7	2,078	97

¹ Average of two measurements per cell

Post-construction quality control strength testing was carried out on FDR-FA and FDR-EE materials sampled from the test track. No testing on sampled materials was attempted on the FDR-PC sections, due to the problems encountered during construction and the associated difficulty of collecting representative samples along the short sections. Instead, pulverized material with no stabilizer was collected from the FDR-NS lane on the test track for strength testing on laboratory prepared specimens at the actual cement contents applied at the selected HVS test section locations. Laboratory testing results are summarized in Table 3.14. The FDR-FA materials had satisfactory strengths. The FDR-EE materials had low strengths as expected, given the problems observed during construction. Realistic FDR-PC strengths were obtained on the materials from Cell #5. Very high strengths were obtained on the materials used in Cells #6, #7, and #8, as expected. Consequently, it was decided that no further laboratory or accelerated loading tests would be undertaken on these sections given that they were not representative of typical FDR-PC pavements.

Table 3.14: Result of Quality Control Strength Tests

Cell		Indirect Tensile Strength		Unconfined Compressive Strength	
		(psi)	(kPa)	(psi)	(MPa)
3b	FDR-EE (W)	43	296	–	–
4a	FDR-FA (E)	105	725	–	–
4b	FDR-FA (W)	107	738	–	–
5	FDR-PC	–	–	440	3.0
6	FDR-PC	–	–	>900	>6.0
7	FDR-PC	–	–	>900	>6.0
8	FDR-PC	–	–	>900	>6.0
1	FDR-NS	Not Tested			
2	FDR-NS				
3a	FDR-EE (W)				
9	FDR-NS				
10	FDR-NS				

3.6 Asphalt Concrete Surfacing

3.6.1 Material Properties

Dense-graded asphalt concrete was sourced from the Teichert Perkins Asphalt Plant in Sacramento, California. Key material design parameters are summarized in Table 3.15. The material met Caltrans specifications for Type A hot-mix asphalt (HMA) with three-quarter inch (19 mm) aggregate gradation and contained 15 percent reclaimed asphalt pavement (RAP).

Table 3.15: Key HMA Mix Design Parameters

Parameter	Wearing Course	
	Actual	Compliance
Grading: 1" (25 mm)	100	100
3/4" (19 mm)	99	94 – 100
1/2" (12.5 mm)	85	94 – 100
#4 (4.75 mm)	49	44 – 58
#8 (2.36 mm)	32	31 – 41
#30 (600 µm)	18	16 – 24
#200 (75 µm)	4	3 – 7
Asphalt binder grade	PG 64-16	–
Asphalt binder content (% by aggregate mass)	4.8	–
Hveem stability at optimum bitumen content	37.0	>37
Air-void content (%)	4.9	2 – 6
Voids in mineral aggregate (LP-2) (%)	13.8	>13
Voids filled with asphalt (LP-3) (%)	64.9	65 – 75
Sand equivalent (%)	72.0	>47
Specific gravity (compacted, Gmb)	2.451	–
Specific gravity (Max, Gmm)	2.576	–

3.6.2 Prime Coat Application

Prime coat was applied on October 15, 2012, 18 days after the full-depth reclamation. Prior to prime coat application, the test track surface was broomed to remove all loose material (Figure 3.34). The FDR-EE

section appeared darker and to have a higher moisture content than the other sections (Figure 3.35), and the surface was easily dented with a hammer blow.



Figure 3.34: Broomed surface of FDR-NS layer.



Figure 3.35: Broomed surface of FDR-EE layer showing dark, moist surface.

An SS-1H asphalt emulsion prime coat was applied to the surface at a rate of 0.15 gal/yd² (0.68 L/m²). Although a consistent application was achieved (Figure 3.36), some differential penetration was observed, which was attributed to patches of near-surface moisture.



Figure 3.36: Prime coat application.

3.6.3 Asphalt Concrete Placement

Asphalt concrete was placed on November 14, 2012, 30 days after application of the prime coat. This extended period between the two activities resulted from a delay in approval to pave, and thereafter because of cold or wet weather.

Construction started at approximately 8:30 a.m. Ambient air temperature was 45°F (7°C) and the relative humidity was 86 percent. Construction was completed at approximately 11:00 a.m., when ambient temperature was 55°F (13°C) and the relative humidity was 70 percent.

Mix was transported using end-dump trucks. Paving was carried out in a west-east direction and followed conventional procedures (Figure 3.37). Work started in Lane #1, followed by Lanes #2, #3, and #4. The second lift on Lane #1 (Cell #2) was placed after completion of the first lift on the other lanes. A breakdown roller closely followed the paver, applying about four passes. A single pass was made with an intermediate rubber-tired roller, followed by another four passes with a finish roller. Compaction of the lower lift appeared to be consistent and no problems were noted (Figure 3.38). On the second lift placed in Cell #2, the mix appeared tender and some shearing was noted (Figure 3.39) in the vicinity of the instrumentation cables (discussed in Section 4.4).



Figure 3.37: Asphalt concrete placement.



Figure 3.38: First lift of asphalt concrete after compaction.



Figure 3.39: Second lift of asphalt concrete showing shearing over instrumentation cables.

3.6.4 Construction Quality Control

Compaction was measured by the UCPRC using a nuclear gauge on the day of construction using the mix design specific gravity values. Measurements were taken at 60 ft (18 m) intervals along the centerline of each lane, with a focus on checking densities in the areas to be used for HVS testing. A summary of the results is provided in Table 3.16. The results indicate that there was some variability in the measurements in the first lift, but that satisfactory compaction had been achieved. Density measurements were generally lower on the second lift and were attributed to tenderness in the mix and problems with shearing in the vicinity of the instrumentation cables.

Table 3.16: Summary of Asphalt Concrete Density Measurements

Position	Lane #1, First Lift			Lane #1, Second Lift		
	Gauge		Relative	Gauge		Relative
	lb/ft ³	kg/m ³	lb/ft ³	lb/ft ³	kg/m ³	(%)
1	146.0	2,339	92.8	141.6	2,269	90.0
2	145.3	2,328	92.4	142.5	2,283	91.0
3	147.8	2,367	93.9	142.3	2,280	90.5
4	143.0	2,290	90.9	–	–	–
5	146.1	2,341	92.9	–	–	–
6	146.5	2,346	93.1	–	–	–
Average	145.8	2,335	92.7	142.1	2,277	90.5
Std. Dev.	1.6	25.6	1.0	0.5	7.4	0.5
RICE	2.520					

Temperatures were systematically measured throughout the placement of the asphalt concrete using infrared temperature guns, thermocouples, and an infrared camera. Average mix temperature behind the paver screed was 297°F (147°C). Temperatures at the start and completion of rolling were 295°F (146°C) and 141°F (61°C), respectively.

A thermal camera image (*FLIR Systems ThermoCAM PM290*) of the mat behind the paver is presented in Figure 3.40 and clearly shows consistent temperature across the mat.

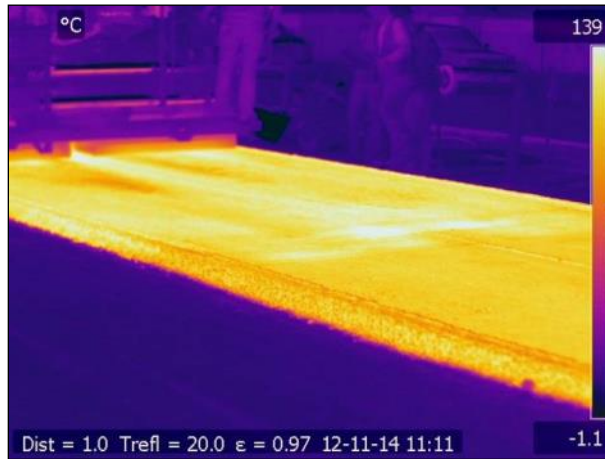


Figure 3.40: Thermal image of test track during construction.

Thickness was monitored with probes by the paving crew throughout the construction process. The thicknesses of cores removed for laboratory testing after construction were measured for quality control purposes. Average thickness of the first lift was 2.6 in. (67 mm). The second lift, placed only in Cell #2, had an average thickness of 2.5 in. (64 mm).

3.6.5 As-Built Layer Thicknesses

As-built layer thicknesses were determined using different methods depending on the layer type. Asphalt concrete layer thicknesses were determined from cores taken near the test section, as described in Section 3.7, and from the cores taken while drilling the instrumentation (multi-depth deflectometer) boreholes. The as-built HMA layer thicknesses for the two test sections are listed in Table 3.17.

Table 3.17: As-Built HMA Layer Thicknesses

Section	Bottom Lift		Top Lift	
	(in.)	(mm)	(in.)	(mm)
FDR-NS (60 mm)	2.5	64	–	–
FDR-NS (120 mm)	2.5	64	2.5	64
FDR-EE	2.6	67	–	–
FDR-FA	2.5	63	–	–
FDR-PC	2.6	67	–	–

Base thicknesses were determined from Dynamic Cone Penetration (DCP) measurements taken in the holes after cores were removed in the sampling area. On the unstabilized sections (FDR-NS), both the recycled and remaining original base layers were assessed. On the stabilized sections, the recycled layer was removed in the core and only the remaining original base layers were assessed. The DCP penetration

curves for the unstabilized (FDR-NS) and stabilized (FDR-EE, FDR-FA, and FDR-PC) sections are shown in Figure 3.41 and Figure 3.42, respectively. Layer interfaces are indicated by the changes in penetration rate. The following observations were made:

- FDR-NS: Tests were done on both the 60 mm and 120 mm thick asphalt concrete sections. Only one distinct change was noted in the penetration rate. This was at approximately 20 in. (500 mm) below the bottom of the asphalt concrete layer, corresponding to the interface between the original base and the subgrade. This indicates that the recycled base and old aggregate base layer had similar mechanical properties. The combined as-built thickness was comparable to the 22.5 in. (570 mm) design thickness.
- FDR-EE, FDR-FA, and FDR-PC: Measurements were consistent with those taken on the FDR-NS sections, with a distinct change between the base and subgrade at approximately 20 in. (500 mm) below the bottom of the asphalt concrete layer.

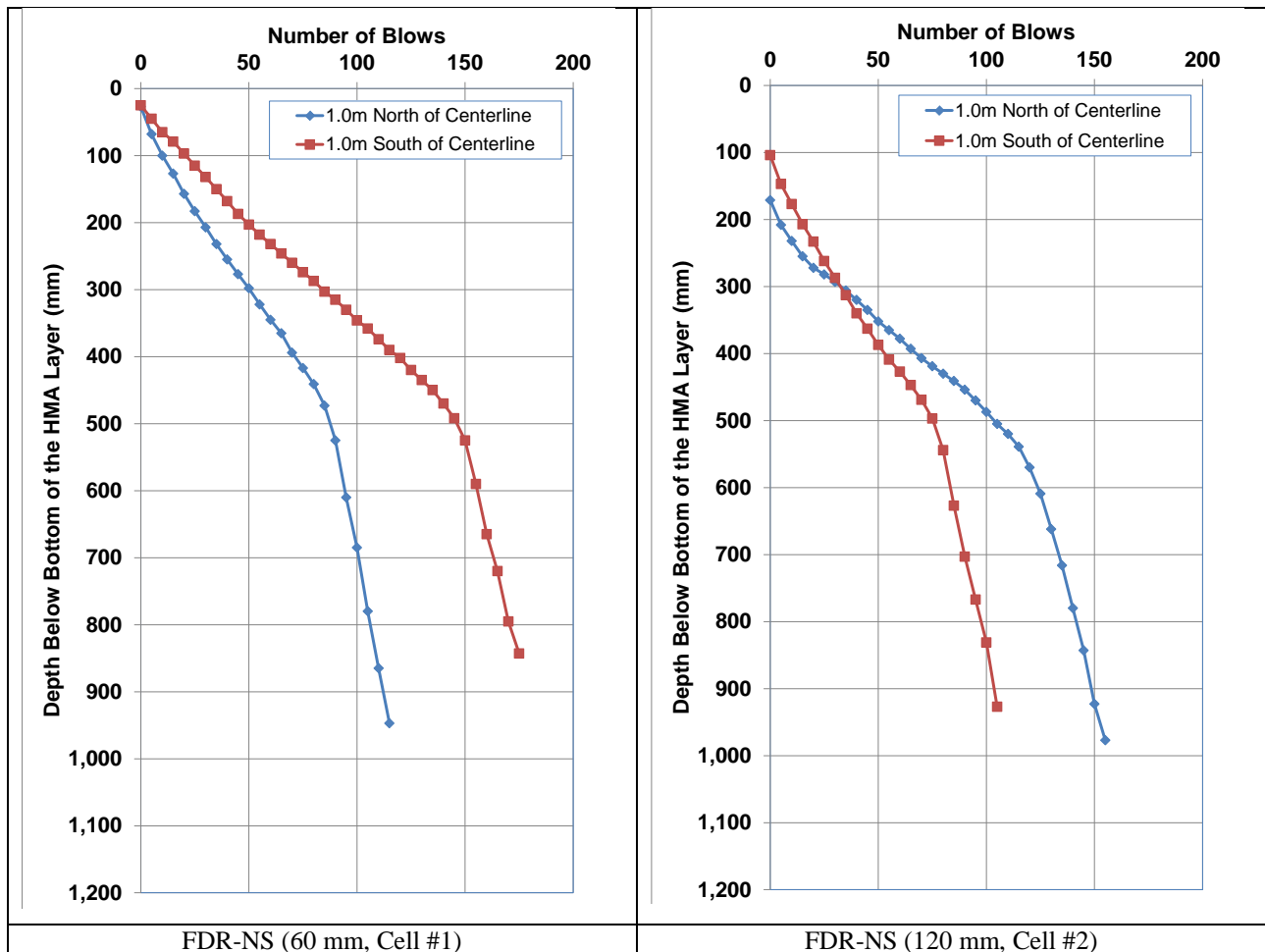


Figure 3.41: Unbound layer DCP penetration curves for unstabilized sections.

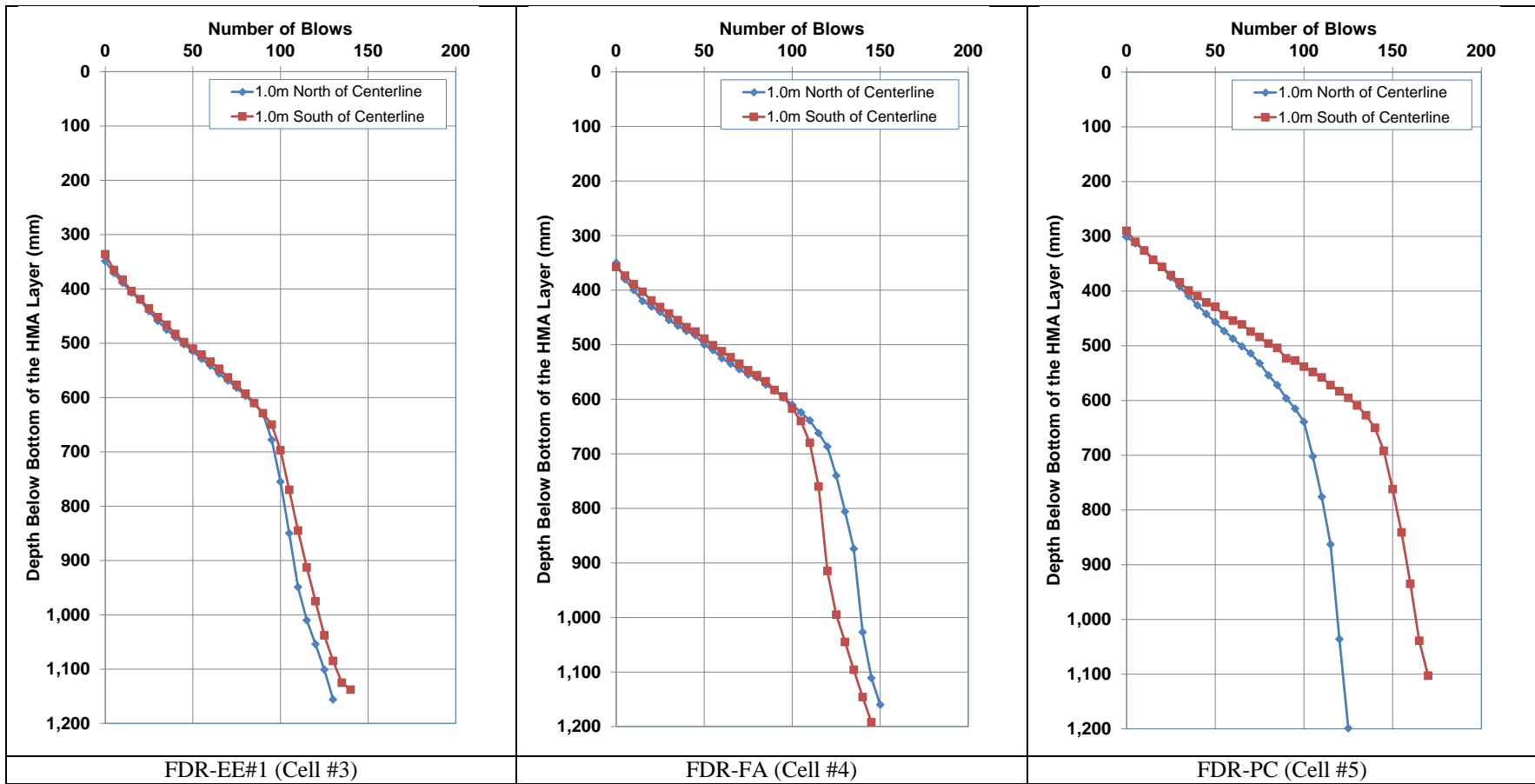


Figure 3.42: Unbound layer DCP penetration curves for stabilized sections.

3.7 Material Sampling

Specimens in the form of 6.0 in. (152 mm) diameter cores and slabs 20 in. by 10 in. (500 mm by 250 mm) were sawn from each section adjacent to the planned HVS test sections for laboratory testing, as shown in Figure 3.43. Slabs were sawn to the bottom of the asphalt concrete layer(s), extracted, stored on pallets, and then transported to the UCPRC Richmond Field Station laboratory. Inspection of the slabs indicated that the asphalt concrete was well bonded to the top of the base-course material, and that the two asphalt layers on the FDR-NS (120 mm) section were well bonded to each other.

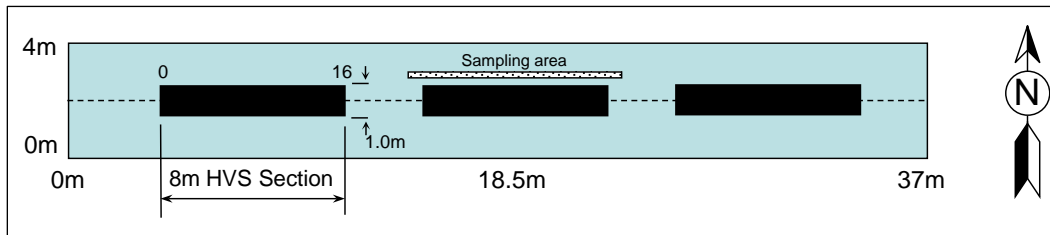


Figure 3.43: Sampling location for laboratory specimens.

3.8 Construction Summary

Key observations from the test track construction process include:

- Based on the results of testing rubberized warm-mix asphalt in a previous study on the UCPRC North Track, it was concluded that preparation of the subgrade and construction of the original base during that study resulted in a generally consistent subgrade and base platform for the FDR study.
- Conventional FDR construction procedures were followed on the FDR-NS lane. Recycling depth was well controlled and the pulverized material had a consistent grading and uniform moisture content. No problems were observed with recycling the relatively new asphalt concrete surface (i.e., limited aging), although some smoke was observed as the cutting teeth milled through the rubberized layer. Satisfactory compaction and a satisfactory surface finish were achieved on the recycled layer.
- Numerous problems were encountered during construction of the FDR-EE lane, including the addition of too much water, blocked nozzles leading to uneven and under- or over-application of asphalt emulsion, which all resulted in uneven compaction.
- Construction of the FDR-FA section followed conventional procedures and no problems were observed. The cement was evenly distributed at the correct application rate and good mixing of the foamed asphalt and cement was achieved. The recycled material had a consistent grading and uniform moisture content. Satisfactory compaction and a satisfactory surface finish were achieved.
- The spread rate of the cement on the FDR-PC section was not well controlled, which led to excess cement being applied. Problems with mixing resulted from this excess cement. Only part of one lane was considered suitable for HVS testing.
- Gradations for the pulverized material on all four lanes were well within the specified limits.

- Densities after compaction met or exceeded the specification on the FDR-NS and FDR-FA lanes, but were slightly lower than specification on the FDR-PC and FDR-EE lanes. The lower than specification densities were attributed to the construction problems on both lanes and, on the FDR-PC lane, to the generalization of the laboratory reference density, given that reference densities were not determined for the range of cement contents actually applied on the day of construction.
- Placement of the hot-mix asphalt followed conventional procedures. Thickness and compaction appeared to be consistent across the test track.

The FDR-NS and FDR-FA lanes and one section of the FDR-PC lane (5 percent measured cement content) were considered satisfactorily uniform for the purposes of accelerated pavement testing. The FDR-EE and the remainder of the FDR-PC sections were not considered representative of typical FDR construction with these stabilization strategies.

4. TRACK LAYOUT, INSTRUMENTATION, AND TEST CRITERIA

4.1 Testing Protocols

The Heavy Vehicle Simulator (HVS) test section layout, test setup, trafficking, and measurements followed standard University of California Pavement Research Center (UCPRC) protocols (51).

4.2 Test Track Layout

The FDR test track layout is shown in Figure 4.1. Two HVS test sections were demarcated in each lane, the first for testing under dry conditions and the second for testing under soaked conditions (this latter testing will take place in Phase 2). Test section locations were selected to ensure that they did not overlap previously tested areas on the original test track. All test sections were located along the centerline of the lane. The section numbers were allocated in order of testing sequence as follows (HB and HC refers to the specific HVS equipment used for testing):

- Section 672HB: FDR-NS (60 mm asphalt concrete)
- Section 673HB: FDR-FA
- Section 674HB: FDR-PC
- Section 675HC: FDR-EE (test #1)
- Section 676HC: FDR-EE (test #2)
- Section 677HC: FDR-NS (120 mm asphalt concrete)

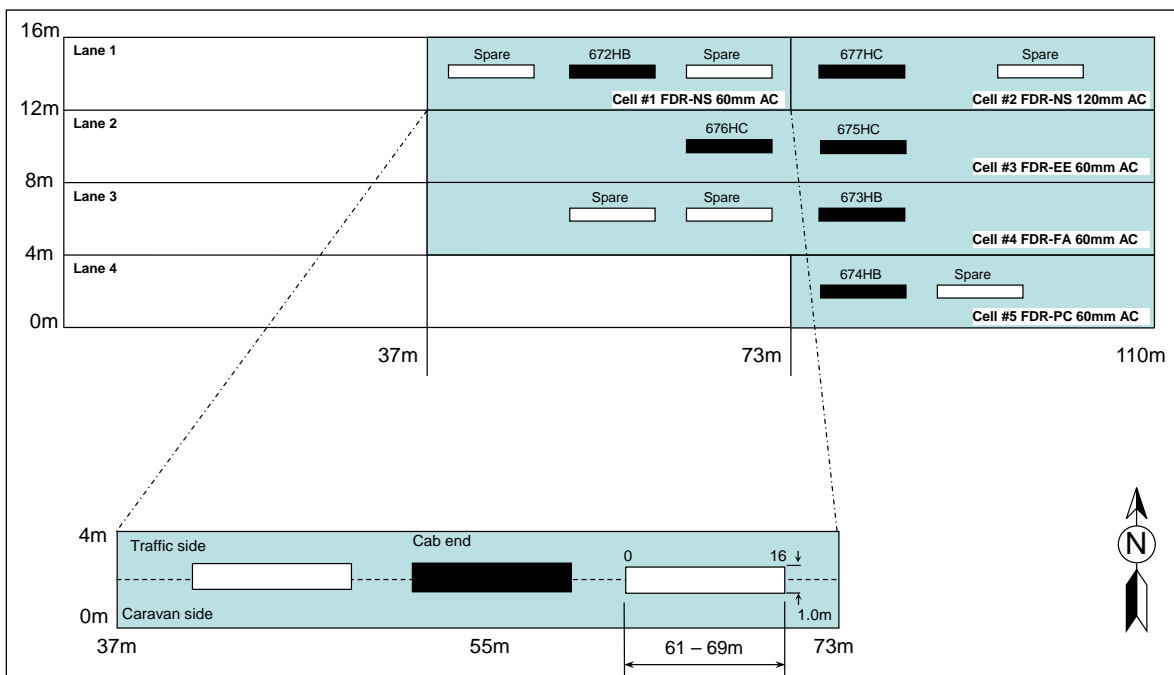


Figure 4.1: Test track layout.

4.3 HVS Test Section Layout

An HVS test section is 26.2 ft (8.0 m) long and 3.3 ft (1.0 m) wide. A schematic in Figure 4.2 shows an HVS test section along with the stationing and coordinate system. Station numbers (0 to 16) refer to fixed points on the test section and are used for measurements and as a reference for discussing performance. Stations are placed at 1.6 ft (0.5 m) increments. A sensor installed at the center of the test section would have an x -coordinate of 4,000 mm and a y -coordinate of 500 mm.

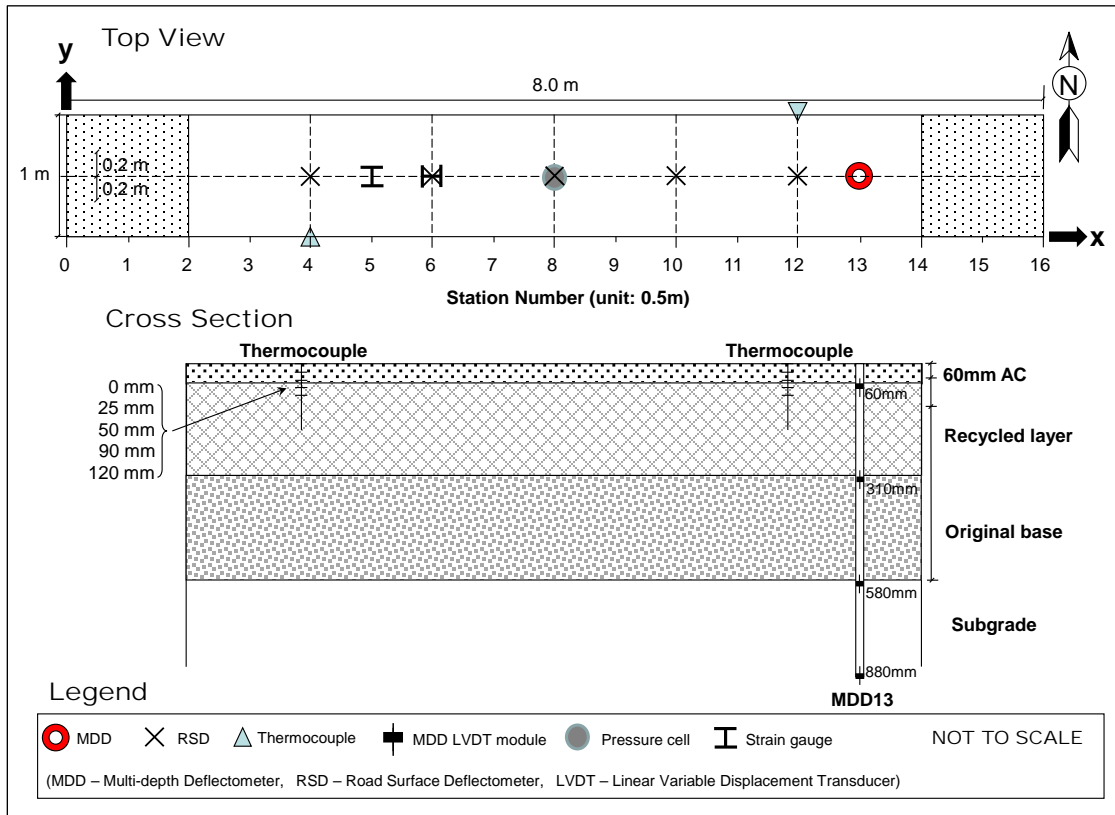


Figure 4.2: Schematic of an HVS test section.

4.4 Test Section Instrumentation

Measurements were taken with the equipment and instruments listed below. Instrument positions are shown in Figure 4.2.

- A laser profilometer was used to measure surface profile; measurements were taken at each station.
- A road surface deflectometer (RSD) was used to measure surface deflection during the test. RSD measurements were taken under a creep-speed 40 kN load at regular intervals. Note that RSD measurements under a creep-speed load will not be the same as those recorded under the trafficking speed load. After load changes, deflections were measured under the new load, as well as under the previous lighter loads. Only the results from testing under the 40 kN load are discussed in this report.

- A falling weight deflectometer (FWD) was used to measure surface deflection on the section before and after HVS testing to evaluate the change in stiffness caused by trafficking. Testing was undertaken on both the trafficked and adjacent untrafficked areas (i.e., 5 m on either end of the 8 m test section) at 500 mm (19.7 in.) intervals. Two sets of tests were undertaken on each day to obtain a temperature range for backcalculation of layer stiffnesses.
- Type-K thermocouples were used to measure pavement and air temperatures (both inside and outside the temperature chamber). Five thermocouples were bundled together to form a “thermocouple tree” for measuring air, pavement surface, and pavement layer temperatures inside the environmental chamber. Pavement layer temperatures were measured at 25 mm, 50 mm, 90 mm, and 120 mm (1 in., 2 in., 3.5 in., and 4.7 in.). Air temperatures were measured with thermocouples attached to the outside walls of the environmental chamber (at least one thermocouple was unshaded during the day). Additional air temperatures were recorded at a weather station at the northwest end of the test track.
- Two *Tokyo Sokki Kenkyujo Inc. KM100-HAS* 350 Ω full bridge strain gauges were installed on each test section, one positioned to measure transverse strain under the moving wheel, and the second positioned to measure longitudinal strain. A paste prepared by mixing sand and asphalt emulsion was used to attach the gauges to the surface of the recycled layer after the prime coat had been applied and had cured (Figure 4.3).
- One *GeoKon 3500-3* pressure cell was installed level with the surface of the recycled layer on each test section (Figure 4.4) to measure vertical pressure (stress) under the moving wheel.



Figure 4.3: Strain gauge installation.



Figure 4.4: Pressure cell installation.

- One multi-depth deflectometer (MDD), which is essentially a stack of linear variable differential transformer (LVDT) modules fixed at different depths in a single borehole, was installed on each test section. The LVDT modules have nonspring-loaded core slugs that are linked together into one long rod that is fixed at the bottom of a 10 ft (3.3 m) borehole. The LVDT modules are fixed to the pavement, which allows permanent vertical deformations at various depths to be recorded, in addition to measurement of the elastic deformation caused by the passage of the HVS wheels. The borehole is 1.5 in. (38 mm) in diameter. A model MDD with five modules is shown in Figure 4.5.



Figure 4.5: A model multi-depth deflectometer (MDD), showing five modules.

4.5 Test Section Measurements

4.5.1 Temperature

Pavement temperatures were controlled using a temperature control chamber. Both air (inside and outside the temperature box) and pavement temperatures were monitored and recorded hourly during the entire loading period. In assessing rutting performance, the temperature at the bottom of the asphalt concrete and the temperature gradient are two important controlling temperature parameters that influence the stiffness of the asphalt concrete and are used to compute plastic strain.

4.5.2 Surface Profile

The following rut parameters were determined from laser profilometer measurements:

- Maximum total rut depth at each station
- Average maximum total rut depth for all stations
- Average deformation for all stations
- Location and magnitude of the maximum rut depth for the section
- Rate of rut development over the duration of the test

The difference between the surface profile after HVS trafficking and the initial surface profile before HVS trafficking is the permanent change in surface profile. Based on the change in surface profile, the maximum total rut is determined for each station, as illustrated in Figure 4.6. The average maximum total rut for the section is the average of all of the maximum total ruts measured between Stations 3 and 13.

4.5.3 Strain

The strain gauges were connected to a *National Instruments NI cDAQ-9237* module. A virtual channel was created for each strain gauge using the *Measurement and Automation Explorer (NI-MAX)* software provided by National Instruments. The strain gauge virtual channel readings were determined as:

$$\text{Strain} = -\frac{V_r}{GF} = -\frac{V_r}{0.5} = -2V_r \quad (4.1)$$

Where: *Strain* is the output of the virtual channel,
GF is the gauge factor in the virtual channel setting, and
V_r is the ratio between output and input voltages of the Wheatstone bridge inside the strain gauge.

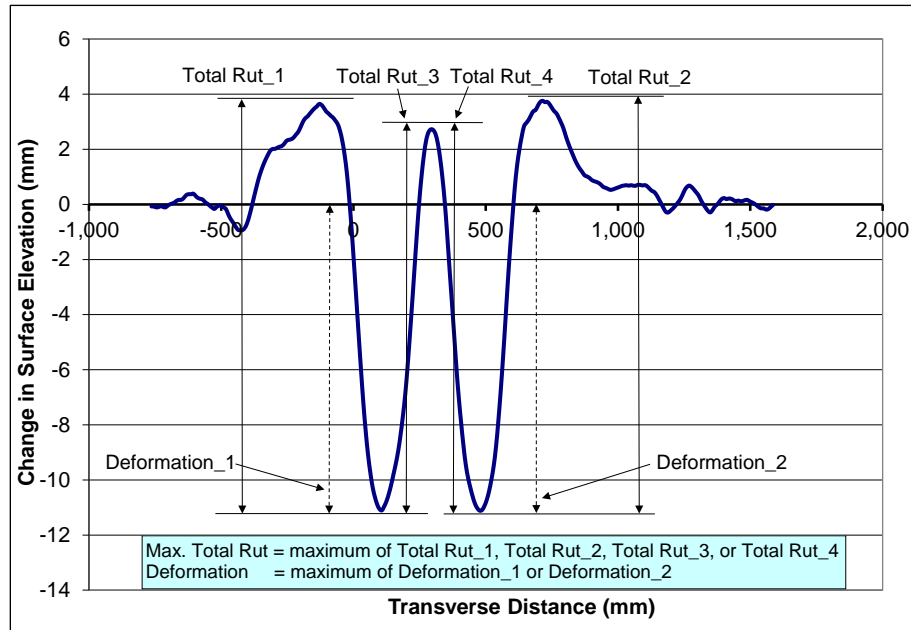


Figure 4.6: Illustration of maximum rut depth and deformation for a leveled profile.

A gauge factor (GF) of 0.5 was used to configure the virtual channel to accommodate the *Tokyo Sokki* calibration coefficient (C_e , [average calibration coefficient of 0.830 was provided by the instrument manufacturer]) for each gauge based on the assumption that the voltage ratio (V_r) is multiplied by 2.0 when converting to strain. The data acquisition software converts the virtual channel reading into microstrain by multiplying it by -0.830×10^6 . The negative sign is necessary to ensure that tensile strain increases with increasing load repetitions.

Strain readings were recorded and loaded into a database where the actual calibration coefficients for each specific strain gauge are stored. When data is extracted from the database, the necessary minor rescaling is built into the query to ensure that the individual gauge factors are used in place of the average value of 0.830.

Example strain data recorded from one of the strain gauges is presented in Figure 4.7, which shows the variation of the strain gauge reading versus wheel position as the wheel travels from one end of the test section to the other. Several quantities are summarized based on the raw readings. Specifically, the reference value is the reading when the wheel is at the far end of the test section. The peak and valley are maximum and minimum values deviating from the reference value, respectively.

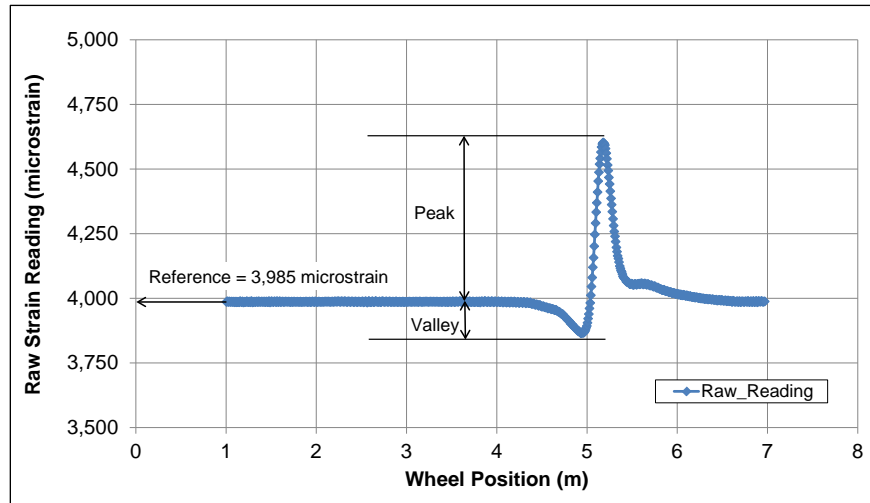


Figure 4.7: Example strain reading and definition of summary quantities.

4.5.4 Pressure

Example data recorded from one of the pressure cells is shown in Figure 4.8. Variation of the pressure reading versus wheel position as the wheel travels from one end of the test section to the other is clearly evident. Several quantities can be summarized from the raw readings, with reference, maximum, and minimum values derived in the same way as that described for strain in Section 4.5.3.

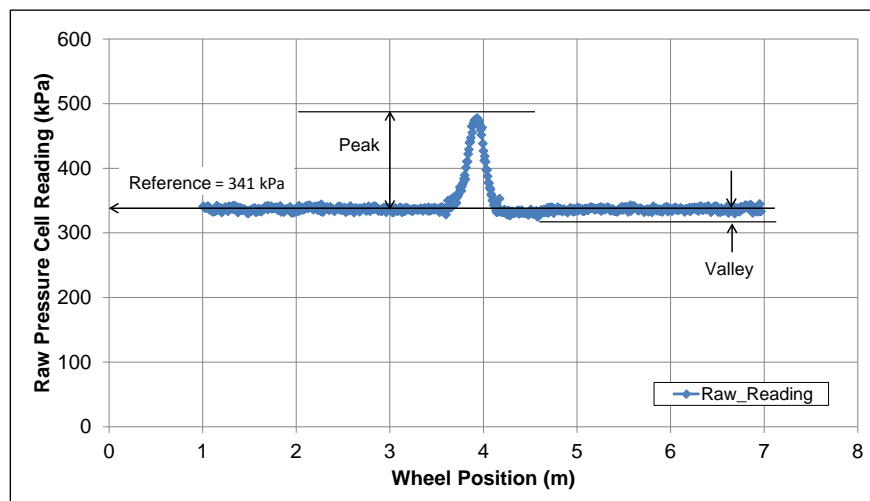


Figure 4.8: Example pressure cell reading and definition of summary quantities.

4.5.5 Elastic Vertical Deflection

An example set of MDD data is presented in Figure 4.9, which shows the variation of the elastic vertical deflections measured at different depths versus wheel position as the wheel travels from one end of the test section to the other. The elastic vertical deflection is the difference between the total vertical

deflection and the reference value, which is the measurement recorded when the wheel is at the far end of the test section. The peak values are the maximum elastic vertical deflection for each individual MDD module.

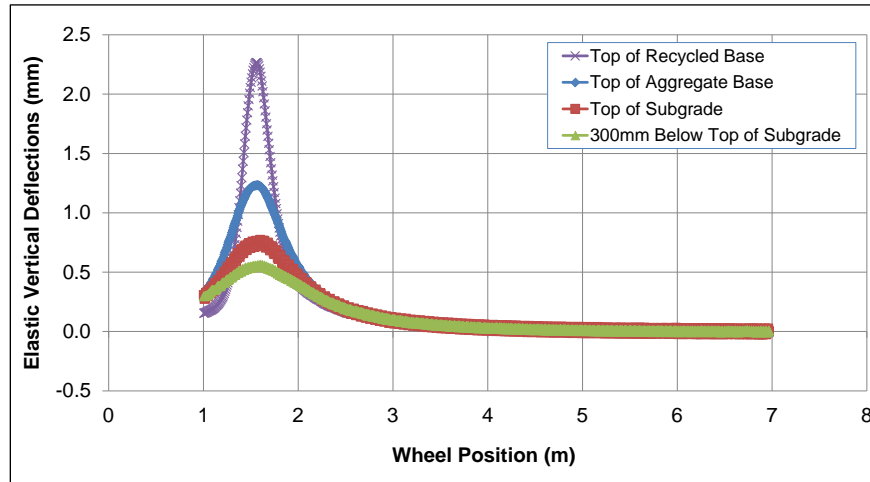


Figure 4.9: Example elastic vertical deflection measured with MDD.

4.6 Phase 1 HVS Test Criteria

4.6.1 Test Section Failure Criteria

An average maximum rut depth of 12.5 mm (0.5 in.) and/or an average crack density of 2.5 m/m² (0.8 ft/ft²) over the full monitored section (Station 3 to Station 13) were set as the failure criteria for the experiment. In some instances, HVS trafficking was continued past these points so the rutting and/or cracking behavior of a test section could be fully understood.

4.6.2 Phase 1 Environmental Conditions

The pavement temperature at 50 mm (2.0 in.) pavement depth was maintained at 30°C±4°C (86°F±7°F) to assess both rutting and cracking potential in the recycled layer under typical pavement conditions. This temperature was considered appropriate for testing the performance of the recycled base. Lower or higher asphalt temperatures could have led to premature cracking or rutting failure of the asphalt concrete, respectively.

Infrared heaters or a chilling unit inside the HVS environmental chamber were used to maintain the pavement temperature. The sections were tested predominantly during dry conditions (2013 was a severe drought year in California), with small amounts of infrequent rainfall recorded during all but one of the tests (FDR-EE#2 [675HC], see Section 5.2). No significant rainfall events occurred and the test sections received no direct rainfall as they were protected by the environmental chamber.

4.6.3 Phase 1 Test Duration

HVS trafficking on each section was initiated and completed as shown in Table 4.1. The sequence of testing was adjusted to accommodate positioning of the two HVS machines on the test sections (i.e., the machines could not test side-by-side on the test track configuration because of space limitations).

Table 4.1: Test Duration for Phase 1 HVS Rutting Tests

Section No.	Stabilization Strategy	Test Sequence	Start Date	Finish Date	Repetitions
672HB	FDR-NS (60 mm)	1	02/05/2013	03/24/2013	713,000
673HB	FDR-FA	2	04/09/2013	06/27/2013	1,000,000
674HB	FDR-PC	4	08/01/2013	11/06/2013	1,560,565
675HC	FDR-EE (Test #1)	5	10/07/2013	10/12/2013	61,500
676HC	FDR-EE (Test #2)	6	10/30/2013	11/07/2013	120,000
677HC	FDR-NS (120 mm)	3	06/07/2013	09/16/2013	1,080,100

4.6.4 Phase 1 Loading Program

The HVS loading program for each section is summarized in Table 4.2. Equivalent Standard Axle Loads (ESALs) were determined using the following Caltrans conversion (Equation 4.1):

$$\text{ESALs} = (\text{axle load}/18,000)^{4.2} \quad (4.1)$$

Table 4.2: Summary of Phase 1 HVS Loading Program

Section	Stabilization Strategy	Wheel Load ¹ (kN)	Repetitions	ESALs ²	Test to Failure
672HB	FDR-NS (60 mm)	40	315,000	315,000	Yes
		60	200,000	1,098,028	
		80	198,000	3,639,076	
Section Total			713,000	5,052,104	
673HB	FDR-FA	40	315,000	315,000	No
		60	200,000	1,098,028	
		80	250,000	4,594,793	
		100	235,000	11,025,947	
Section Total			1,000,000	17,033,768	
674HB	FDR-PC	40	315,000	315,000	No
		60	200,000	1,098,028	
		80	250,000	4,594,793	
		100	795,565	37,327,053	
Section Total			1,560,565	43,334,874	
675HC	FDR-EE (Test #1)	40	61,500	61,500	Yes
Section Total			61,500	61,500	
676HC	FDR-EE (Test #2)	40	120,000	120,000	Yes
Section Total			120,000	120,000	
677HC	FDR-NS (120 mm)	40	315,000	315,000	Yes
		60	200,000	1,098,028	
		80	250,000	4,594,793	
		100	315,100	14,784,153	
Section Total			1,080,100	20,791,974	
Project Total			4,535,165	86,394,220	

¹ 40 kN = 9,000 lb.; 60 kN = 13,500 lb.; 80 kN = 18,000 lb.; 100 kN = 22,500 lb

² ESAL: Equivalent Standard Axle Load

All trafficking was carried out with a dual-wheel configuration, using radial truck tires (Goodyear G159 - 11R22.5- steel belt radial) inflated to a pressure of 720 kPa (104 psi), in a bidirectional loading mode with wander (i.e., trafficking in both directions in line with standard procedures for testing base layer performance). Load was checked with a portable weigh-in-motion pad at the beginning of each test, after each load change, and at the end of each test.

Blank page

5. PHASE 1 HVS TEST DATA SUMMARY

5.1 Introduction

This chapter provides a summary of the data collected from the six HVS tests (Sections 672HB through 677HC) and a brief discussion of the first-level analysis. Data collected includes:

- Rainfall
- Air temperatures outside and inside the temperature control chamber
- Pavement temperatures at 0 mm, 25 mm, 90 mm, and 120 mm below the surface
- Surface permanent deformation (rutting)
- Transverse and longitudinal strain at the top of the recycled layer (i.e., bottom of the asphalt concrete surfacing)
- Pressure (stress) at the top of the recycled layer
- Elastic vertical deflection at the top of the recycled layer, top of the original base layer, and top of the subgrade
- Permanent deformation at the top of the recycled layer, top of the original base layer, and top of the subgrade
- Pavement deflection and layer stiffnesses

5.2 Rainfall

Figure 5.1 shows the monthly rainfall data from January 2013 through December 2013 as measured at the weather station next to the test track. Some rainfall was recorded during all the tests except during the test on FDR-EE#1 (675HC). However, rainfall amounts were very small. There were no high rainfall events during the year.

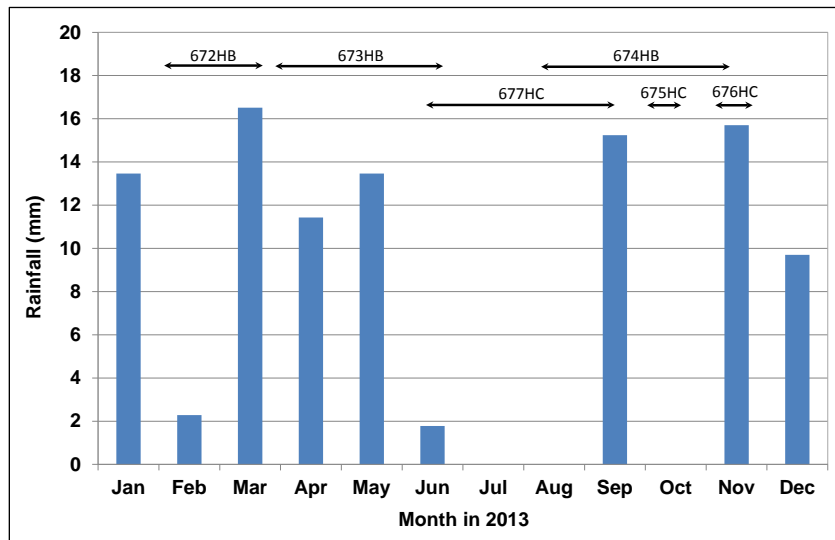


Figure 5.1: Measured rainfall during Phase 1 HVS testing.

5.3 Section 672HB: No Stabilizer with 60 mm Surfacing (FDR-NS [60 mm])

5.3.1 Test Summary

Loading commenced with a 40 kN (9,000 lb) half-axle load on February 5, 2013, and ended with an 80 kN (18,000 lb) load on March 24, 2013. A total of 713,000 load repetitions were applied and 49 datasets were collected. Load was increased from 40 kN to 60 kN (13,500 lb) and then to 80 kN (18,000 lb) after 315,000 and 515,000 load repetitions, respectively. No breakdowns occurred during testing on this section. The HVS loading history for Section 672HB is shown in Figure 5.2.

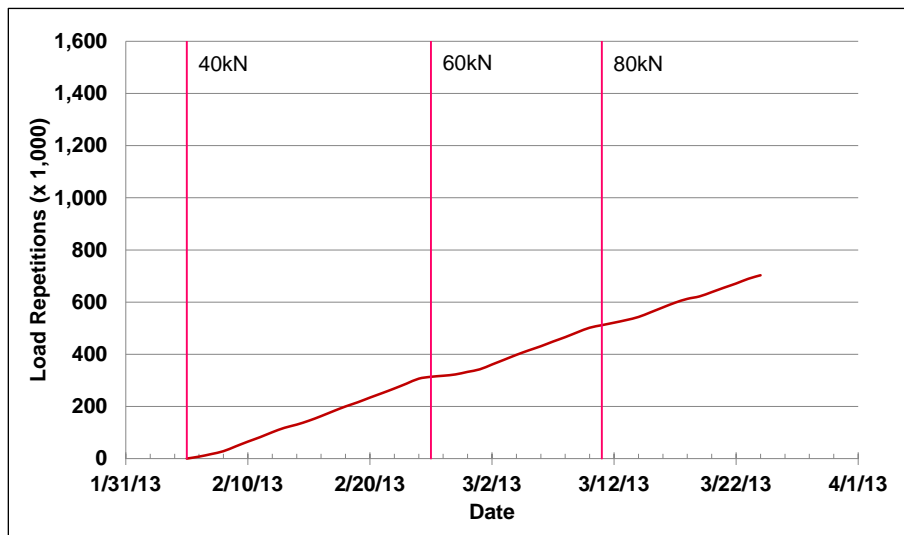


Figure 5.2: 672HB: HVS loading history.

Moisture contents in the various layers were determined on materials sampled from augur holes drilled on either side of the test section just before the start of testing. Moisture contents in the recycled layer, original aggregate base, and subgrade were 4.4, 5.0, and 15.8 percent of the dry weight of the materials, respectively.

5.3.2 Air Temperatures

Outside Air Temperatures

Daily average outside air temperatures are summarized in Figure 5.3. Vertical error bars on each point on the graph show the daily temperature range. Temperatures ranged from -0.7°C to 29°C (19°F to 84°F) during the course of HVS testing, with a daily average of 12°C (54°F), an average minimum of 5°C (41°F), and an average maximum of 20°C (68°F).

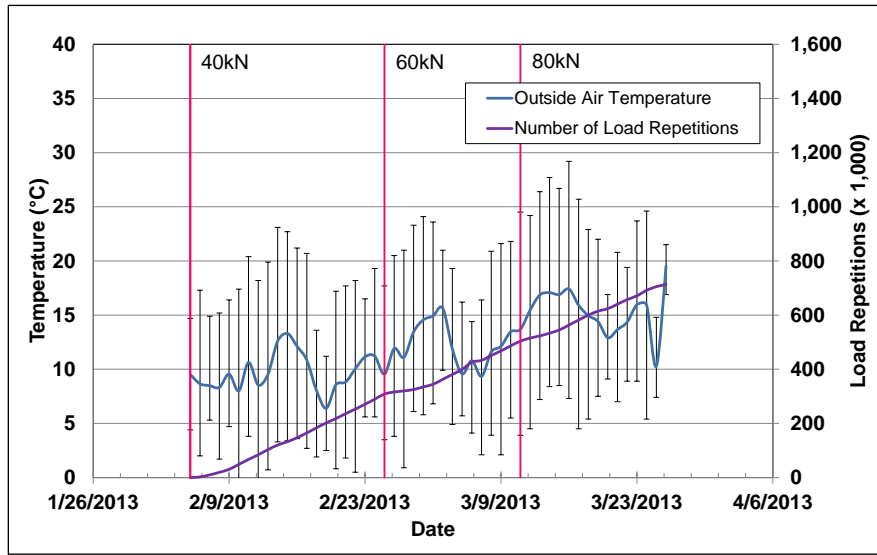


Figure 5.3: 672HB: Daily average air temperatures outside the environmental chamber.

Air Temperatures in the Environmental Chamber

During the test, air temperatures inside the temperature control chamber ranged from 14°C to 34°C (57°F to 93°F) with an average of 24°C (75°F) and a standard deviation of 1.8°C (3.2°F). Air temperature was adjusted to maintain a pavement temperature of 30°C±4°C (86°F±7°F) at a pavement depth of 50 mm (2.0 in.). The recorded pavement temperatures discussed in Section 5.3.3 indicate that the inside air temperatures were adjusted appropriately to maintain the required pavement temperature. The daily average air temperatures recorded in the environmental chamber, calculated from the hourly temperatures recorded during HVS operation, are shown in Figure 5.4. Vertical error bars on each point on the graph show the daily temperature range.

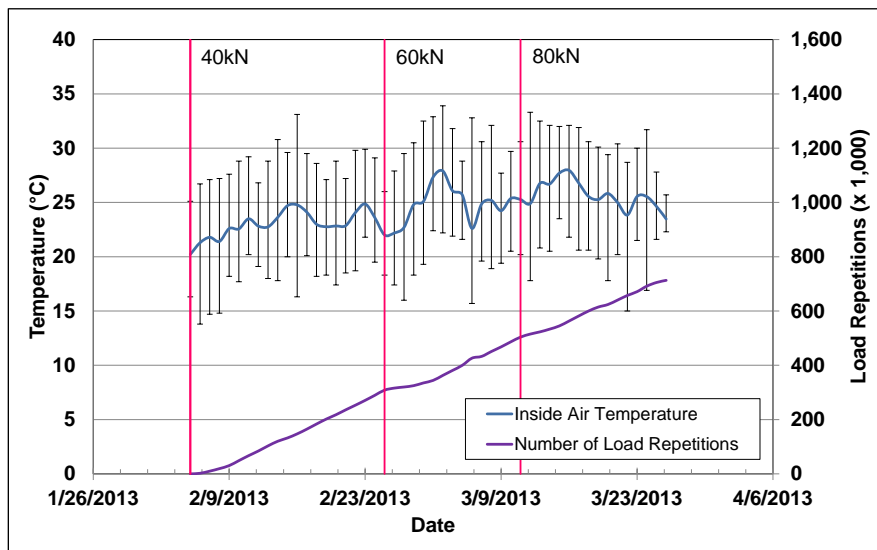


Figure 5.4: 672HB: Daily average air temperatures inside the environmental chamber.

5.3.3 Pavement Temperatures

Daily averages of the surface and in-depth temperatures of the asphalt concrete and recycled layers are listed in Table 5.1 and shown in Figure 5.5. Pavement temperatures increased slightly with increasing depth in the asphalt concrete. Temperatures in the top of the recycled layer were slightly cooler than the asphalt concrete, which was expected as there is usually a thermal gradient between the top and bottom of asphalt concrete pavement layers.

Table 5.1: 672HB: Temperature Summary for Air and Pavement

Temperature	Layer	Average (°C)	Std. Dev. (°C)	Average (°F)	Std. Dev. (°F)
Outside air	-	12	3.1	54	5.6
Inside air	-	24	1.8	75	3.2
Pavement surface	AC	29	0.6	84	1.1
- 25 mm below surface	AC	30	0.3	86	0.5
- 50 mm below surface	AC	30	0.3	86	0.5
- 90 mm below surface	FDR	29	0.4	84	0.7
- 120 mm below surface	FDR	29	0.5	84	0.9

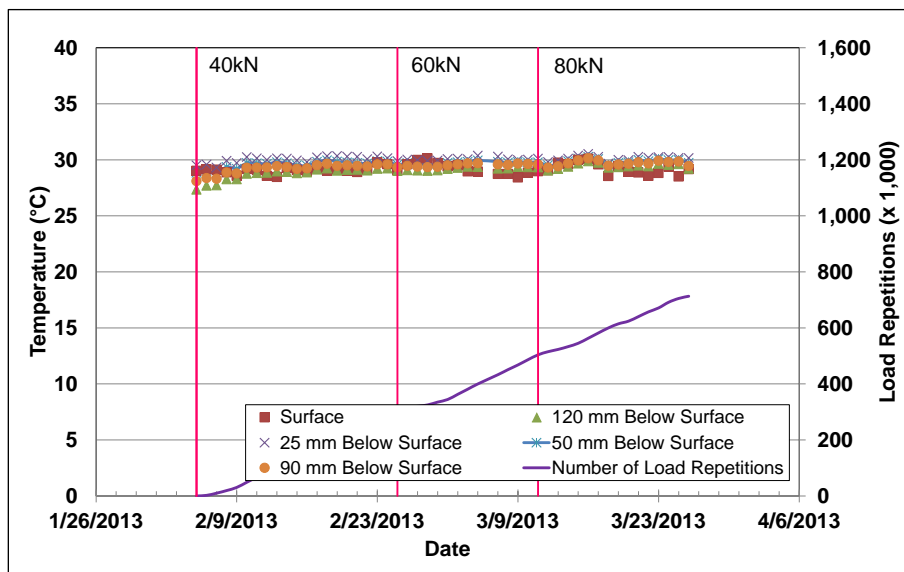


Figure 5.5: 672HB: Daily average pavement temperatures.

5.3.4 Permanent Deformation on the Surface (Rutting)

Figure 5.6 shows the average transverse cross section measured with the laser profilometer at various stages of the test. This plot clearly shows the increase in rutting and deformation over time. Figure 5.7 shows the development of permanent deformation (average maximum total rut and average deformation) with load repetitions. The two plots show that most of the deformation was in the form of a depression (i.e., deformation was below the zero elevation point at the surface [Figure 4.6]) rather than upward and outward displacement of the material above the zero elevation point.

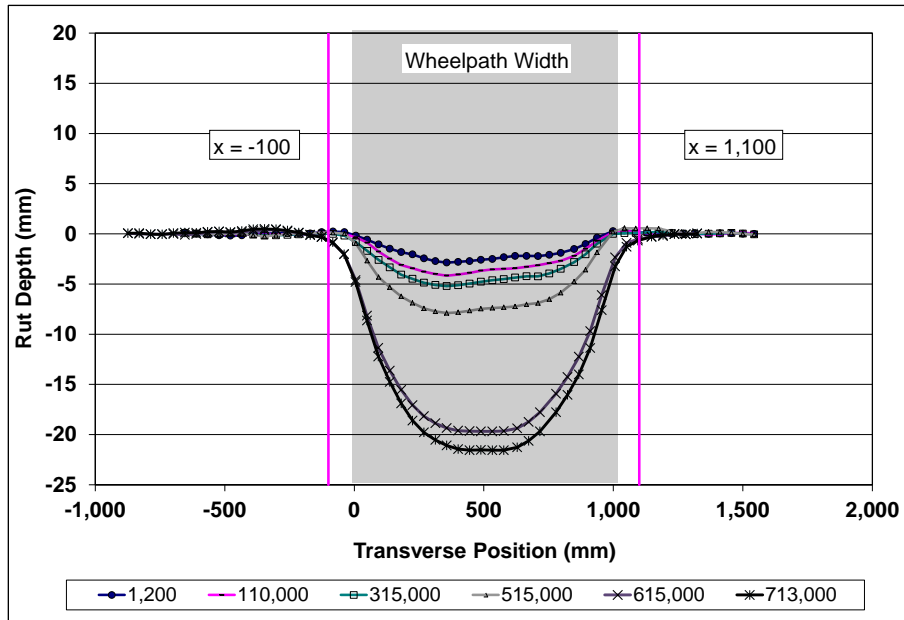


Figure 5.6: 672HB: Profilometer cross section at various load repetitions.

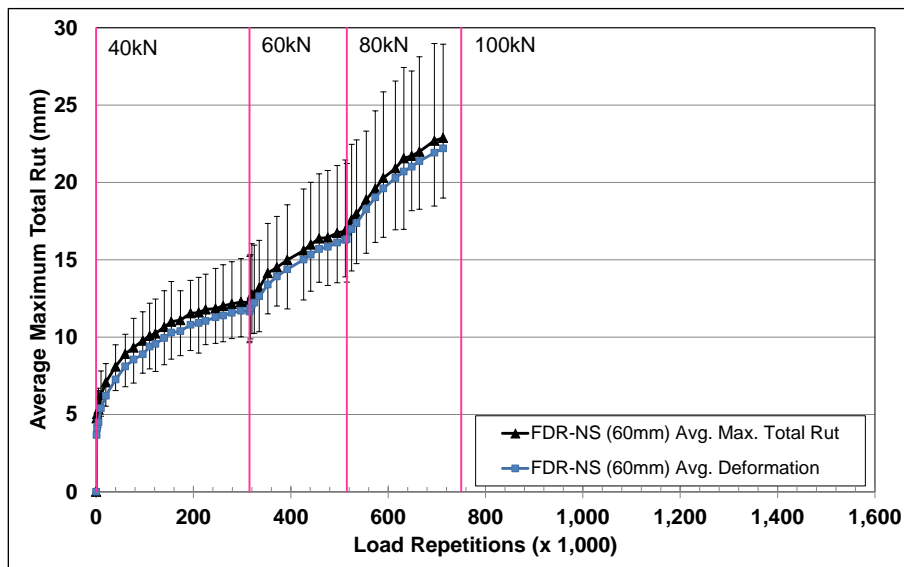


Figure 5.7: 672HB: Average maximum total rut and average deformation.

During HVS testing, rutting usually occurs at a high rate initially, and then it typically diminishes as trafficking progresses until reaching a steady state. This initial phase is referred to as the “embedment” phase. The embedment phase in this test, although relatively short in terms of the number of load repetitions (i.e., $\pm 5,000$), ended with a fairly significant early rut of about 6.0 mm (0.25 in.) that was attributed to the relatively high air-void content in the asphalt concrete, as discussed in Section 3.6.4. The rate of rut depth increase after the embedment phase was also relatively fast, which was attributed to the generally weak base (unstabilized recycled material and original base). Increases in the applied load (to

60 kN and then to 80 kN) resulted in short embedment phases after each event. The rate of rut depth increase also accelerated after both load changes. Error bars on the average maximum total rut reading indicate that there was some variation along the length of the section. Analysis of the data showed that the rut was slightly deeper between Stations 8 and 13, compared to that measured between Stations 3 and 7 (see Figure 4.2 for schematic of the test section layout).

Figure 5.8 shows contour plots of the pavement surface at the start and end of the test (713,000 load repetitions) that also indicate the deeper rut at one end of the section. Terminal rut (12.5 mm [0.5 in.]) was reached after approximately 320,000 load repetitions. However, testing was continued for approximately 400,000 additional load repetitions to further assess rutting trends at the higher loads.

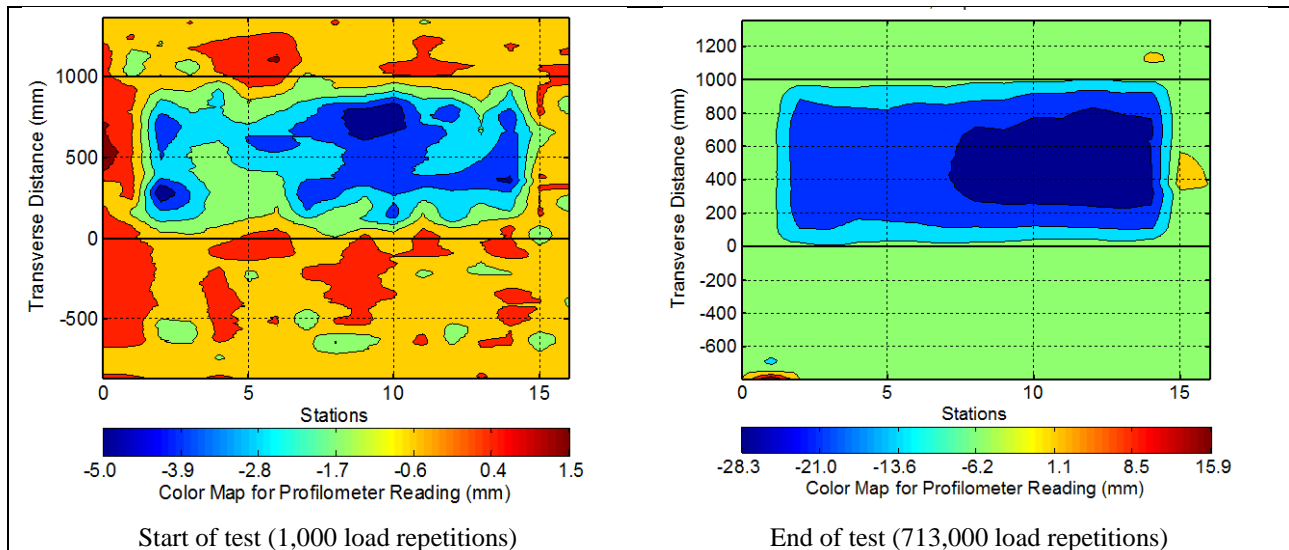


Figure 5.8: 672HB: Contour plots of permanent surface deformation.
(Note different scales in legends.)

After completion of trafficking, the average maximum rut depth and the average deformation were 22.9 mm (0.90 in.) and 22.2 mm (0.87 in.), respectively. The maximum rut depth measured on the section was 28.3 mm (1.11 in.), recorded at Station 12.

5.3.5 Permanent Deformation in the Underlying Layers

Permanent deformation in the underlying layers, recorded with a multi-depth deflectometer (MDD) at Station 13 and compared to the surface layer (laser profilometer deformation [not total rut] measurement at Station 13), is shown in Figure 5.9. The MDD measurements were consistent with the laser profilometer measurements. Deformation in each of the layers is summarized in Table 5.2. After 320,000 load repetitions, when the terminal rut for the test (average maximum total rut [12.5 mm] measured over the full section) was reached, most of the deformation at Station 13 was in the recycled base, followed by

the asphalt concrete surfacing and existing aggregate base. Noticeable permanent deformation was only recorded in the subgrade after the load increase to 60 kN. After completion of the test (713,000 load repetitions), most of the deformation measured was still in the recycled layer; however, a sharp increase in the deformation in the aggregate base was also recorded. A forensic investigation will be undertaken on completion of the Phase 2 HVS testing to validate these measurements.

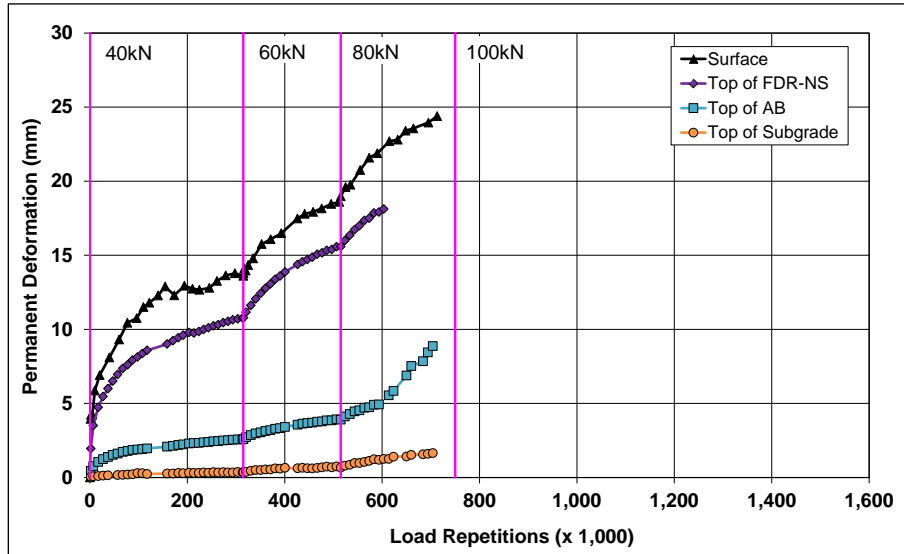


Figure 5.9: 672HB: Permanent deformation in the underlying layers.

Table 5.2: 672HB: Deformation in Each Layer

Layer	Layer Thickness		Deformation at Terminal Rut ¹		Deformation at End of Test	
	(mm)	(in.)	(mm)	(in.)	(mm)	(in.)
Surface	60	2.4	4.2	0.17	3.6	0.14
Recycled	250	10.0	8.5	0.33	11.9	0.47
Aggregate Base	320	12.6	2.3	0.09	7.3	0.29
Subgrade	-	-	0.4	0.02	1.6	0.06
Total MDD Measured Deformation			15.4	0.61	24.4	0.96
Laser Measured Deformation at Station 13			15.4	0.61	24.4	0.96

¹ Terminal rut for test section

5.3.6 Tensile Strain at the Bottom of the Asphalt Concrete Layer

Figure 5.10 shows the peak traffic-induced tensile strain at the bottom of the asphalt concrete layer. Longitudinal strain remained fairly constant throughout the test, apart from a small decrease during the first 200,000 load repetitions and some small spikes when the wheel load was increased. The figure indicates relatively constant transverse strain readings for the first 200,000 load repetitions with a slight decrease thereafter until the first load change, suggesting gradual layer stiffening resulting from densification caused by the HVS trafficking. Strains increased after each load change but then showed similar decreasing trends, indicating continued densification under loading. Apart from the permanent

deformation discussed in Section 5.3.4 and Section 5.3.5, no other surface distresses associated with the increase in strain measured in the recycled layer were noted during the course of the study.

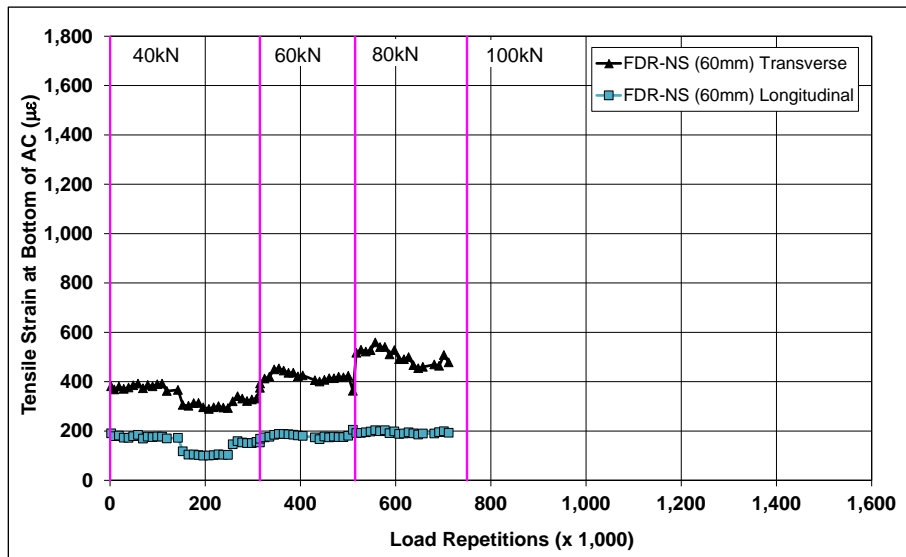


Figure 5.10: 672HB: Tensile strain at the bottom of the asphalt concrete layer.

5.3.7 Vertical Pressure at the Top of the Recycled Layer

Figure 5.11 shows the traffic-induced vertical pressure at the top of the recycled base layer. Pressure readings were stable, but sensitive to load change, for the duration of the test. Increases in recorded pressures occurred after the load changes, as expected. The reason for the decrease in pressure at the end of the test is unclear, but it is assumed that either the instrumentation was damaged or support conditions under the pressure cell changed.

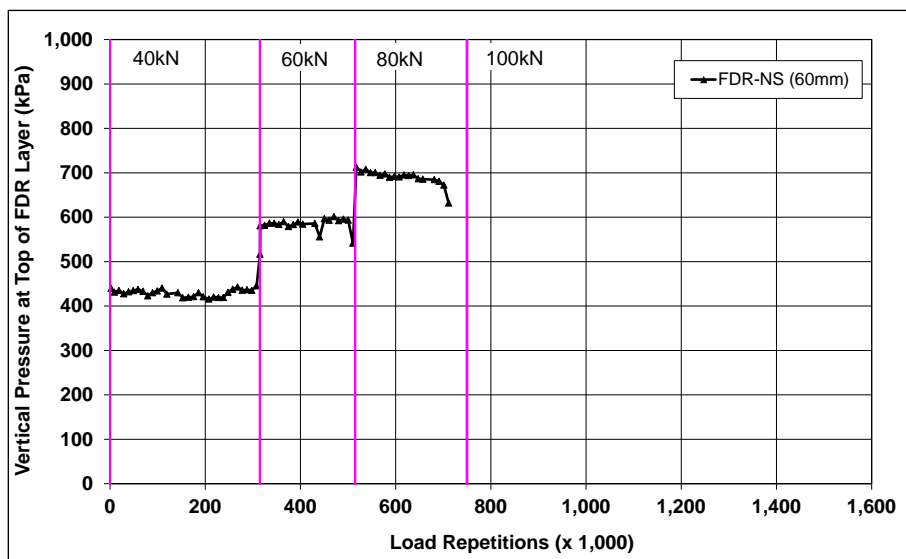


Figure 5.11: 672HB: Vertical pressure at the top of the recycled layer.

5.3.8 Deflection on the Surface (Road Surface Deflectometer)

Figure 5.12 compares elastic surface deflections measured with a road surface deflectometer (RSD) under a 40 kN half-axle load. Some problems were experienced with the data acquisition system during the 60 kN load test phase and the data points are not shown. However, the line on the plot shows the trend in increasing deflection during that time. Note that RSD measurements were taken under a creep-speed load and would not be the same as those recorded under the trafficking speed load. Slight increases in absolute surface deflection were recorded on the section after each load change, as expected, but it remained stable thereafter, indicating that there was no significant stiffness change in the pavement structure over time.

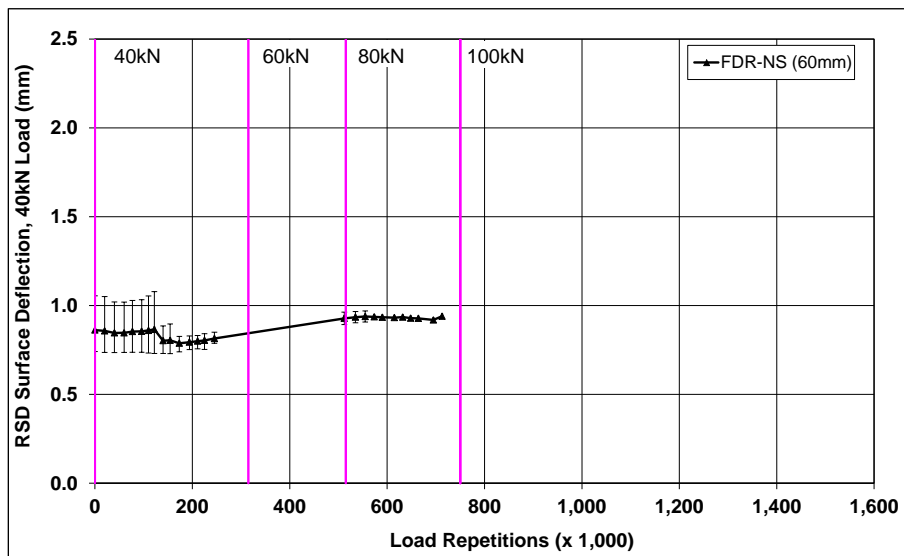


Figure 5.12: 672HB: Surface deflection (RSD).

5.3.9 Deflection in the Underlying Layers (Multi-Depth Deflectometer)

Figure 5.13 shows the history of in-depth elastic deflections measured by the LVDTs in the multi-depth deflectometer in the FDR-NS section. These readings are consistent with the surface deflections measured with the RSD shown in Figure 5.12. Deflections increased with increased load, as expected, but decreased after the embedment phase with increasing number of load repetitions, suggesting some stiffening/densification in the recycled layer attributable to HVS trafficking. Deflection decreased with increasing depth, but the LVDTs at the different depths showed similar trends over the course of the test.

5.3.10 Deflection in the Pavement Structure (Falling Weight Deflectometer)

Surface deflection measured with a falling weight deflectometer (FWD) on the FDR-NS section is summarized in Figure 5.14 (“trafficked area” and “untrafficked area” represent the FWD measurements taken on the HVS test section and adjacent to the HVS test section, respectively). The results were consistent with the RSD measurements discussed above, with the section exhibiting a large increase in

surface deflection of about 450 microns after completion of HVS trafficking. Deflections in the subgrade did not appear to change during the course of testing.

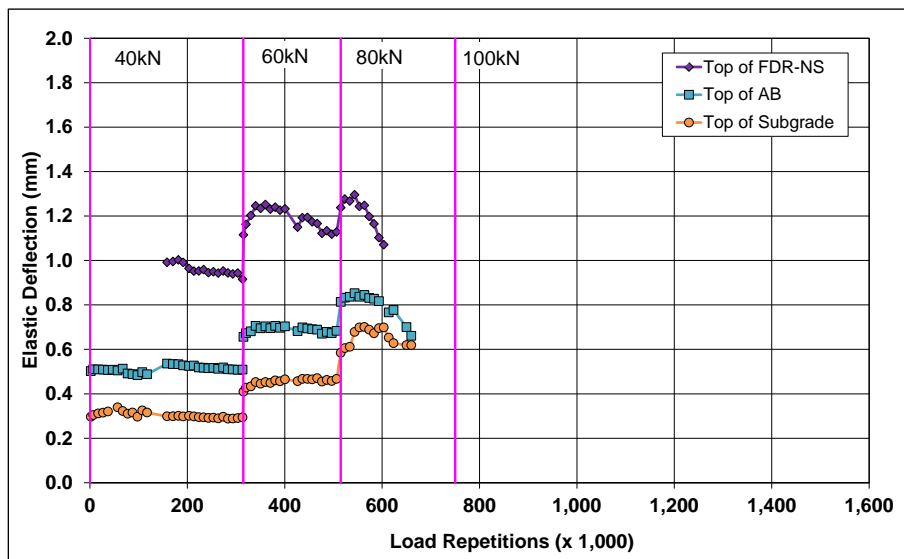


Figure 5.13: 672HB: Elastic deflection in the underlying layers.

The recycled layer stiffness was backcalculated from the deflection measurements using the *CalBack* software package and the results are summarized in Figure 5.15. The stiffness of the recycled layer was generally low at the start of the test, consistent with unstabilized materials, and it did not decrease significantly (drop of about 30 MPa) as a result of the HVS trafficking. The presence of the recycled asphalt concrete material did not appear to affect the stiffness of the layer. The stiffness of the untrafficked areas at either end of the test section did not change over time.

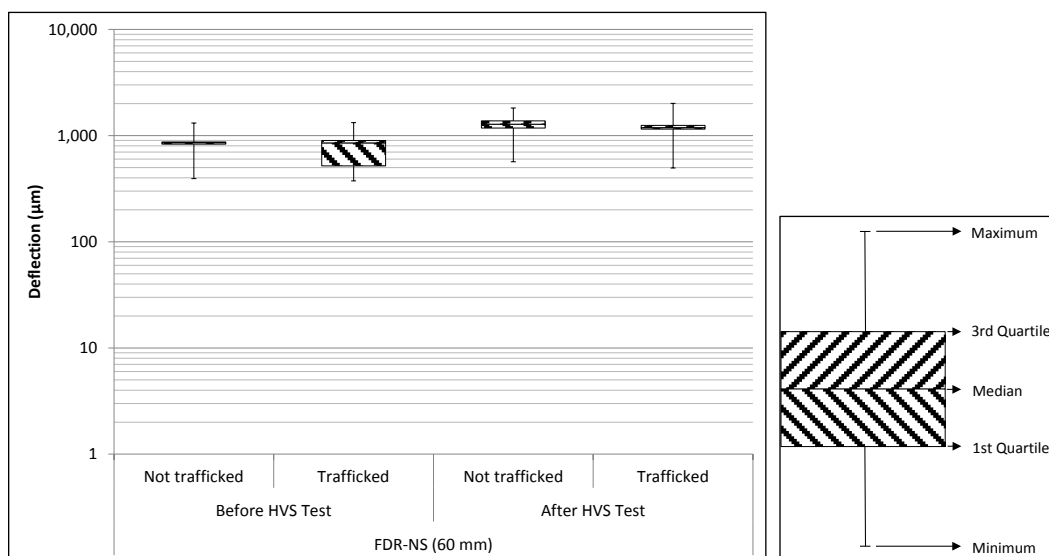


Figure 5.14: 672HB: Surface deflection (FWD).

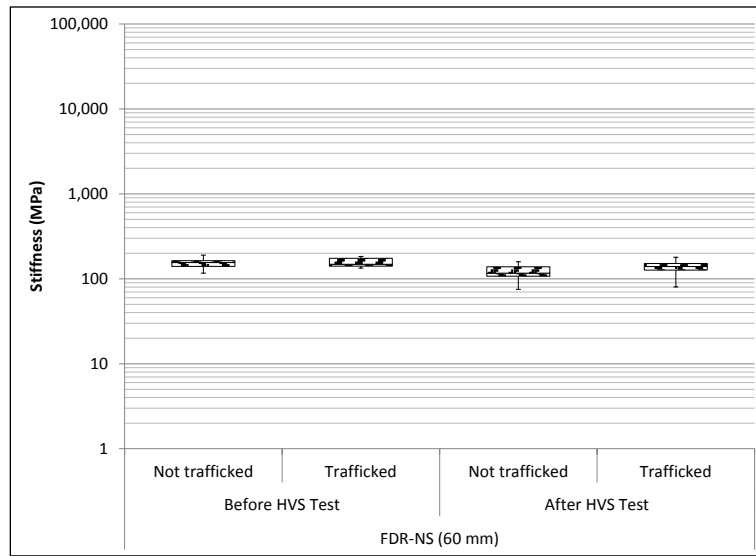


Figure 5.15: 672HB: Backcalculated stiffness of recycled layer (FWD).

5.3.11 Visual Assessment

Apart from rutting, no other distress was recorded on the section. Photographs of the test section after HVS testing are shown in Figure 5.16.

5.4 Section 677HC: No Stabilizer with 120 mm Surfacing (FDR-NS [120 mm])

5.4.1 Test Summary

Loading commenced with a 40 kN (9,000 lb) half-axle load on June 7, 2013, and ended with a 100 kN (22,500 lb) load on September 16, 2013. A total of 1,080,100 load repetitions were applied and 103 datasets were collected. Load was increased from 40 kN to 60 kN (13,500 lb) and then to 80 kN (18,000 lb) and 100 kN (22,500 lb.) after 315,000, 515,000, and 750,000 load repetitions, respectively. No breakdowns occurred during testing on this section. The HVS loading history for Section 677HC is shown in Figure 5.17.

At the start of the test, moisture contents in the recycled layer, original aggregate base, and subgrade layers were 4.3, 4.9, and 15.0 percent of the dry weight of the materials, respectively.



General view of test section looking from east to west



General view of test section looking from west to east



Close-ups of surface

Figure 5.16: 672HB: Test section photographs.

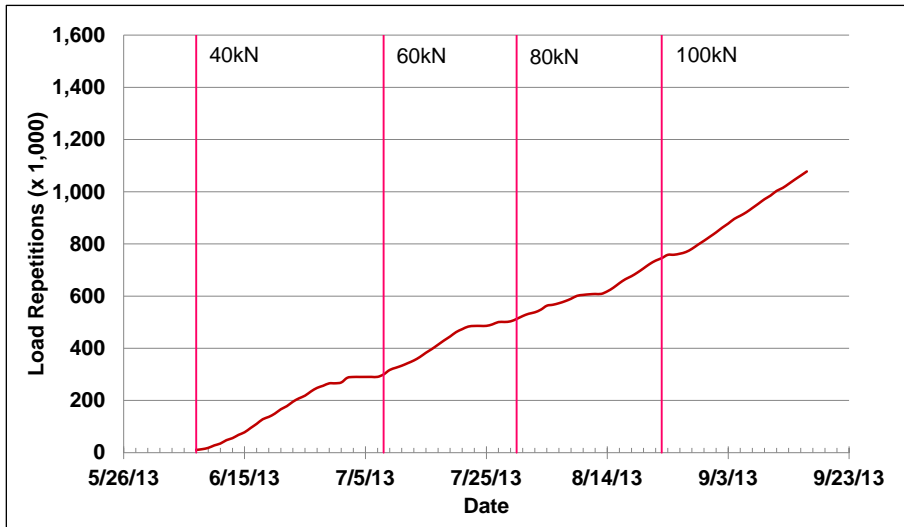


Figure 5.17: 677HC: HVS loading history.

5.4.2 Air Temperatures

Outside Air Temperatures

Daily average outside air temperatures are summarized in Figure 5.18. Vertical error bars on each point on the graph show the daily temperature range. Temperatures ranged from 10°C to 47°C (50°F to 117°F) during the course of HVS testing, with a daily average of 24°C (75°F), an average minimum of 15°C (59°F), and an average maximum of 36°C (97°F).

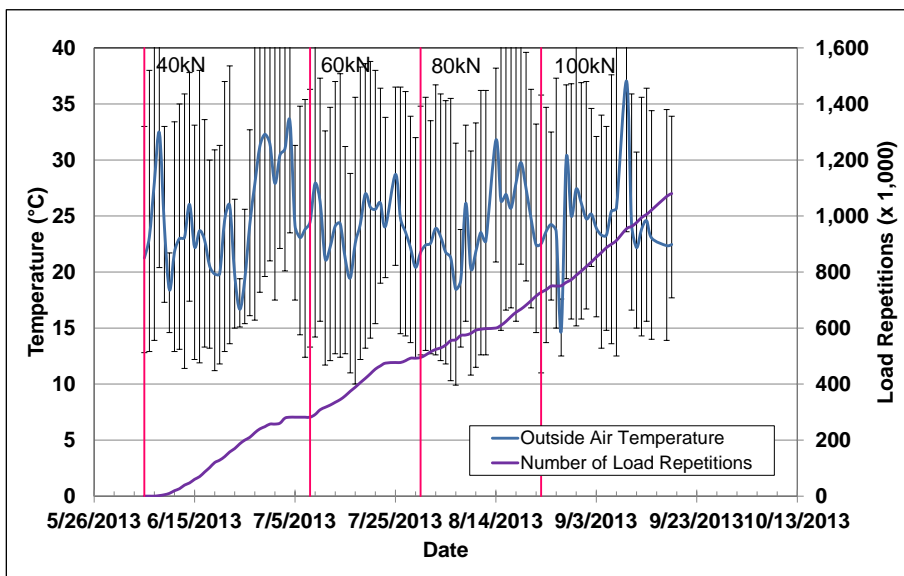


Figure 5.18: 677HC: Daily average air temperatures outside the environmental chamber.

Air Temperatures in the Environmental Chamber

During the test, air temperatures inside the temperature control chamber ranged from 14°C to 61°C (57°F to 142°F) with an average of 29°C (84°F) and a standard deviation of 2.9°C (5.2°F). Air temperature was adjusted to maintain a pavement temperature of 30°C±4°C (86°F±7°F) at a pavement depth of 50 mm (2.0 in.). The recorded pavement temperatures discussed in Section 5.4.3 indicate that the inside air temperatures were adjusted appropriately to maintain the required pavement temperature. The daily average air temperatures recorded in the environmental chamber, calculated from the hourly temperatures recorded during HVS operation, are shown in Figure 5.19. Vertical error bars on each point on the graph show the daily temperature range.

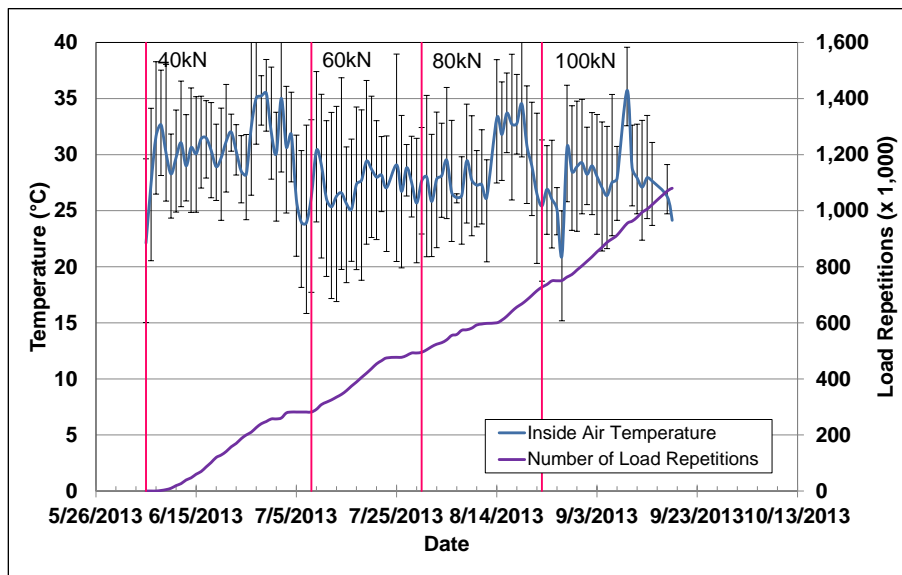


Figure 5.19: 677HC: Daily average air temperatures inside the environmental chamber.

5.4.3 Pavement Temperatures

Daily averages of the surface and in-depth temperatures of the asphalt concrete and recycled layers are listed in Table 5.3 and shown in Figure 5.20. Pavement temperatures were constant throughout the top 120 mm (4.7 in.) of the pavement.

Table 5.3: 677HC: Temperature Summary for Air and Pavement

Temperature	Layer	Average (°C)	Std. Dev. (°C)	Average (°F)	Std. Dev. (°F)
Outside air	-	24	3.7	75	6.7
Inside air	-	29	2.9	84	5.2
Pavement surface	AC	29	2.7	84	4.9
- 25 mm below surface	AC	30	1.9	86	3.4
- 50 mm below surface	AC	30	1.9	86	3.4
- 90 mm below surface	FDR	30	1.7	86	3.1
- 120 mm below surface	FDR	30	1.5	86	2.7

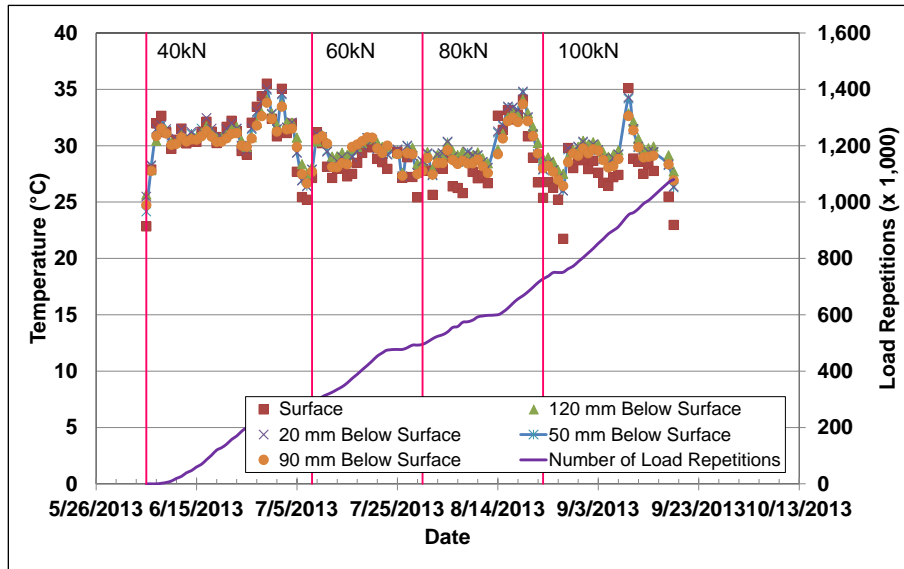


Figure 5.20: 677HC: Daily average pavement temperatures.

5.4.4 Permanent Deformation on the Surface (Rutting)

Figure 5.21 shows the average transverse cross section measured with the laser profilometer at various stages of the test and illustrates the increase in rutting and deformation over time. Figure 5.22 shows the development of permanent deformation (average maximum rut and average deformation) with load repetitions for the test section. The results for the FDR-NS (60 mm) section (Section 672HB) are shown for comparison. The two plots show that most of the deformation was in the form of a depression rather than upward and outward displacement of the material above the zero elevation point.

The embedment phase on the FDR-NS (120 mm) section was of a similar duration to that on the FDR-NS (60 mm) section in terms of the number of load repetitions (i.e., $\pm 5,000$), but ended with significantly less rutting compared to Section 672HB. The average maximum total rut at the end of the embedment phase was about 3.5 mm (0.13 in.). The rate of rut depth increase after the embedment phase was also considerably slower than that on Section 672HB, which was attributed to the generally stiffer structure resulting from the thicker asphalt concrete surfacing. Increases in the applied load (to 60 kN and then to 80 kN and 100 kN) did not result in any noticeable embedment phases after each event. However, the rate of rut depth increase did accelerate slightly after each load change. Error bars on the average maximum total rut reading indicate that there was some variation along the length of the section. Analysis of the data showed that variability was across the entire section and not confined to one half as with the rut on Section 672HB.

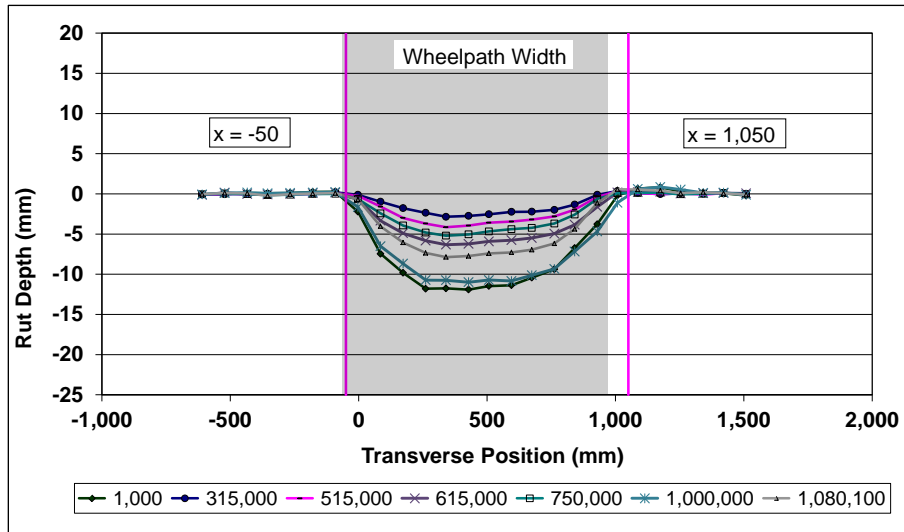


Figure 5.21: 677HC: Profilometer cross section at various load repetitions.

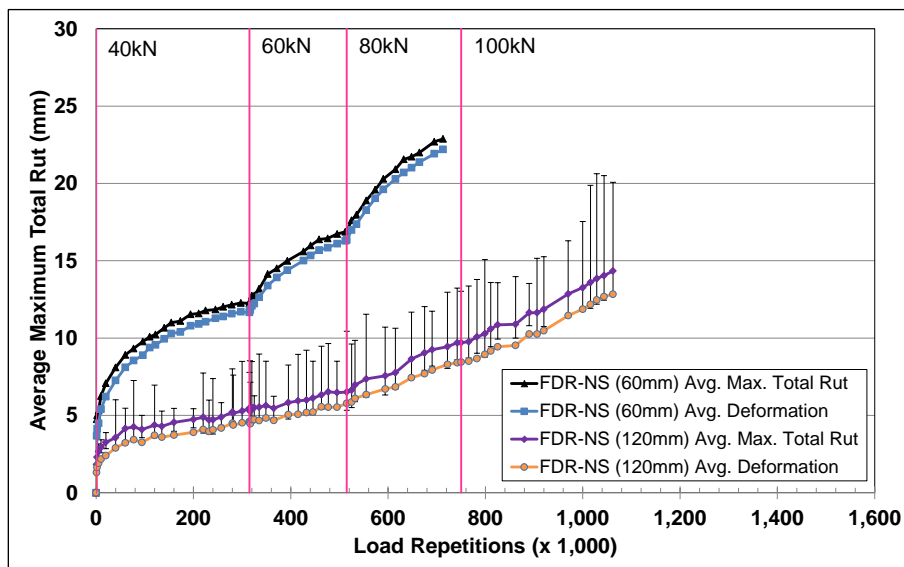


Figure 5.22: 677HC: Average maximum total rut and average deformation.

Figure 5.23 shows contour plots of the pavement surface at the start and end of the test (1,080,100 load repetitions). The plot indicates that the deepest ruts were at the start and end of the test section where the wheel changed direction. Terminal rut (12.5 mm [0.5 in.]) was reached after approximately 950,000 load repetitions.

After completion of trafficking, the average maximum total rut depth and the average deformation were 14.3 mm (0.56 in.) and 12.8 mm (0.50 in.), respectively. The maximum rut depth measured on the section was 19.4 mm (0.76 in.), recorded at Station 13.

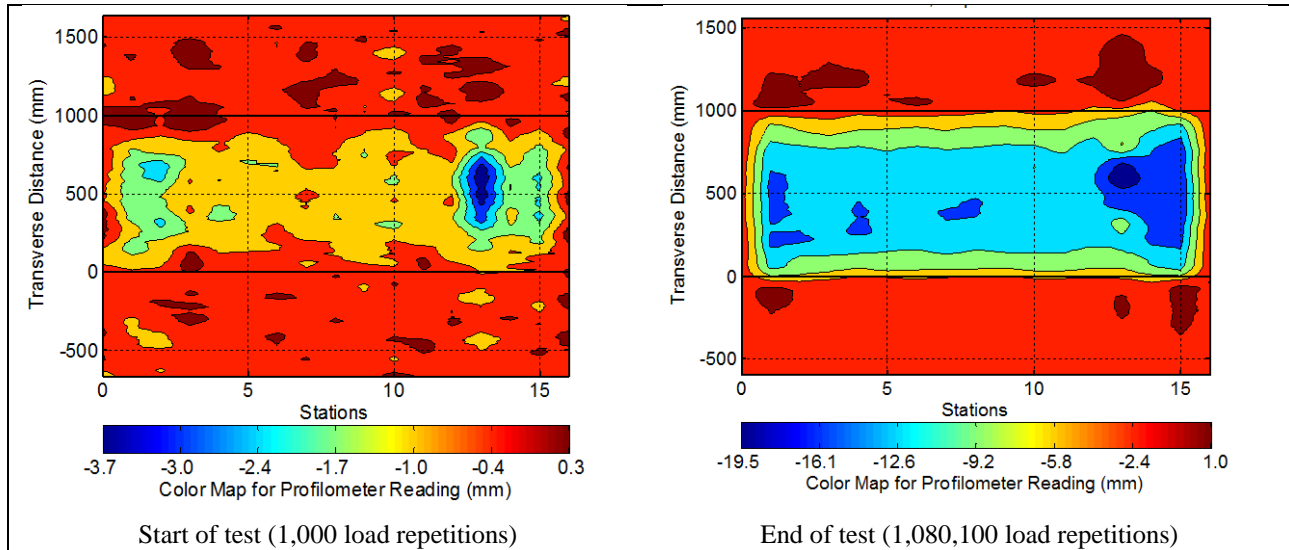


Figure 5.23: 677HC: Contour plots of permanent surface deformation.
 (Note different scales in legends.)

5.4.5 Permanent Deformation in the Underlying Layers

Permanent deformation in the underlying layers, recorded with a multi-depth deflectometer (MDD) at Station 13 and compared to the surface layer laser profilometer measurements, is shown in Figure 5.24.

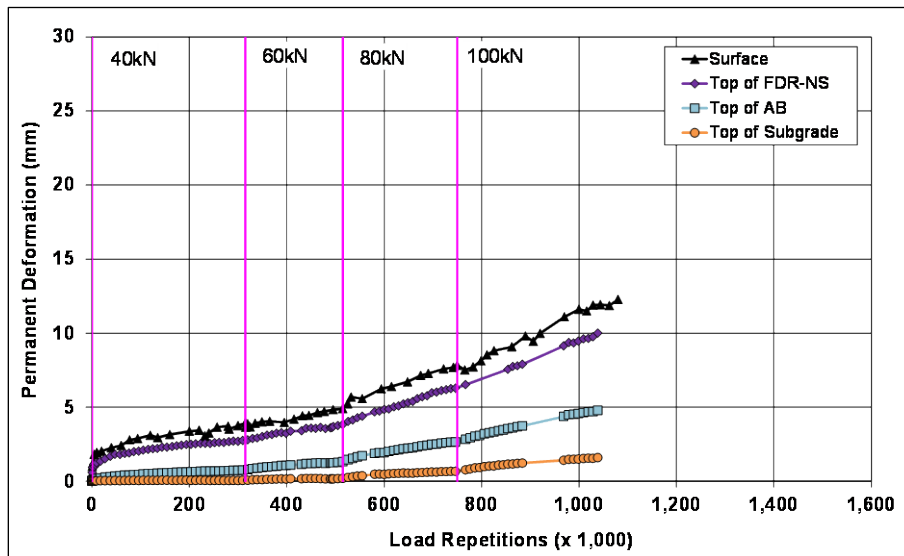


Figure 5.24: 677HC: Permanent deformation in the underlying layers.

The MDD measurements were consistent with the laser profilometer measurements. Deformation in each of the layers is summarized in Table 5.4 (results for Section 672HB are included for comparison). After 950,000 load repetitions, when the terminal rut for the test (average maximum total rut [12.5 mm] measured over the full section) was reached, most of the deformation at Station 13 was in the recycled

base, followed by the existing aggregate base and asphalt concrete surfacing. Noticeable permanent deformation was only recorded in the subgrade after the load increase to 80 kN. Similar ratios between the different layers were recorded after completion of the test (1,080,100 load repetitions). A forensic investigation will be undertaken on completion of the Phase 2 HVS testing to validate these measurements.

Table 5.4: 677HC: Deformation in Each Layer

Layer	Layer Thickness		677HC		672HB	
			Deformation at Terminal Rut ¹		Deformation at Terminal Rut ¹	
	(mm)	(in.)	(mm)	(in.)	(mm)	(in.)
Surface	120	4.8	2.1	0.08	4.2	0.17
Recycled	250	10.0	4.6	0.18	8.5	0.33
Aggregate Base	320	12.6	3.0	0.12	2.3	0.09
Subgrade	-	-	1.4	0.06	0.4	0.02
Total MDD Measured Deformation			11.1	0.44	15.4	0.61
Laser Measured Deformation at Station 13			11.1	0.44	15.4	0.61
¹ Terminal rut for test section						

5.4.6 Tensile Strain at the Bottom of the Asphalt Concrete Layer

Figure 5.25 shows the peak traffic-induced tensile strain at the bottom of the asphalt concrete layer. Transverse strain measurements from the FDR-NS (60 mm) section are included in the figure for comparison.

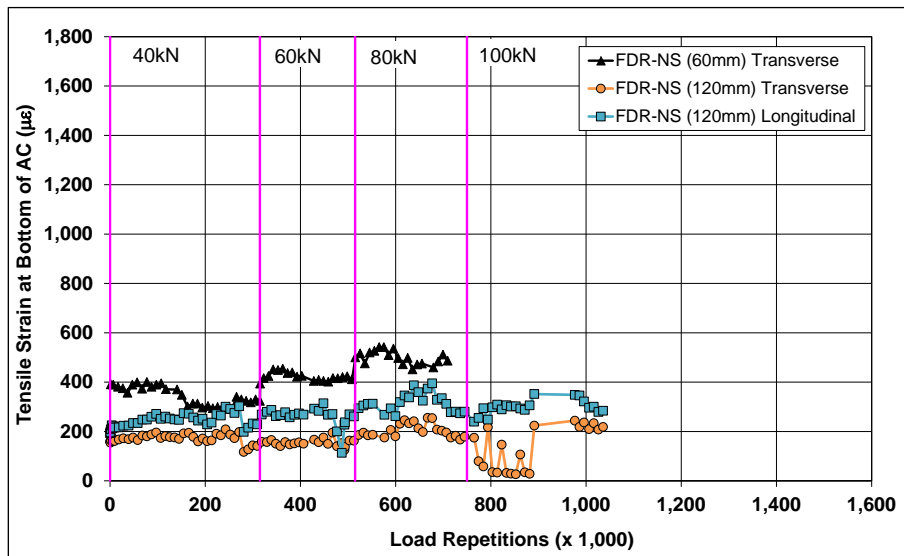


Figure 5.25: 677HC: Tensile strain at the bottom of the asphalt concrete layer.

Longitudinal strains were slightly higher than the transverse strains on the FDR-NS (120 mm) section, the opposite of that recorded on the FDR-NS (60 mm) section. Transverse strains on the FDR-NS (120 mm) section were lower than those measured on the FDR-NS (60 mm) section as expected, this being attributed

to the thicker asphalt concrete surfacing layer. Transverse and longitudinal strains showed similar trends on the FDR-NS (120 mm) section. Strains increased in the initial stages of the test, and then stabilized or decreased slightly, suggesting gradual layer stiffening resulting from densification caused by the HVS trafficking. Strains increased after each load change but then showed similar decreasing trends, indicating continued densification under loading. It is not clear what caused the variations in the transverse strain measurements after the load change to 100 kN. This will be assessed during the forensic investigation after completion of Phase 2 HVS testing. Apart from the permanent deformation discussed in Section 5.4.4 and Section 5.4.5, no other surface distresses associated with the increase in strain measured in the recycled layer were noted during the course of the study.

5.4.7 Vertical Pressure at the Top of the Recycled Layer

Figure 5.26 shows a comparison of traffic-induced vertical pressure at the top of the recycled base layer for the FDR-NS (120 mm) and FDR-NS (60 mm) sections. Pressure readings were lower on the FDR-NS (120 mm) section, as expected. Pressure readings were also sensitive to load changes. Measurements were erratic toward the end of the test after the load change to 100 kN. The reason for this is unclear, but it is assumed that either the instrumentation was damaged or support conditions under the pressure cell changed.

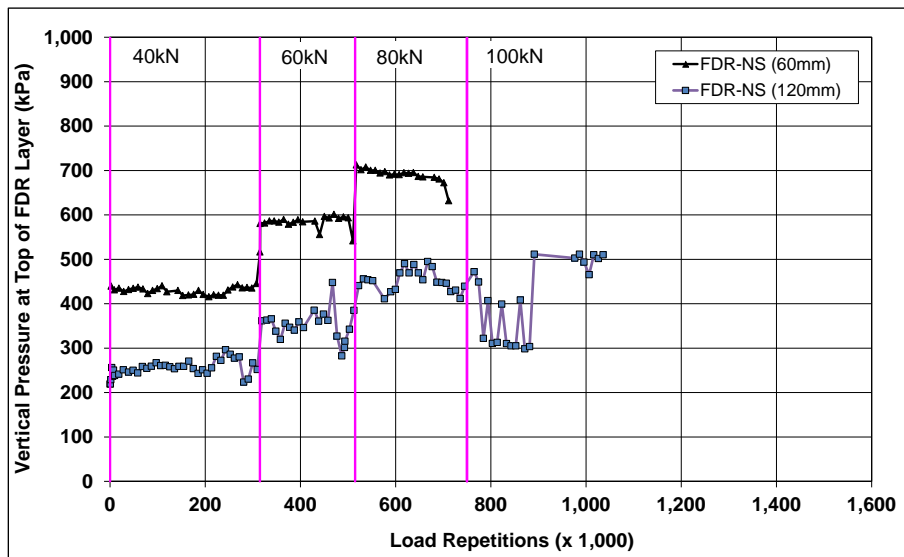


Figure 5.26: 677HC: Vertical pressure at the top of the recycled layer.

5.4.8 Deflection on the Surface (Road Surface Deflectometer)

Figure 5.27 compares elastic surface deflections measured with an RSD on the FDR-NS (120 mm) and FDR-NS (60 mm) sections under a 40 kN half-axle load. Deflections were notably lower on the FDR-NS (120 mm) section, as expected. Slight increases in absolute surface deflection were recorded after each

load change, but it stabilized after initial embedment, indicating that there was no significant change in the stiffness of the pavement structure over time.

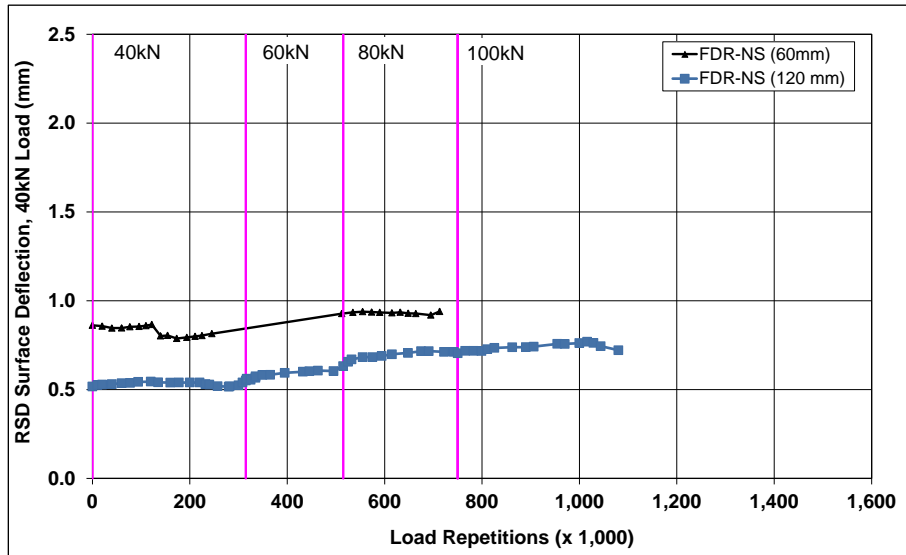


Figure 5.27: 677HC: Surface deflection (RSD).

5.4.9 Deflection in the Underlying Layers (Multi-Depth Deflectometer)

Figure 5.28 shows the history of in-depth elastic deflections measured by the LVDTs in the multi-depth deflectometer in the FDR-NS (120 mm) section. These readings are consistent with the surface deflections measured with the RSD and those recorded on the FDR-NS (60 mm) section. However, initial deflection on the top of the recycled layer was lower on the FDR-NS (120 mm) section, as expected, due to the confinement provided by the thicker asphalt concrete surfacing. Deflections increased with increased load, as expected, but stabilized after the embedment phase with increasing number of load repetitions, which suggests some stiffening/densification in the recycled layer attributable to HVS trafficking. Deflections decreased with increasing depth, but the LVDTs at the different depths all showed similar trends over the course of the test.

5.4.10 Deflection in the Pavement Structure (Falling Weight Deflectometer)

Surface deflection measured with an FWD is summarized in Figure 5.29. Results from the FDR-NS (60 mm) test section are included for comparison. The results were generally consistent with the RSD measurements discussed above, with the section exhibiting very little change in surface deflection after completion of HVS trafficking. Deflections in the subgrade did not appear to change during the course of testing.

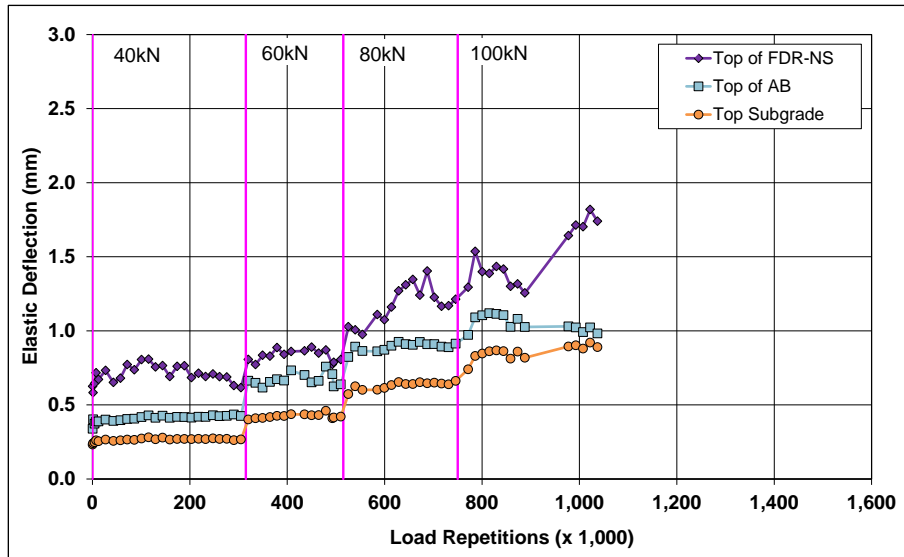


Figure 5.28: 677HC: Elastic deflection in the underlying layers.

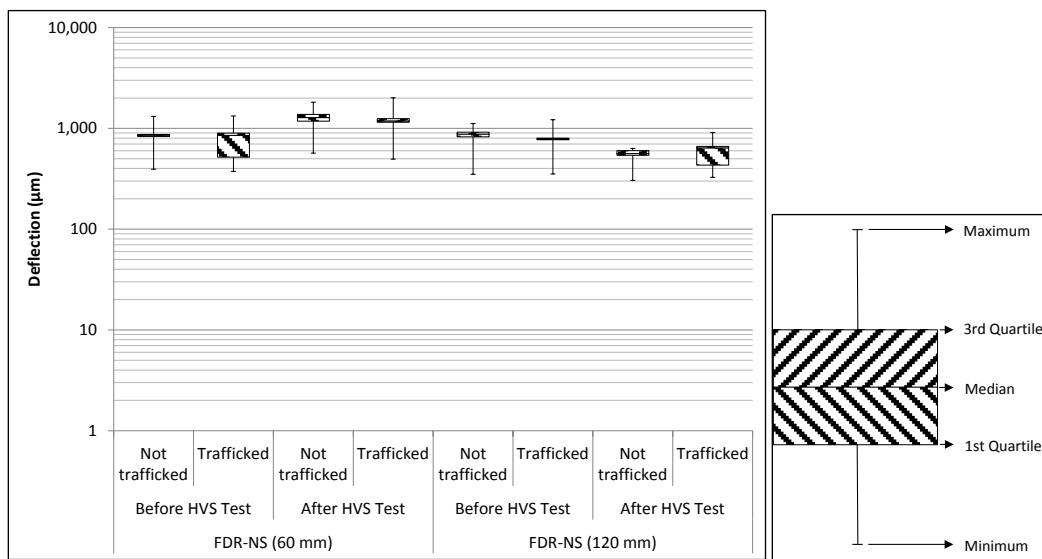


Figure 5.29: 677HC: Surface deflection (FWD).

The recycled layer stiffness was backcalculated from the deflection measurements using the *CalBack* software package, and the results are summarized in Figure 5.30. The stiffness of the unstabilized recycled layer was generally low at the start of the test and similar to that recorded on the FDR-NS (60 mm) section, as expected. At the end of the HVS test, average stiffness measured along the length of the test section had dropped by about 150 MPa, consistent with the loading that had been applied (~ 20.8 million ESALs). The presence of the recycled asphalt concrete material did not appear to affect the stiffness of the layer. There was no change in the stiffness of the untrafficked areas on either side of the test section.

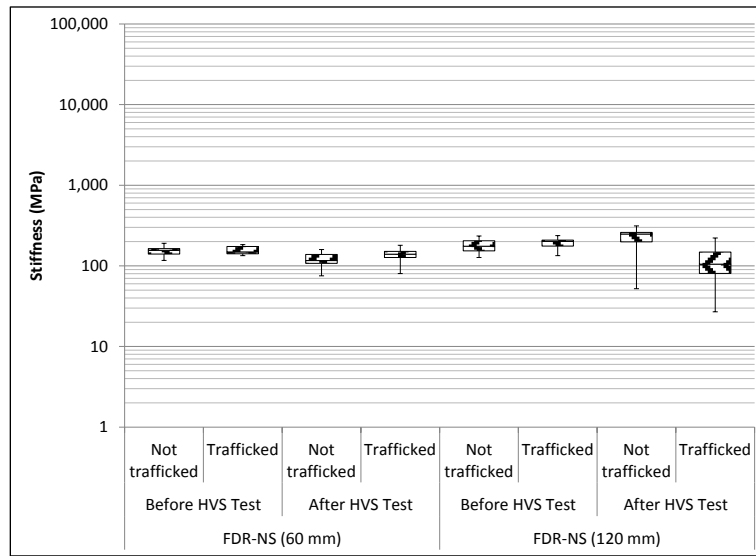


Figure 5.30: 677HC: Backcalculated stiffness of recycled layer (FWD).

5.4.11 Visual Assessment

Apart from rutting, no other distress was recorded on the section. Photographs of the test section after HVS testing are shown in Figure 5.31.

5.5 Section 673HB: Foamed Asphalt with Portland Cement (FDR-FA)

5.5.1 Test Summary

Loading commenced with a 40 kN (9,000 lb) half-axle load on April 9, 2013, and ended with a 100 kN (22,500 lb) load on June 27, 2013. A total of 1,000,000 load repetitions were applied and 81 datasets were collected. Loading on this section was terminated after one million load repetitions, well before the terminal rut or crack density criteria were reached, in the interests of completing the project within the project time and financial constraints. Load was increased from 40 kN to 60 kN (13,500 lb) and then to 80 kN (18,000 lb) and 100 kN (22,500 lb.) after 315,000, 515,000, and 750,000 load repetitions, respectively. No breakdowns occurred during testing on this section. The HVS loading history for Section 673HB is shown in Figure 5.32.

At the start of the test, moisture contents in the recycled layer, original aggregate base, and subgrade were 3.2, 4.5, and 12.9 percent of the dry weight of the materials, respectively.

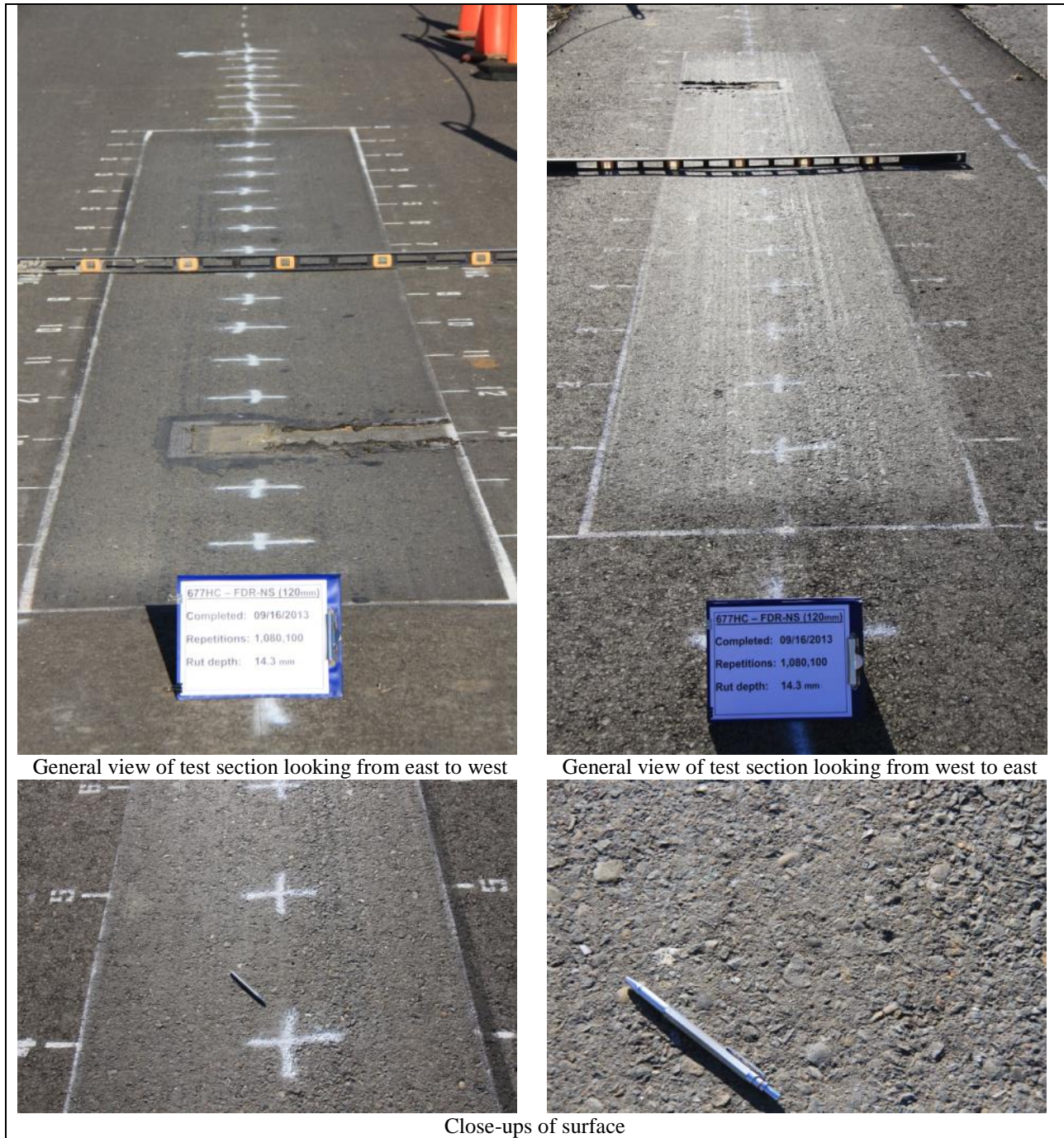


Figure 5.31: 677HC: Test section photographs.

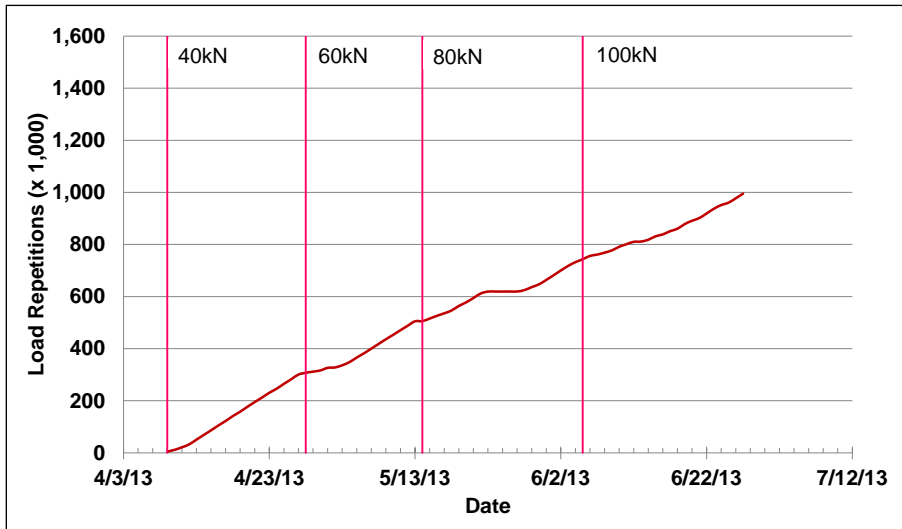


Figure 5.32: 673HB: HVS loading history.

5.5.2 Air Temperatures

Outside Air Temperatures

Daily average outside air temperatures are summarized in Figure 5.33. Vertical error bars on each point on the graph show the daily temperature range. Temperatures ranged from 9°C to 39°C (48°F to 102°F) during the course of HVS testing, with a daily average of 23°C (73°F), an average minimum of 15°C (59°F), and an average maximum of 31°C (88°F).

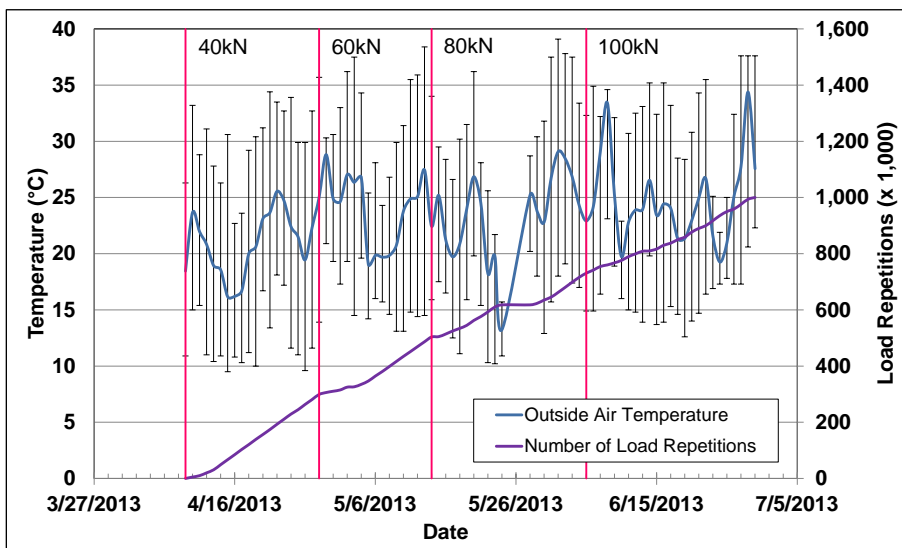


Figure 5.33: 673HB: Daily average air temperatures outside the environmental chamber.

Air Temperatures in the Environmental Chamber

During the test, air temperatures inside the temperature control chamber ranged from 18°C to 40°C (64°F to 104°F) with an average of 29°C (84°F) and a standard deviation of 2.0°C (3.6°F). Air temperature was adjusted to maintain a pavement temperature of 30°C±4°C (86°F±7°F) at a pavement depth of 50 mm (2.0 in.). The recorded pavement temperatures discussed in Section 5.5.3 indicate that the inside air temperatures were adjusted appropriately to maintain the required pavement temperature. The daily average air temperatures recorded in the environmental chamber, calculated from the hourly temperatures recorded during HVS operation, are shown in Figure 5.34. Vertical error bars on each point on the graph show the daily temperature range.

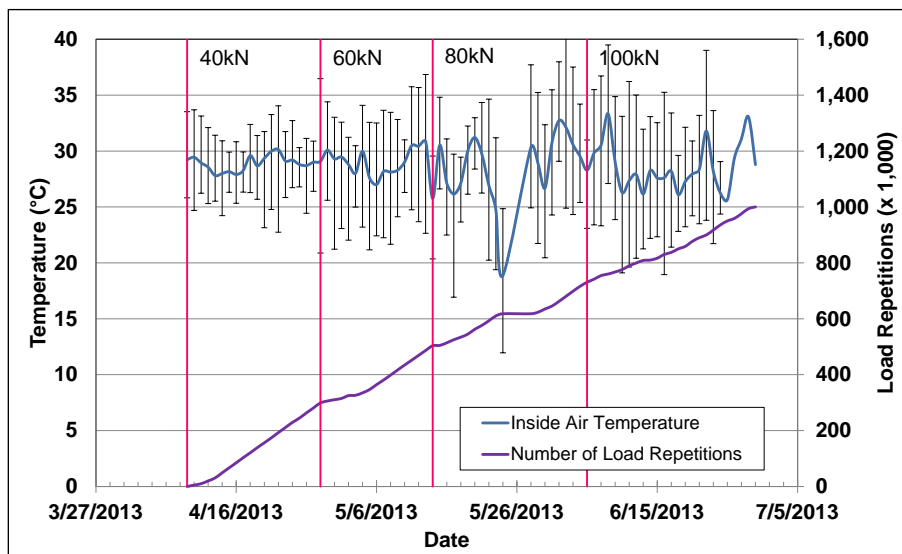


Figure 5.34: 673HB: Daily average air temperatures inside the environmental chamber.

5.5.3 Pavement Temperatures

Daily averages of the surface and in-depth temperatures of the asphalt concrete and recycled layers are listed in Table 5.5 and shown in Figure 5.35. Pavement temperatures increased slightly with increasing depth in the asphalt concrete. Temperatures in the top of the recycled layer were slightly cooler than the asphalt concrete, which was expected as there is usually a thermal gradient between the top and bottom of asphalt concrete pavement layers.

Table 5.5: 673HB: Temperature Summary for Air and Pavement

Temperature	Layer	Average (°C)	Std. Dev. (°C)	Average (°F)	Std. Dev. (°F)
Outside air	-	23	3.7	73	6.7
Inside air	-	29	2.0	84	3.6
Pavement surface	AC	30	0.9	86	1.6
- 25 mm below surface	AC	30	0.9	86	1.6
- 50 mm below surface	AC	30	1.2	86	2.2
- 90 mm below surface	FDR	29	1.9	84	3.4
- 120 mm below surface	FDR	29	1.2	84	2.2

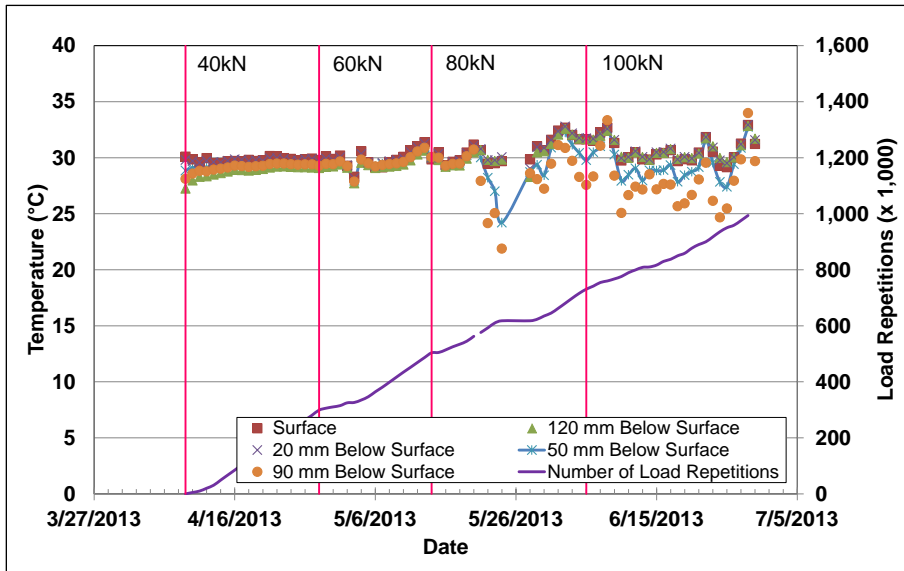


Figure 5.35: 673HB: Daily average pavement temperatures.

5.5.4 Permanent Deformation on the Surface (Rutting)

Figure 5.36 shows the average transverse cross section measured with the laser profilometer at various stages of the test and illustrates the increase in rutting and deformation over time. Figure 5.37 shows the development of permanent deformation (average maximum rut and average deformation) with load repetitions for the test section. The results for the FDR-NS (60 mm) section are shown for comparison. The two plots show that most of the deformation was in the form of a depression rather than upward and outward displacement of the material above the zero elevation point.

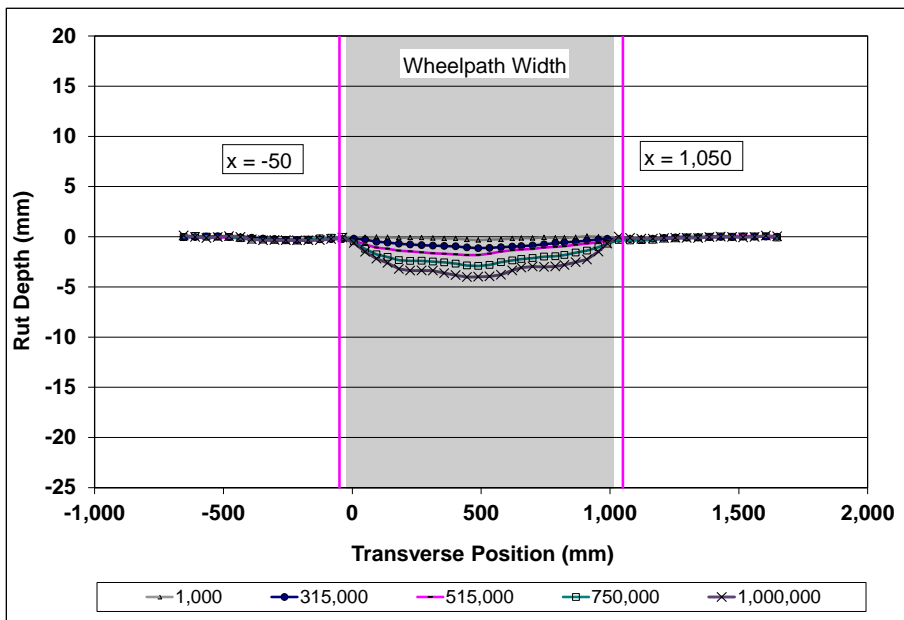


Figure 5.36: 673HB: Profilometer cross section at various load repetitions.

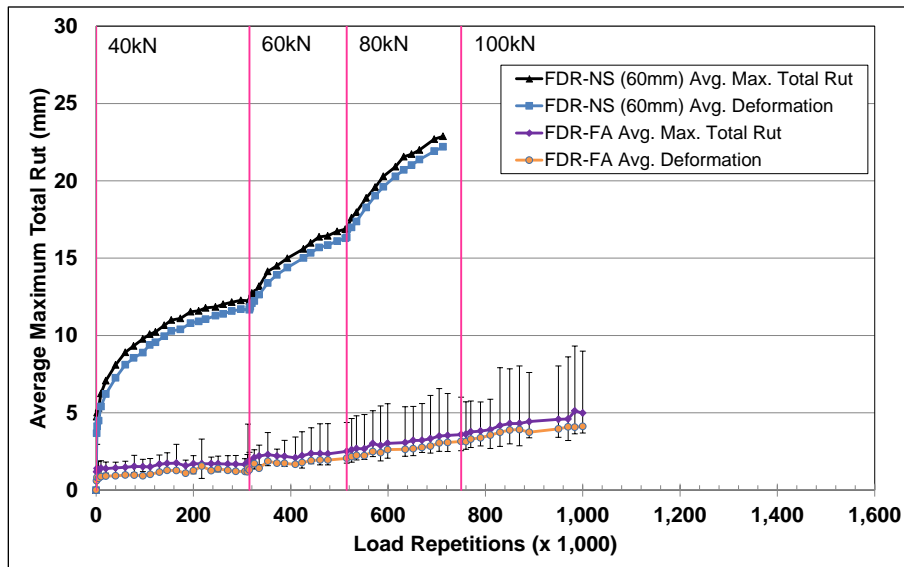


Figure 5.37: 673HB: Average maximum total rut and average deformation.

The embedment phase on the FDR-FA section was of a similar duration to that on the FDR-NS (60 mm) section in terms of the number of load repetitions (i.e., $\pm 5,000$), but ended with significantly less rutting. The average maximum total rut at the end of the embedment phase was about 1.1 mm (0.04 in.). The rate of rut depth increase after the embedment phase was also very slow compared to that on Sections 672HB and 677HC, which was attributed to the stiffer nature of the stabilized recycled material. A short embedment phase with an increased rate of rutting was evident after the 60 kN load change, but not after the load changes to 80 kN and 100 kN. The rate of rut depth increased very slowly during the course of loading. Error bars on the average maximum total rut reading indicate that there was very little variation along the length of the section. The test was halted when the average maximum total rut depth reached 5.0 mm (0.2 in.) due to time and budget limitations.

Figure 5.38 shows contour plots of the pavement surface at the start and end of the test (1,000,000 load repetitions). The plot shows the relative uniformity of the rut depth over the length of the section. The small area of distress at Station 8 was attributed to some mechanical damage on the surface and not to rutting (see Section 5.5.11). After completion of trafficking, the average maximum rut depth and the average deformation were 5.0 mm (0.20 in.) and 4.1 mm (0.16 in.), respectively. The maximum total rut depth measured on the section was 8.2 mm (0.32 in.), recorded at Station 8 in the area of mechanical damage on the surface.

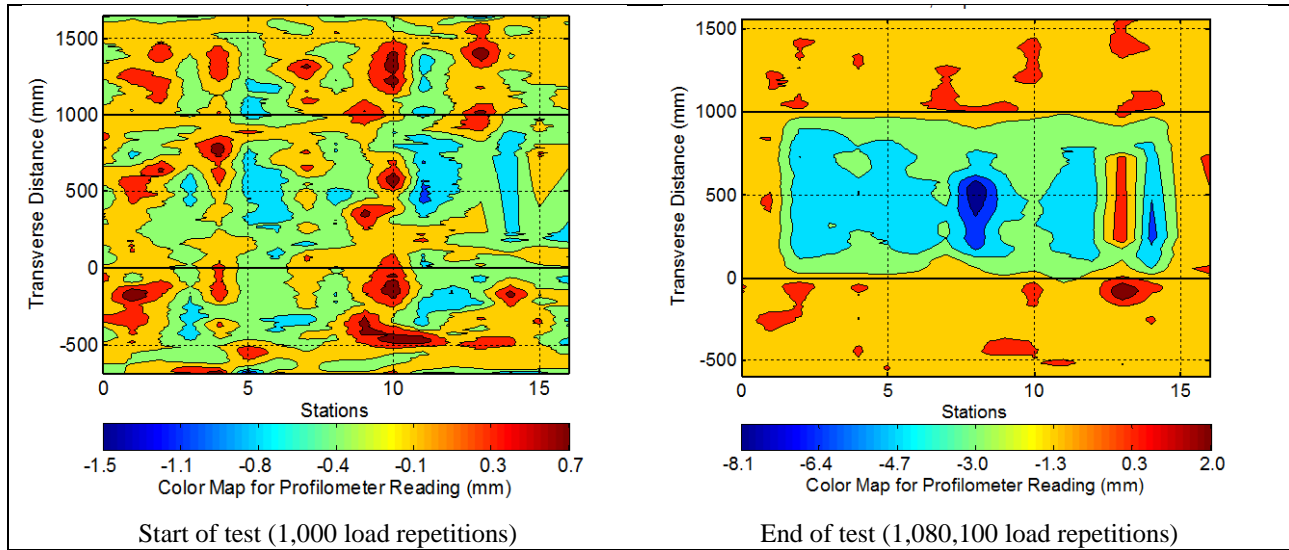


Figure 5.38: 673HB: Contour plots of permanent surface deformation.
 (Note different scales in legends.)

5.5.5 Permanent Deformation in the Underlying Layers

Permanent deformation in the underlying layers, recorded with a multi-depth deflectometer (MDD) at Station 13 and compared to the surface layer laser profilometer measurements is shown in Figure 5.39.

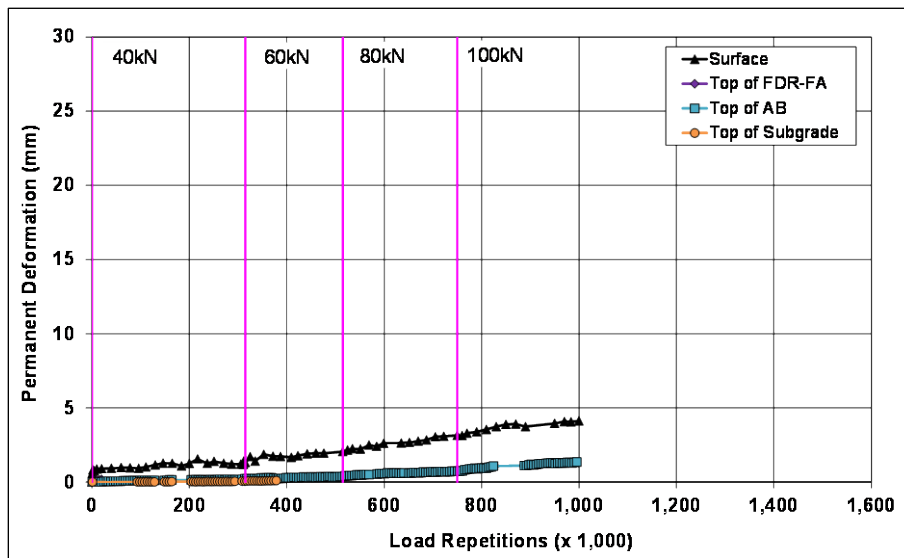


Figure 5.39: 673HB: Permanent deformation in the underlying layers.

The LVDT at the top of the FDR layer failed early in the test and consequently there were no measurements for this layer. The LVDT in the subgrade failed after approximately 400,000 load repetitions, leaving only one functioning LVDT at the top of the aggregate base. No deformation was recorded in the subgrade up to the point that the subgrade LVDT failed. Deformation at the top of the

existing aggregate base reached 1.3 mm at the end of the test (1,000,000 load repetitions). Based on the results obtained from the two unstabilized sections (Sections 672HB and 677HC), it is assumed that most of the remaining deformation occurred in the asphalt concrete surfacing, with very little deformation in the FDR-FA and subgrade layers. Deformation in each of the layers is summarized in Table 5.6 with assumptions made for the recycled and subgrade layers (results for the FDR-NS [60 mm] section are included for comparison). A forensic investigation will be undertaken on completion of the Phase 2 HVS testing to validate these measurements.

Table 5.6: 673HB: Deformation in Each Layer

Layer	Layer Thickness		673HB		672HB	
			Deformation at End of Test ¹		Deformation at End of Test ²	
	(mm)	(in.)	(mm)	(in.)	(mm)	(in.)
Surface	60	2.4	2.0 ³	0.08	3.6	0.14
Recycled	250	10.0	0.3 ³	0.01	11.9	0.47
Aggregate Base	320	12.6	1.3	0.05	7.3	0.29
Subgrade	-	-	0.5 ³	0.02	1.6	0.06
Total MDD Measured Deformation			4.1	0.16	24.4	0.96
Laser Measured Deformation at Station 13			4.1	0.16	24.4	0.96
¹ 1,000,000 load repetitions (~ 17,033,768 ESALs) ² 713,000 load repetitions (~ 5,5052,104 ESALs) ³ Assumed value						

5.5.6 Tensile Strain at the Bottom of the Asphalt Concrete Layer

Figure 5.40 shows the peak traffic-induced transverse tensile strain at the bottom of the asphalt concrete layer. The strain gauge installed to measure longitudinal strain was damaged during placement of the asphalt concrete surfacing and therefore no readings were obtained. Transverse strain measurements from the FDR-NS (60 mm) section are included in the figure for comparison. Trends in the transverse strains measured on the FDR-FA section differed from those measured on the FDR-NS sections. Initial transverse strains were significantly lower than those recorded on the unstabilized section, but they showed a relatively sharp increase in the first 50,000 load repetitions attributable to initial breakdown of the portland cement bonds. The strains stabilized thereafter at similar levels to those recorded on the FDR-NS (60 mm) section for the remainder of the 40 kN wheel load trafficking. The increase in strain immediately after the load change was not as sharp as that recorded on the FDR-NS section, but it continued to increase for the remainder of the test suggesting further weakening of the structure (probably attributed to microcracking in the recycled base) caused by trafficking. Variability in the strain measurements recorded in the latter part of the test was attributed to a combination of temperature changes and their effect on microcracks under the strain gauge. No surface distresses associated with the increase in strain measured in the recycled layer were noted during the course of the study.

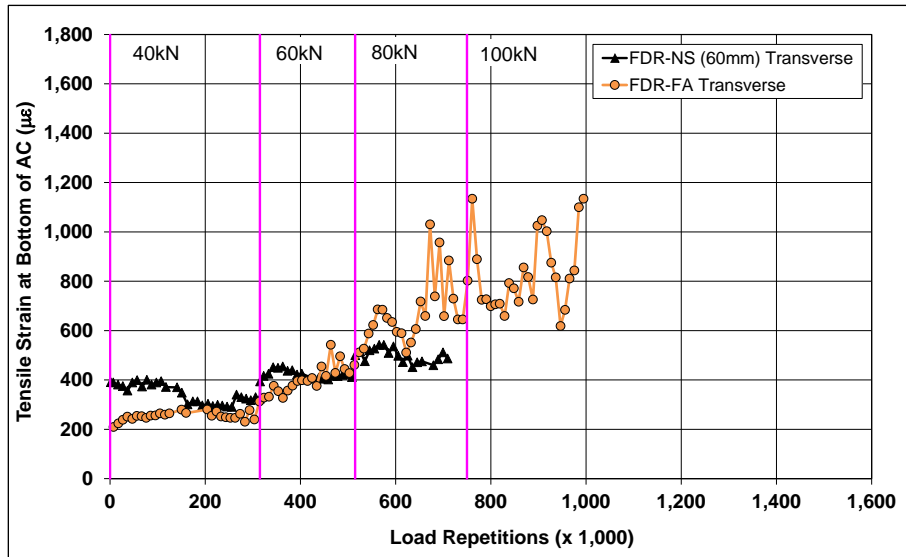


Figure 5.40: 673HB: Tensile strain at the bottom of the asphalt concrete layer.

5.5.7 Vertical Pressure at the Top of the Recycled Layer

Figure 5.41 shows the comparison of traffic-induced vertical pressure at the top of the recycled base layer for the FDR-NS (60 mm) and FDR-FA sections.

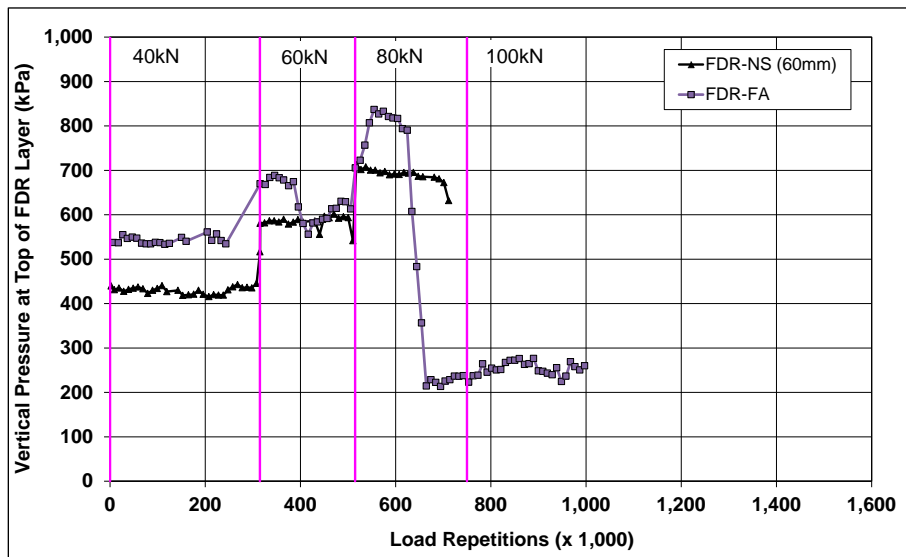


Figure 5.41: 673HB: Vertical pressure at the top of the recycled layer.

Pressure readings were stable and sensitive to load changes for most of the FDR-FA test. Initial pressure was higher on the FDR-FA section compared to the FDR-NS section, which was expected based on layer elastic theory and considering the much higher stiffness of the FDR-FA section. Increases in recorded pressures occurred after the load changes, as expected. A rapid increase followed by a significant drop in

pressure was recorded on the section between 520,000 and 620,000 load repetitions. The reason for this is unclear, but it is assumed that either the instrumentation was damaged or that support conditions under the pressure cell changed, given that no evidence of distress was observed on the section and that similar abrupt changes in measurements were not recorded on the other instruments.

5.5.8 Deflection on the Surface (Road Surface Deflectometer)

Figure 5.42 compares elastic surface deflections measured with an RSD on the FDR-FA and FDR-NS (60 mm) sections under a 40 kN half-axle load. Deflections were notably lower on the FDR-FA section, as expected, this being attributed to the higher stiffnesses associated with the stabilized layer. Slight increases in absolute surface deflection were recorded after each load change, but levelled off after initial embedment.

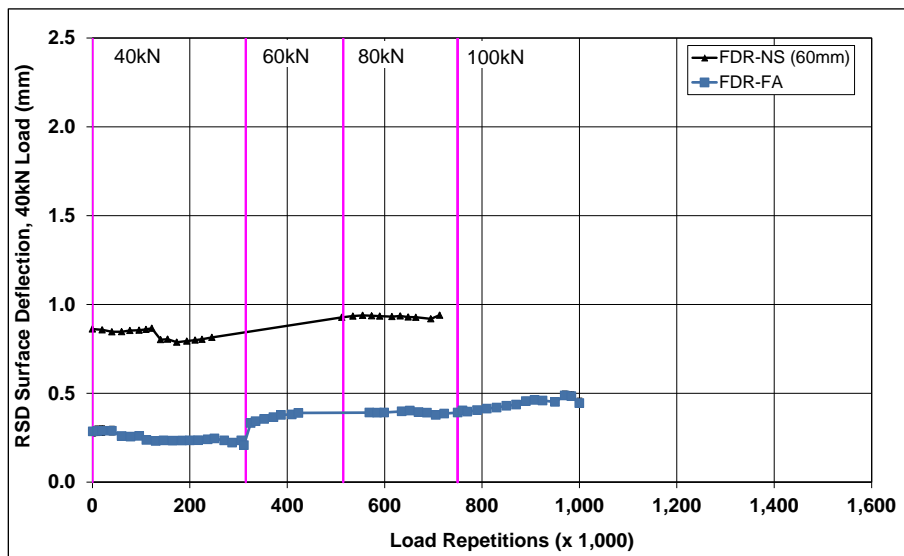


Figure 5.42: 673HB: Surface deflection (RSD).

5.5.9 Deflection in the Underlying Layers (Multi-Depth Deflectometer)

Figure 5.43 shows the history of in-depth elastic deflections, measured by the LVDTs at the top of the existing aggregate base and top of the subgrade in the multi-depth deflectometer in the FDR-FA section. The LVDT at the top of the recycled layer failed early in the experiment and no data is available for this location. The readings are consistent with the surface deflections measured with the RSD, and those recorded on the FDR-NS (60 mm) section. However, the deflections measured were lower than those recorded on the unstabilized sections, as expected due to the higher stiffnesses associated with the stabilized recycled layer. Deflections increased with increased load, as expected, but stabilized after each embedment phase with increasing number of load repetitions, which suggests continued stiffening/densification during HVS trafficking and the absence of any distress in the recycled layer.

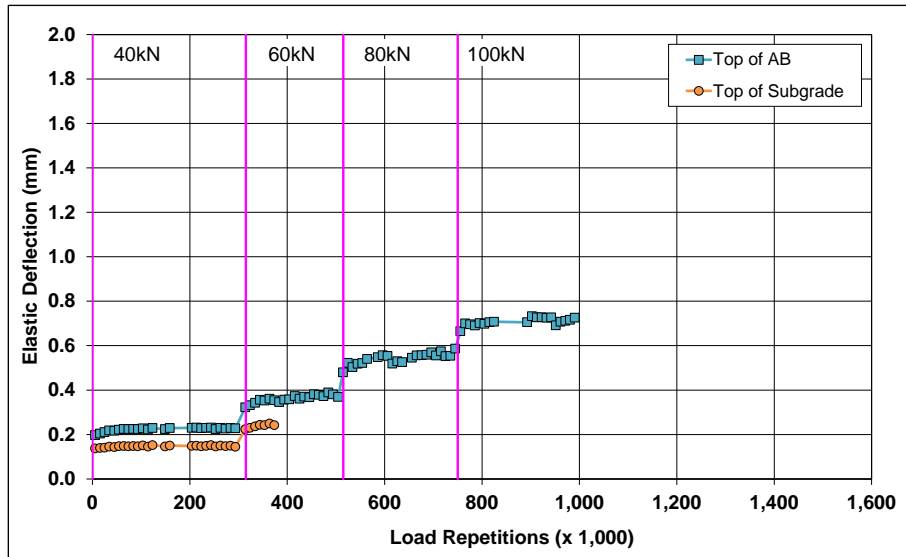


Figure 5.43: 673HB: Elastic deflection in the underlying layers.

5.5.10 Deflection in the Pavement Structure (Falling Weight Deflectometer)

Surface deflection measured with an FWD is summarized in Figure 5.44. Results from the FDR-NS (60 mm) test section are included for comparison. The results were generally consistent with the RSD measurements discussed above, with the section exhibiting a small increase in surface deflection (approximately 150 microns) after completion of HVS trafficking. Deflections in the subgrade did not appear to change during the course of testing.

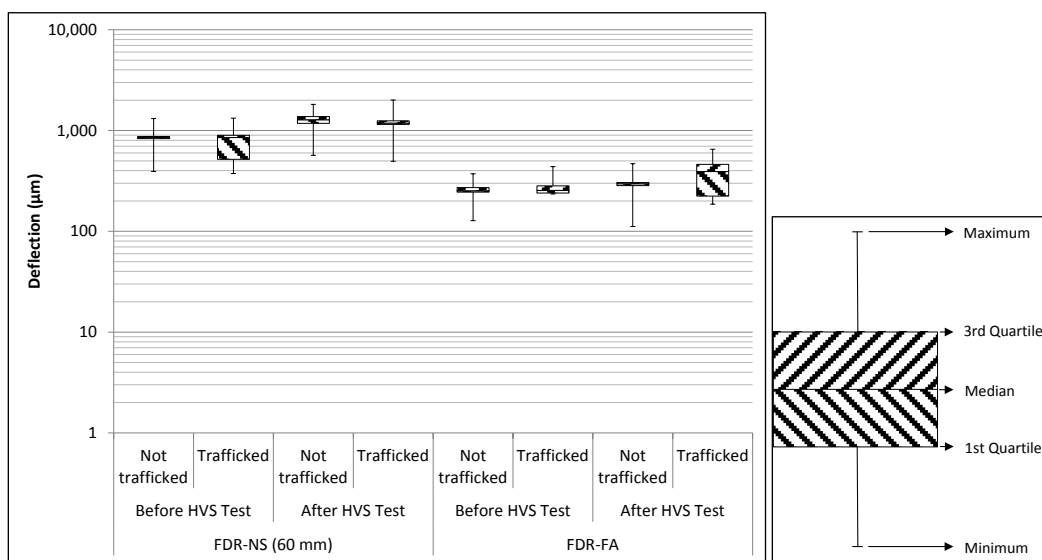


Figure 5.44: 673HB: Surface deflection (FWD).

The recycled layer stiffness was backcalculated from the deflection measurements using the *CalBack* software package, and the results are summarized in Figure 5.45. The stiffness of the FDR-FA stabilized layer was an order of magnitude stiffer than the unstabilized layer in the FDR-NS (60 mm) section, and consistent with data collected on a range of field projects (1). There was a notable drop (~ 3,500 MPa) in the stiffness of the FDR-FA recycled layer after HVS trafficking, which was attributed to some breaking of the asphalt and cement bonds under loading and consequent damage in the form of microcracking. However, the recycled layer stiffness was still significantly higher compared to the FDR-NS (60 mm) section after completion of trafficking (~ 1,500 MPa compared to ~ 150 MPa) despite the significantly higher number of equivalent standard axle loads applied on the FDR-FA section (17,034 million compared to 5,052 million). The presence of the recycled asphalt concrete material did not appear to affect the stiffness of the layer. The stiffness of the untrafficked areas at either end of the test section did not change over time.

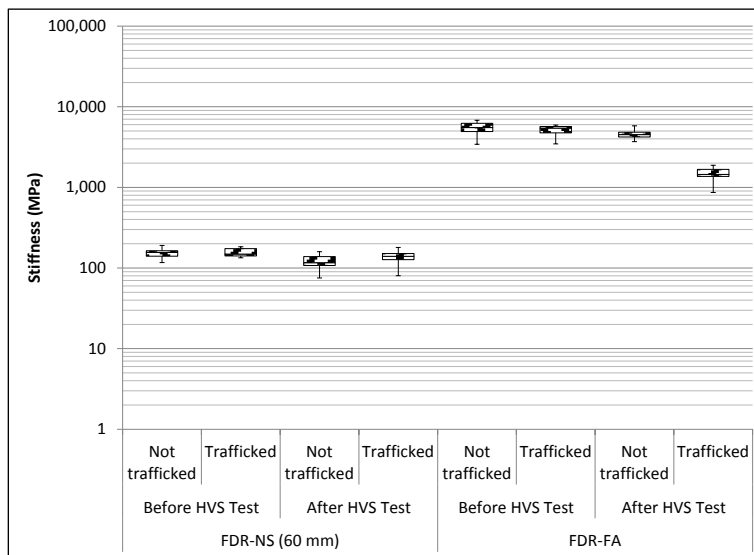


Figure 5.45: 673HB: Backcalculated stiffness of recycled layer (FWD).

5.5.11 Visual Assessment

Apart from rutting, no other distress was recorded on the section. Photographs of the test section after HVS testing are shown in Figure 5.46. The use of a different bituthene tape to cover the wires connecting the MDD resulted in some rubber and adhesive deposits on the surface. A small area of stone loss in the vicinity of Station 8 occurred after removal of one of the adhesive deposits and was not related to the performance of the pavement structure.

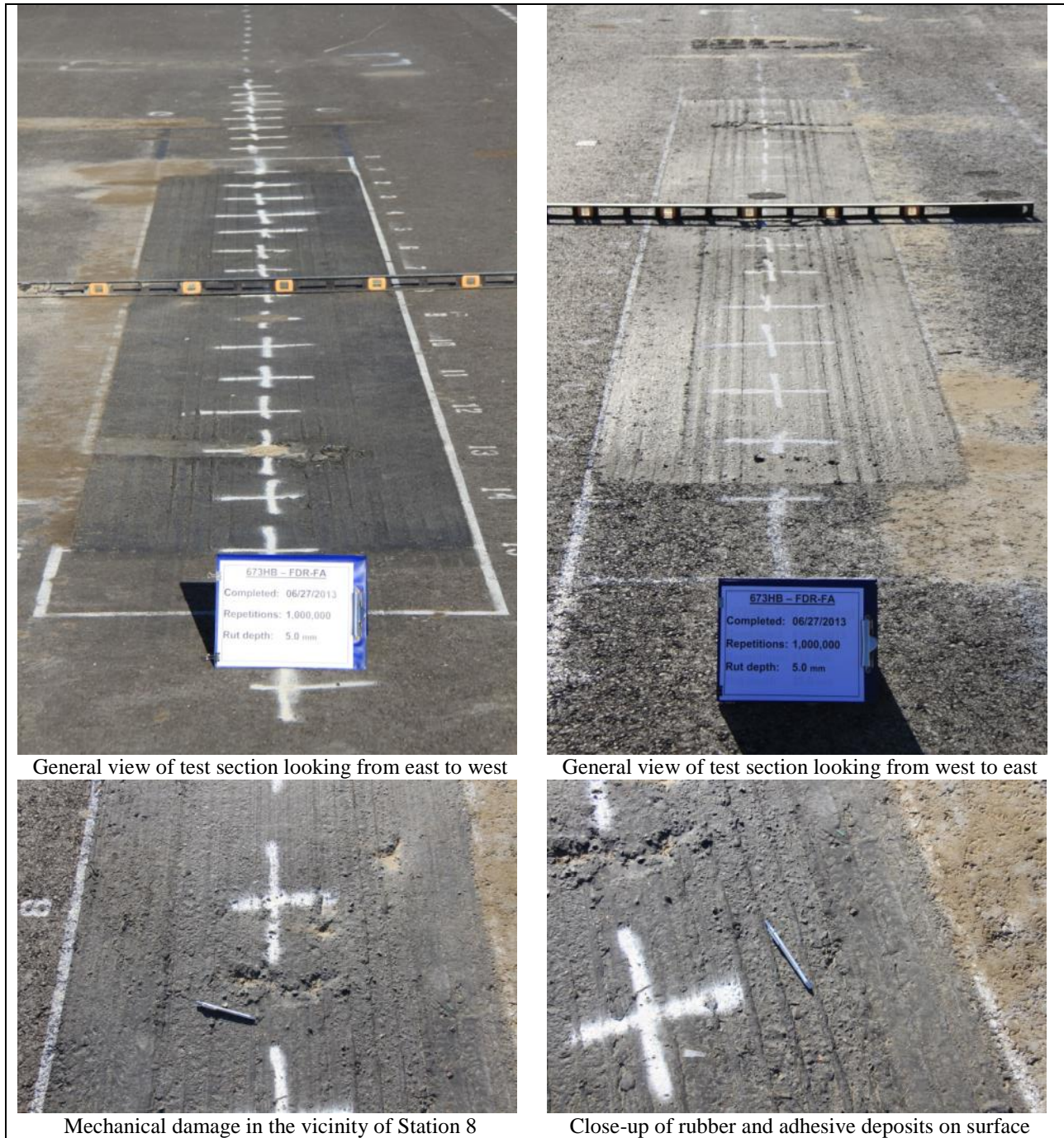


Figure 5.46: 673HB: Test section photographs.

5.6 Section 674HB: Portland Cement (FDR-PC)

5.6.1 Test Summary

Loading commenced with a 40 kN (9,000 lb) half-axle load on August 1, 2013, and ended with a 100 kN (22,500 lb) load on November 6, 2013. A total of 1,560,565 load repetitions were applied and 99 datasets were collected. Loading on this section was terminated at this point, well before the terminal rut or crack

density criteria were reached, in the interests of completing the project within the project time and financial constraints. Load was increased from 40 kN to 60 kN (13,500 lb) and then to 80 kN (18,000 lb) and 100 kN (22,500 lb.) after 315,000, 515,000, and 750,000 load repetitions, respectively. No breakdowns occurred during testing on this section. The HVS loading history for Section 674HB is shown in Figure 5.47.

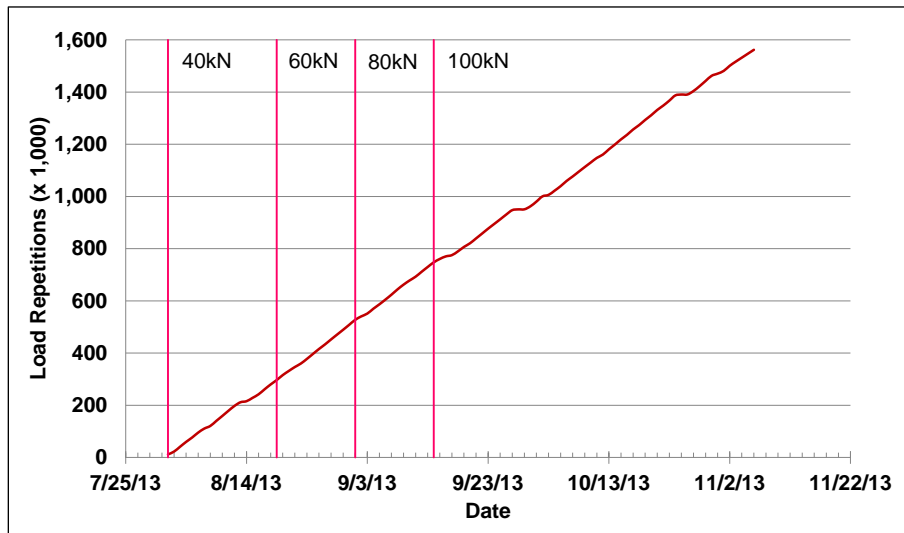


Figure 5.47: 674HB: HVS loading history.

At the start of the test, moisture contents in the recycled layer, original aggregate base, and subgrade layers were 1.8, 6.0, and 12.6 percent of the dry weight of the materials, respectively.

5.6.2 Air Temperatures

Outside Air Temperatures

Daily average outside air temperatures are summarized in Figure 5.48. Vertical error bars on each point on the graph show the daily temperature range. Temperatures ranged from 6°C to 38°C (43°F to 100°F) during the course of HVS testing, with a daily average of 22°C (72°F), an average minimum of 15°C (59°F), and an average maximum of 30°C (86°F).

Air Temperatures in the Environmental Chamber

During the test, air temperatures inside the temperature control chamber ranged from 15°C to 36°C (59°F to 97°F) with an average of 27°C (81°F) and a standard deviation of 2.4°C (4.3°F). Air temperature was adjusted to maintain a pavement temperature of 30°C±4°C (86°F±7°F) at a pavement depth of 50 mm (2.0 in.). The recorded pavement temperatures discussed in Section 5.6.3 indicate that the inside air temperatures were adjusted appropriately to maintain the required pavement temperature. The daily

average air temperatures recorded in the environmental chamber, calculated from the hourly temperatures recorded during HVS operation, are shown in Figure 5.49. Vertical error bars on each point on the graph show the daily temperature range.

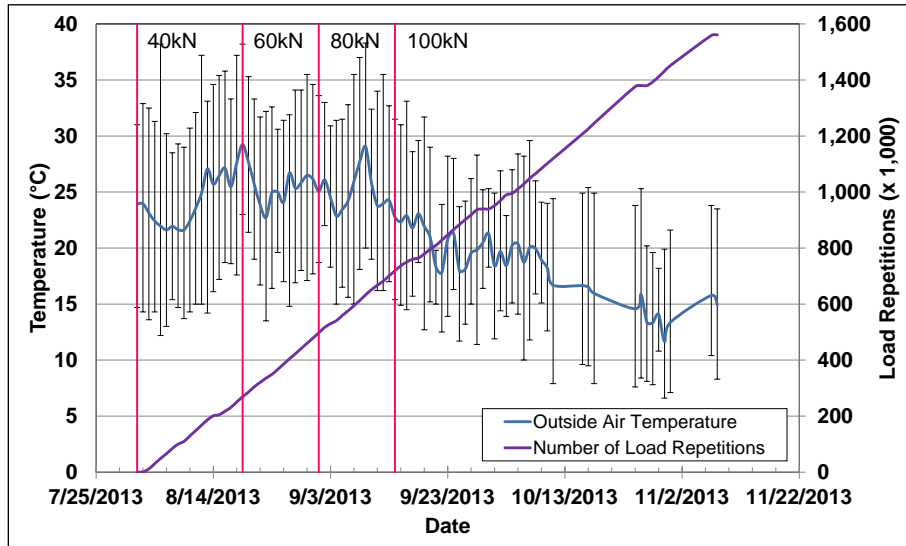


Figure 5.48: 674HB: Daily average air temperatures outside the environmental chamber.

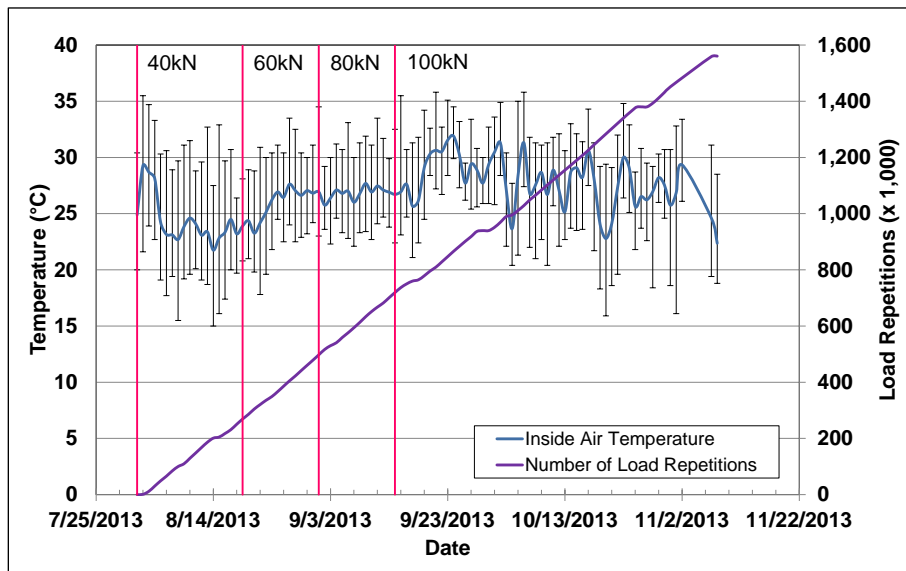


Figure 5.49: 674HB: Daily average air temperatures inside the environmental chamber.

5.6.3 Pavement Temperatures

Daily averages of the surface and in-depth temperatures of the asphalt concrete and recycled layers are listed in Table 5.7 and shown in Figure 5.50. Pavement temperatures increased slightly with increasing

depth in the asphalt concrete. Temperatures were consistent throughout the measured depth of the pavement.

Table 5.7: 674HB: Temperature Summary for Air and Pavement

Temperature	Layer	Average (°C)	Std. Dev. (°C)	Average (°F)	Std. Dev. (°F)
Outside air	-	22	4.1	72	7.4
Inside air	-	27	2.4	81	4.3
Pavement surface	AC	29	0.8	84	1.4
- 25 mm below surface	AC	29	0.8	84	1.4
- 50 mm below surface	AC	29	0.8	84	1.4
- 90 mm below surface	FDR	29	0.7	84	1.3
- 120 mm below surface	FDR	29	0.7	84	1.3

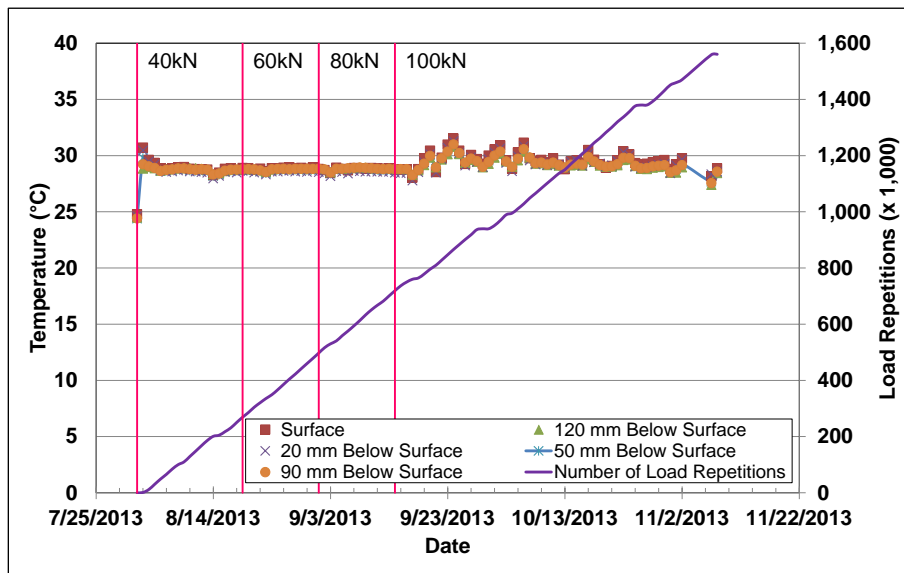


Figure 5.50: 674HB: Daily average pavement temperatures.

5.6.4 Permanent Deformation on the Surface (Rutting)

Figure 5.51 shows the average transverse cross section measured with the laser profilometer at various stages of the test and illustrates the increase in rutting and deformation over the duration of the test. Figure 5.52 shows the development of permanent deformation (average maximum rut and average deformation) with load repetitions for the test section. The results for the FDR-NS (60 mm) section are shown for comparison. The two plots show that most of the deformation was in the form of a depression rather than upward and outward displacement of the material above the zero elevation point. The plots also show similar performance trends to that measured on the FDR-FA section (Section 673HB).

The embedment phase on the FDR-PC section was very short with very little measurable rutting. The average maximum total rut at the end of the embedment phase was about 1.0 mm (0.04 in.). The rate of rut depth increase after the embedment phase was also very slow compared to that on the two sections with

unstabilized bases (Sections 672HB and 677HC), which was attributed to the much stiffer nature of the stabilized recycled material. A short embedment phase with increased rate of rutting was evident after the 100 kN load change, but not after the earlier load changes to 60 kN and 80 kN. The rate of rut depth increased very slowly during the course of loading. Error bars on the average maximum total rut reading indicate that there was very little variation along the length of the section. The test was halted when the average maximum total rut depth reached 3.0 mm (0.12 in.) due to time and budget limitations.

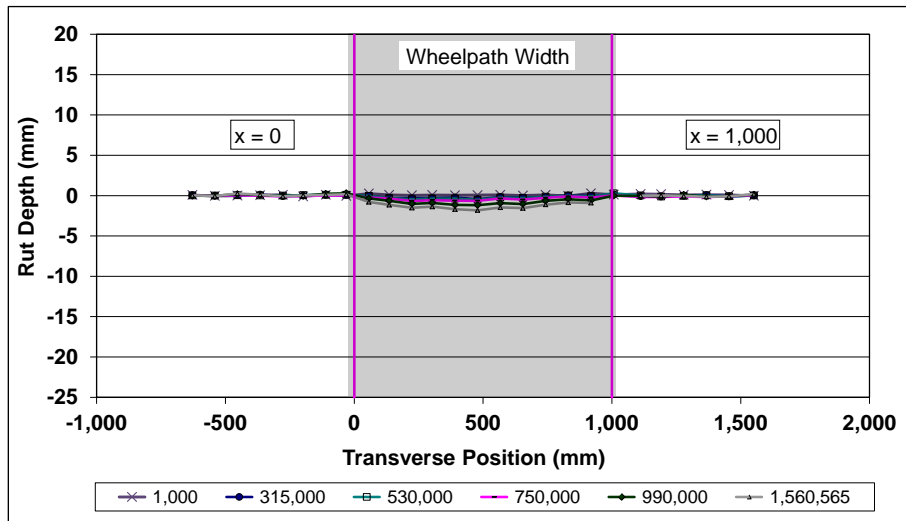


Figure 5.51: 674HB: Profilometer cross section at various load repetitions.

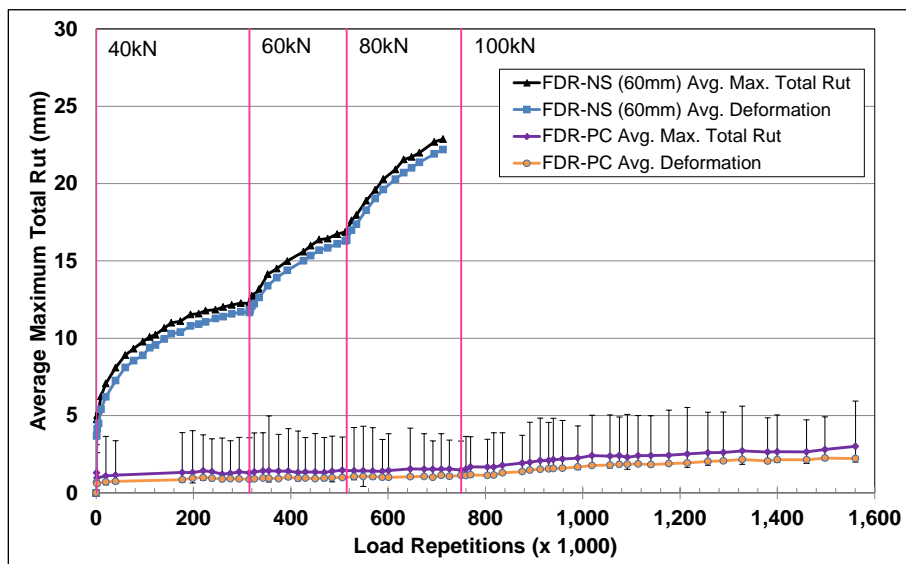


Figure 5.52: 674HB: Average maximum total rut and average deformation.

Figure 5.53 shows contour plots of the pavement surface at the start and end of the test (1,560,565 load repetitions). The plot shows the relative uniformity of the rut depth over the length of the section. After

completion of trafficking, the average total maximum rut depth and the average deformation were 3.0 mm (0.12 in.) and 2.2 mm (0.09 in.), respectively. The maximum rut depth measured on the section was 5.9 mm (0.23 in.), recorded at Station 13, close to the wheel stop/start location.

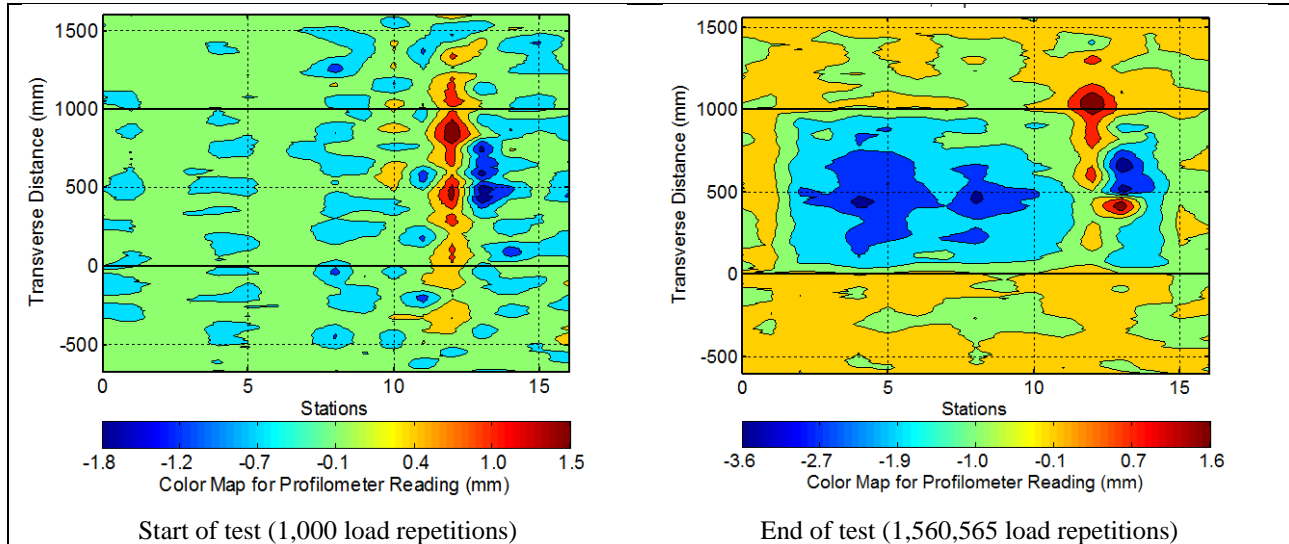


Figure 5.53: 674HB: Contour plots of permanent surface deformation.
(Note different scales in legends.)

5.6.5 Permanent Deformation in the Underlying Layers

Permanent deformation in the underlying layers, recorded with a multi-depth deflectometer (MDD) at Station 13 and compared to the surface layer laser profilometer measurements is shown in Figure 5.54.

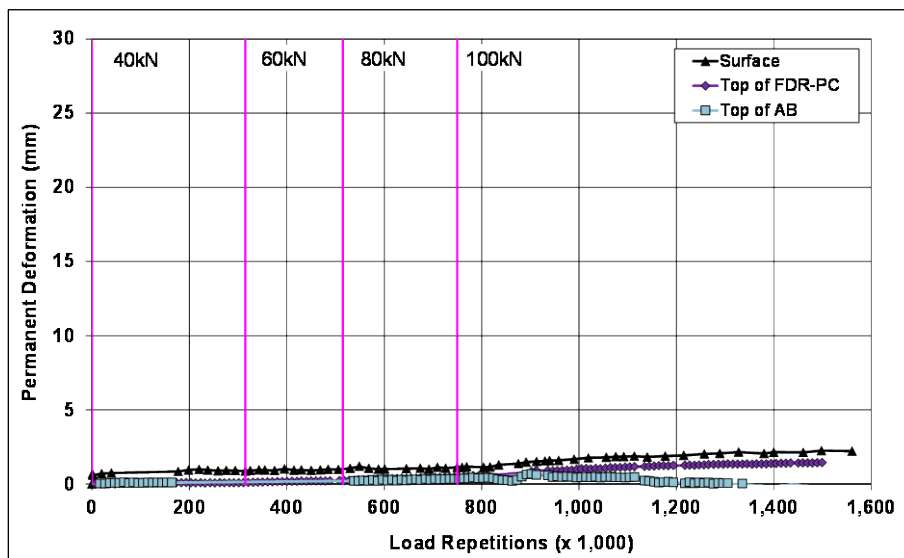


Figure 5.54: 674HB: Permanent deformation in the underlying layers.

The MDD measurements were consistent with the laser profilometer measurements. The LVDT at the top of the subgrade failed early in the test and consequently there were no measurements for this location in the pavement structure. Deformation in each of the layers is summarized in Table 5.8 with an assumption made for the subgrade layer (results for the FDR-NS [60 mm] section are included for comparison). Very little deformation was measured on this test section, with small contributions (< 1.0 mm) attributed to each layer. A forensic investigation will be undertaken on completion of the Phase 2 HVS testing to validate these measurements.

Table 5.8: 674HB: Deformation in Each Layer

Layer	Layer Thickness		674HB		672HB	
			Deformation at End of Test ¹		Deformation at End of Test ²	
	(mm)	(in.)	(mm)	(in.)	(mm)	(in.)
Surface	60	2.4	0.9	0.04	3.6	0.14
Recycled	250	10.0	0.9	0.04	11.9	0.47
Aggregate Base	320	12.6	0.5	0.02	7.3	0.29
Subgrade	-	-	0.0 ³	0.09	1.6	0.06
Total MDD Measured Deformation			2.3	0.16	24.4	0.96
Laser Measured Deformation at Station 13			2.3	0.16	24.4	0.96

¹ 1,560,565 load repetitions (~ 43,334,874 ESALs)
² 713,000 load repetitions (~ 5,5052,104 ESALs)
³ Assumed value

5.6.6 Tensile Strain at the Bottom of the Asphalt Concrete Layer

Figure 5.55 shows the traffic-induced tensile strain at the bottom of the asphalt concrete layer. Transverse strain measurements from the FDR-NS (60 mm) section are included in the figure for comparison.

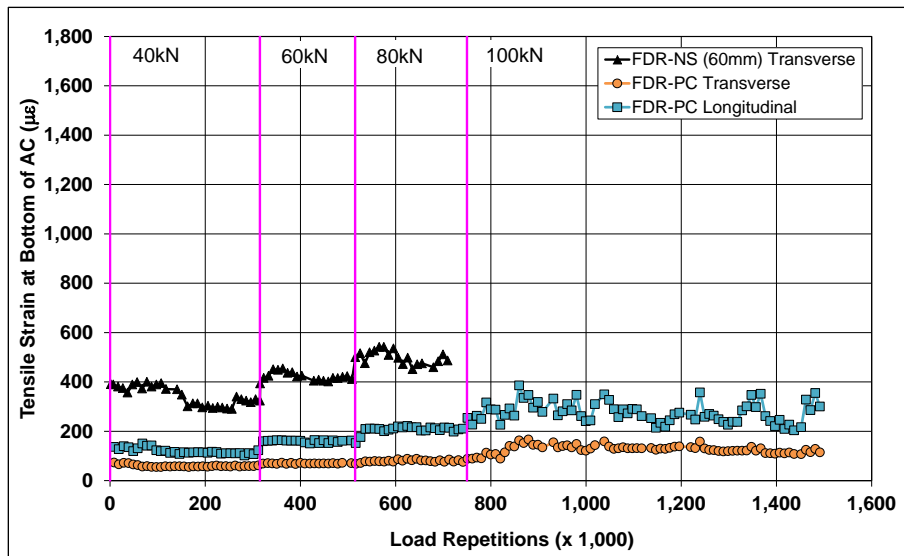


Figure 5.55: 674HB: Tensile strain at the bottom of the asphalt concrete layer.

Strains were generally low on the FDR-PC section, this being attributed to the very stiff recycled layer underneath the strain gauges. Longitudinal strains were slightly higher than the transverse strains, and increased after each load change. The longitudinal strains also showed some variability after the load change to 100 kN. This was attributed to a combination of temperature changes and their effect on microcracks under the strain gauge, which were related to damage in the layer caused by the heavier loads. Transverse strains remained constant throughout the first three loading cycles (40 kN, 60 kN, and 80 kN), but increased slightly after the load change to 100 kN, indicating that some damage (e.g., microcracks) had resulted from the heavier loading. However, transverse strain did not continue to increase, indicating that the integrity of the layer was not deteriorating at the time the testing was halted. No surface distresses associated with the increase in strain measured in the recycled layer were noted during the course of the study.

5.6.7 Vertical Pressure at the Top of the Recycled Layer

Figure 5.56 shows the comparison of traffic-induced vertical pressure at the top of the recycled base layer for the FDR-NS (60 mm) and FDR-PC sections. Pressure readings were stable and sensitive to load changes for most of the FDR-PC test. Initial pressure dropped considerably on the FDR-PC section, which was unexpected given that layer elastic theory would suggest higher pressures considering the much higher stiffness of the FDR-PC section. This anomaly could be attributed to movement of the gauge. After the first load change, the pressure readings appeared to stabilize and increases were consistent with later load changes. Variability and a reduction in recorded pressures after the load change to 100 kN were attributed to problems with the instrument at the higher load level.

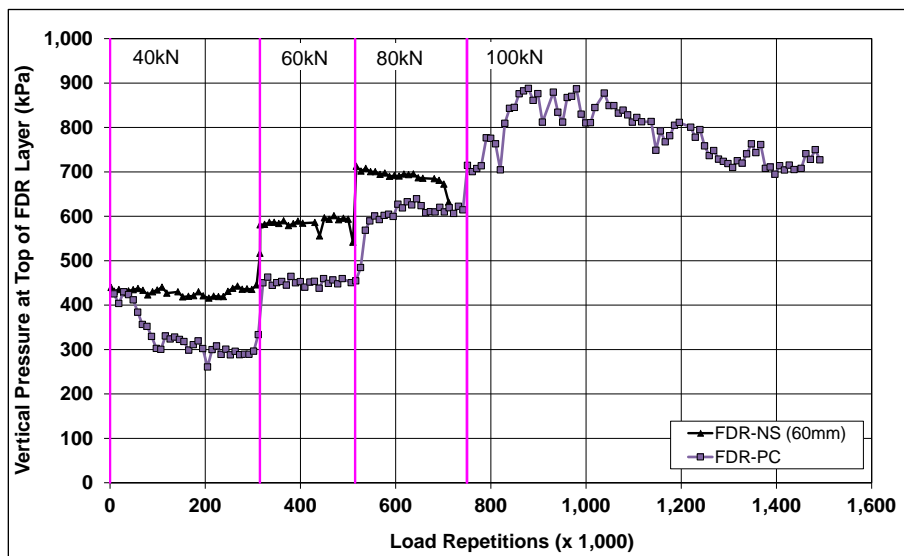


Figure 5.56: 674HB: Vertical pressure at the top of the recycled layer.

5.6.8 Deflection on the Surface (Road Surface Deflectometer)

Figure 5.57 compares elastic surface deflections measured with an RSD on the FDR-PC and FDR-NS (60 mm) sections under a 40 kN half-axle load. Deflections were notably lower on the FDR-PC section, as expected, this being attributed to the higher stiffnesses associated with the stabilized layer. Slight increases in absolute surface deflection were recorded after each load change, but levelled off after initial embedment.

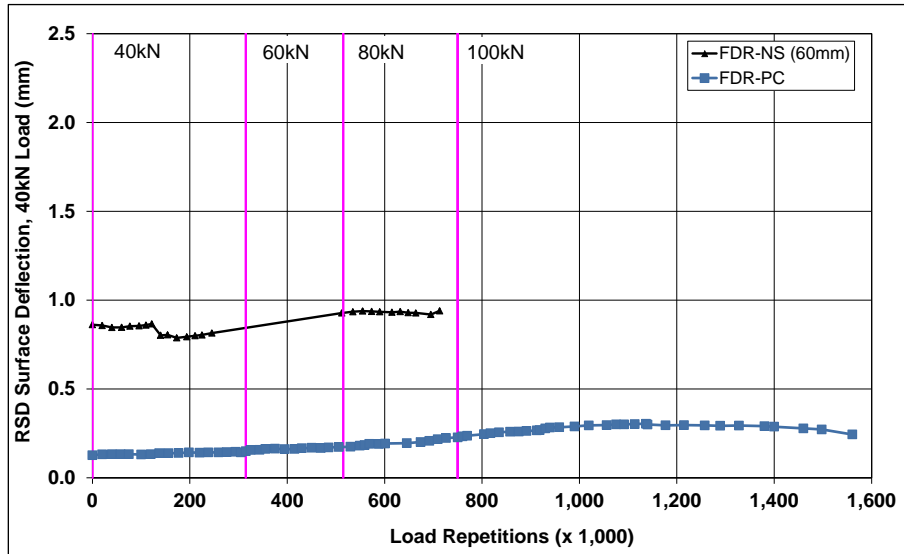


Figure 5.57: 674HB: Surface deflection (RSD).

5.6.9 Deflection in the Underlying Layers (Multi-Depth Deflectometer)

Figure 5.58 shows the history of in-depth elastic deflections measured by the LVDTs at the top of the recycled layer and top of existing aggregate base in the multi-depth deflectometer in the FDR-PC section. The LVDT at the top of the subgrade failed early in the experiment and no data is available for this location. The readings are consistent with the surface deflections measured with the RSD, and those recorded on the FDR-NS (60 mm) section. However, the deflections measured were lower than those recorded on the unstabilized sections, as expected due to the higher stiffnesses associated with the stabilized recycled layer. Deflections increased with increased load, as expected, but stabilized after each embedment phase with increasing number of load repetitions, suggesting the absence of any significant distress in the recycled layer.

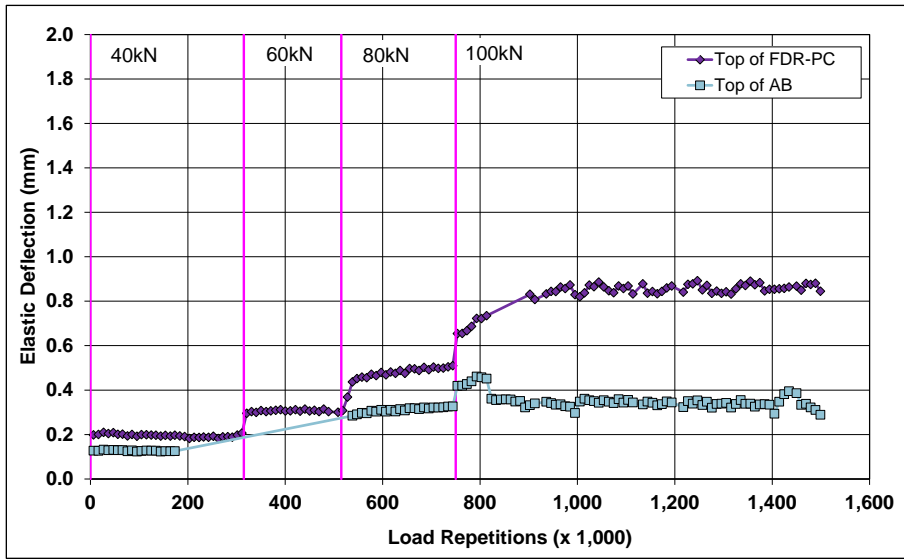


Figure 5.58: 674HB: Elastic deflection in the underlying layers.

5.6.10 Deflection in the Pavement Structure (Falling Weight Deflectometer)

Surface deflection measured with an FWD is summarized in Figure 5.59. Results from the FDR-NS (60 mm) test section are included for comparison. The results were generally consistent with the RSD measurements discussed above, with the section exhibiting very little change in surface deflection after completion of HVS trafficking. Deflections in the subgrade did not appear to change during the course of testing.

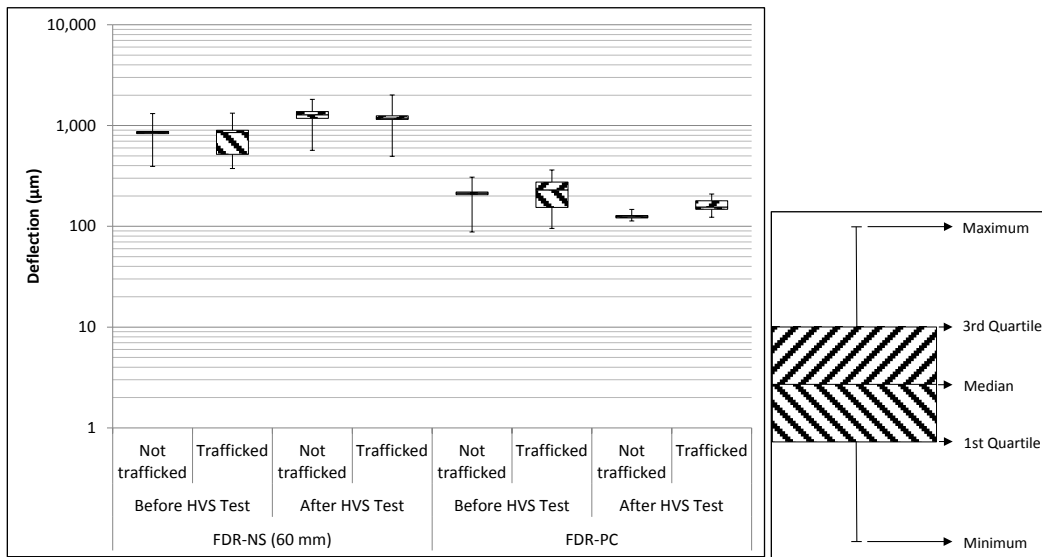


Figure 5.59: 674HB: Surface deflection (FWD).

The recycled layer stiffness was backcalculated from the deflection measurements using the *CalBack* software package, and the results are summarized in Figure 5.60. The stiffness of the cement-stabilized layer was an order of magnitude stiffer than the unstabilized layer in the FDR-NS (60 mm) section. There was, however, a notable drop (~ 7,000 MPa) in the stiffness of the recycled layer after HVS trafficking, which was attributed to breaking of the cement bonds under loading and consequent damage in the form of microcracking. However, the recycled layer stiffness was still significantly higher compared to the recycled layer in the FDR-NS (60 mm) section after completion of trafficking (~ 6,000 MPa compared to ~ 150 MPa) despite the significantly higher number of equivalent standard axle loads applied on the FDR-PC section (43,334 million compared to 5,052 million). The presence of the recycled asphalt concrete material did not appear to affect the stiffness of the layer. The stiffness of the untrafficked areas at either end of the test section did not change over time.

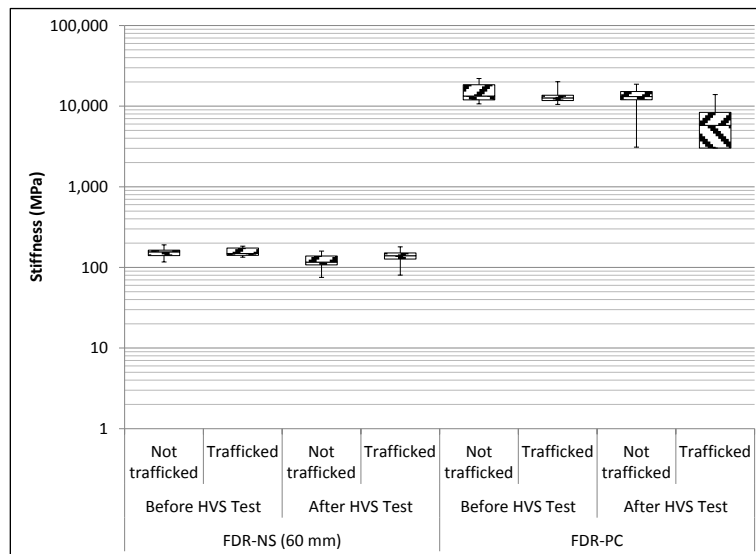


Figure 5.60: 674HB: Backcalculated stiffness of recycled layer (FWD).

5.6.11 Visual Assessment

Apart from rutting, no other distress was recorded on the section. Photographs of the test section after HVS testing are shown in Figure 5.61.

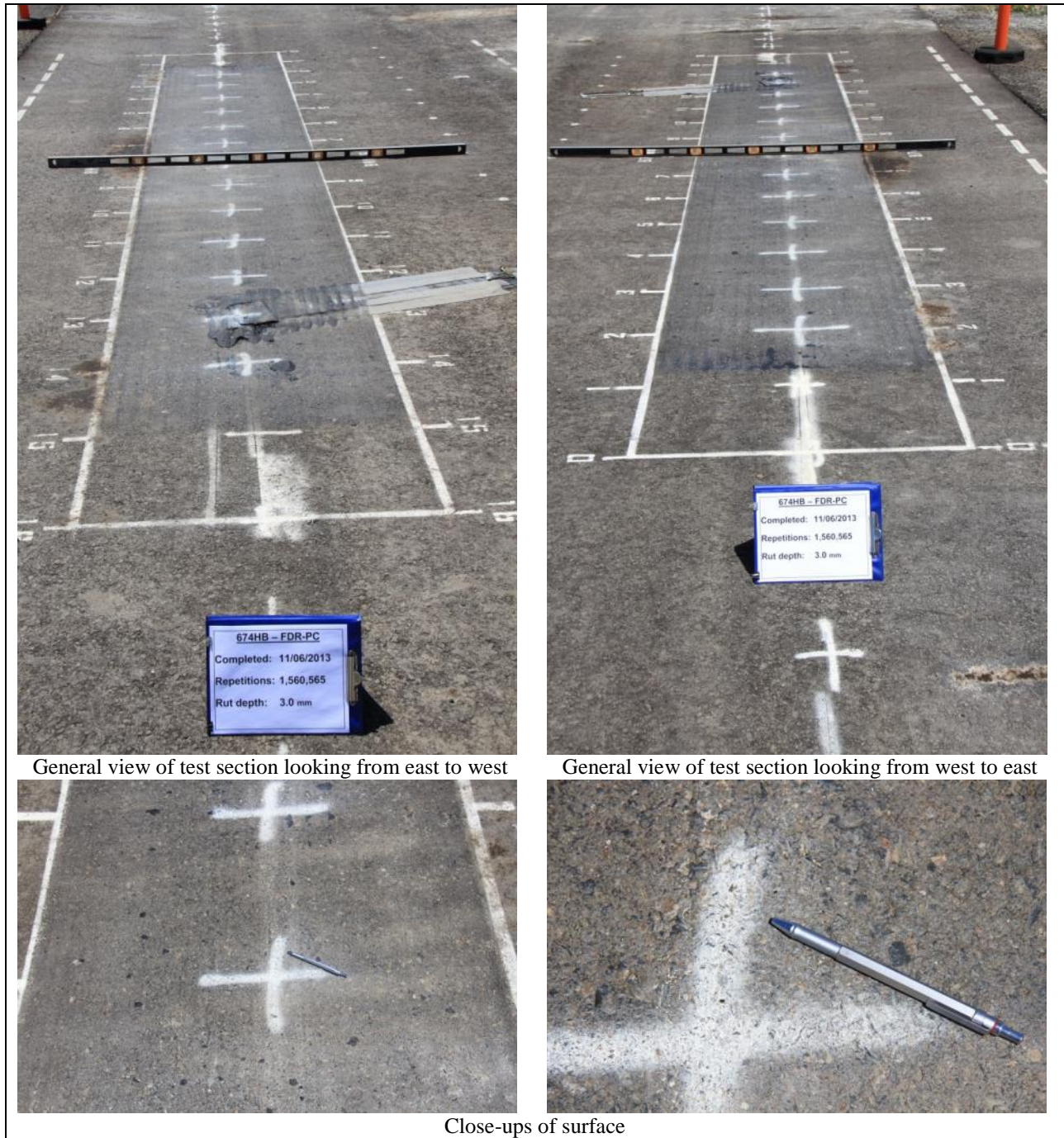


Figure 5.61: 674HB: Test section photographs.

5.7 Section 675HC: Engineered Emulsion (FDR-EE #1)

5.7.1 Test Summary

Loading commenced with a 40 kN (9,000 lb) half-axle load on October 7, 2013, and ended on October 12, 2013. A total of just 61,500 load repetitions were applied and six datasets were collected. Load was not

increased. No breakdowns occurred during testing on this section. The HVS loading history for Section 675HC is shown in Figure 5.62.

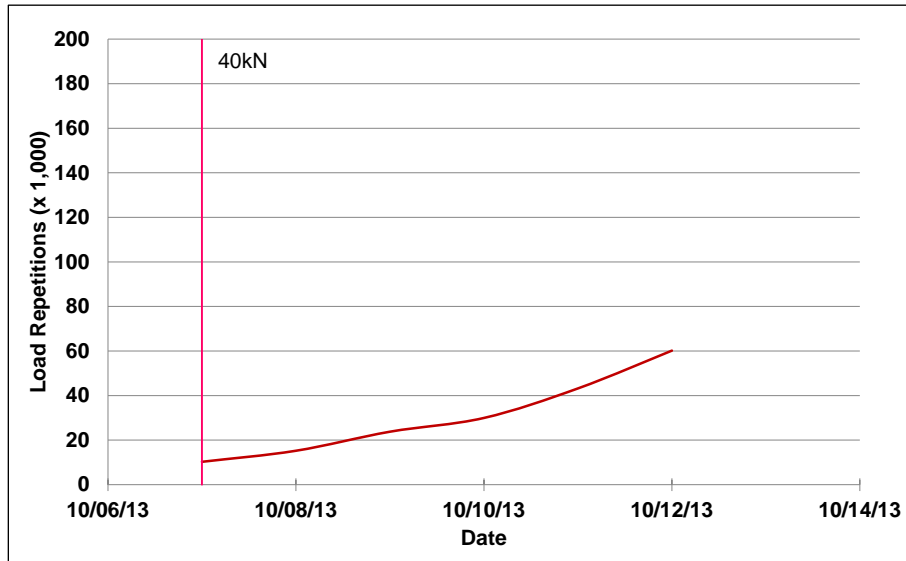


Figure 5.62: 675HC: HVS loading history.

At the start of the test, moisture contents in the recycled layer, original aggregate base, and subgrade layers were 6.0, 5.5, and 13.1 percent of the dry weight of the materials, respectively.

5.7.2 Air Temperatures

Outside Air Temperatures

Daily average outside air temperatures are summarized in Figure 5.63. Vertical error bars on each point on the graph show the daily temperature range. Temperatures ranged from 6°C to 32°C (43°F to 90°F) during the course of HVS testing, with a daily average of 26°C (79°F), an average minimum of 12°C (54°F), and an average maximum of 18°C (64°F).

Air Temperatures in the Environmental Chamber

During the test, air temperatures inside the temperature control chamber ranged from 22°C to 33°C (72°F to 91°F) with an average of 27°C (81°F) and a standard deviation of 1.3°C (2.3°F). Air temperature was adjusted to maintain a pavement temperature of 30°C±4°C (86°F±7°F) at a pavement depth of 50 mm (2.0 in.). The recorded pavement temperatures discussed in Section 5.7.3 indicate that the inside air temperatures were adjusted appropriately to maintain the required pavement temperature. The daily average air temperatures recorded in the environmental chamber, calculated from the hourly temperatures recorded during HVS operation, are shown in Figure 5.64. Vertical error bars on each point on the graph show the daily temperature range.

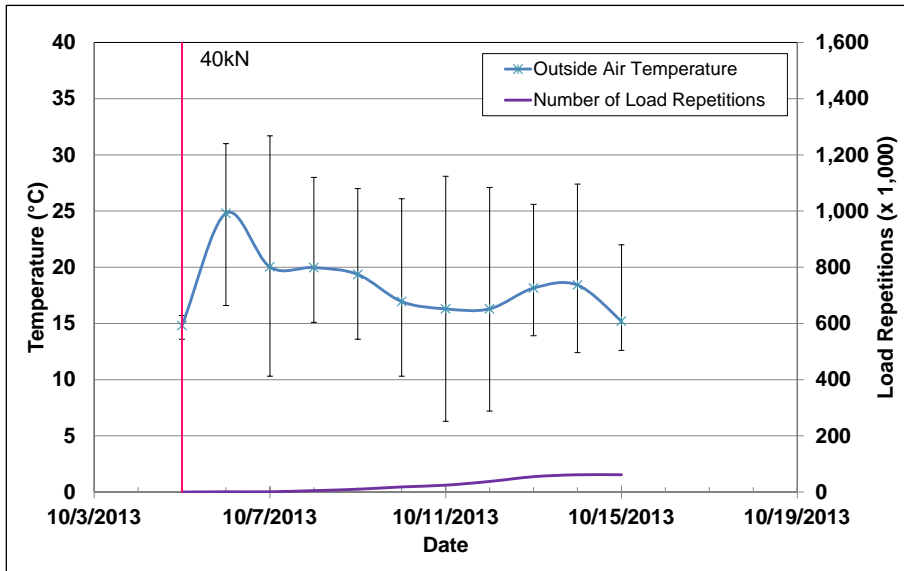


Figure 5.63: 675HC: Daily average air temperatures outside the environmental chamber.

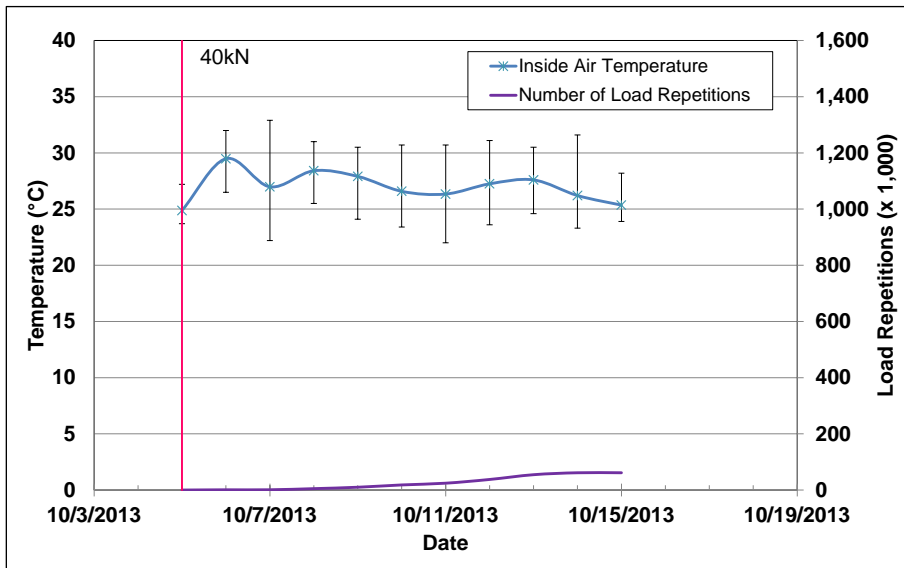


Figure 5.64: 675HC: Daily average air temperatures inside the environmental chamber.

5.7.3 Pavement Temperatures

Daily averages of the surface and in-depth temperatures of the asphalt concrete and recycled layers are listed in Table 5.9 and shown in Figure 5.65. Pavement temperatures increased slightly with increasing depth in the asphalt concrete. Temperatures were consistent throughout the measured depth of the pavement.

Table 5.9: 675HC: Temperature Summary for Air and Pavement

Temperature	Layer	Average (°C)	Std. Dev. (°C)	Average (°F)	Std. Dev. (°F)
Outside air	-	26	2.8	79	5.0
Inside air	-	27	1.3	81	2.3
Pavement surface	AC	29	0.4	84	0.7
- 25 mm below surface	AC	29	0.4	84	0.7
- 50 mm below surface	AC	29	0.3	84	0.5
- 90 mm below surface	FDR	29	0.3	84	0.5
- 120 mm below surface	FDR	29	0.3	84	0.5

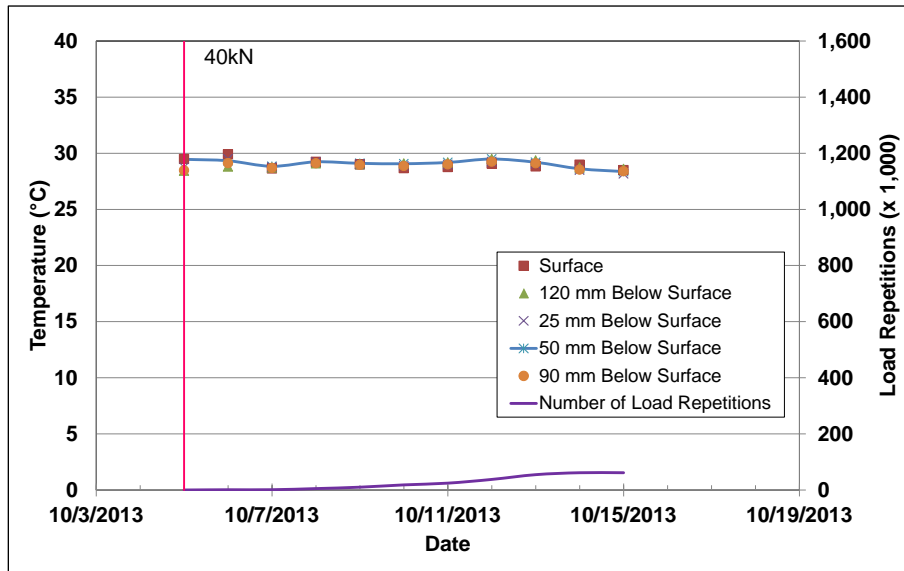


Figure 5.65: 675HC: Daily average pavement temperatures.

5.7.4 Permanent Deformation on the Surface (Rutting)

Figure 5.66 shows the average transverse cross section measured with the laser profilometer at various stages of the test and illustrates the rapid increase in rutting and deformation over the short duration of trafficking that was attributed to the construction problems (excess fluids, poor distribution of asphalt emulsion, poor compaction, and slow rate of curing) discussed in Section 3.5.2. Figure 5.67 shows the development of permanent deformation (average maximum rut and average deformation) with load repetitions for the test section. The results for the FDR-NS (60 mm) section are shown for comparison. The two plots show that depression and upward and outward displacement (shear) both contributed to the average maximum total rut depth. The rate of rut depth increase of this test was very high and the test was terminated before the embedment phase was complete given that the terminal rut depth (12.5 mm [0.5 in.]) had already been exceeded.

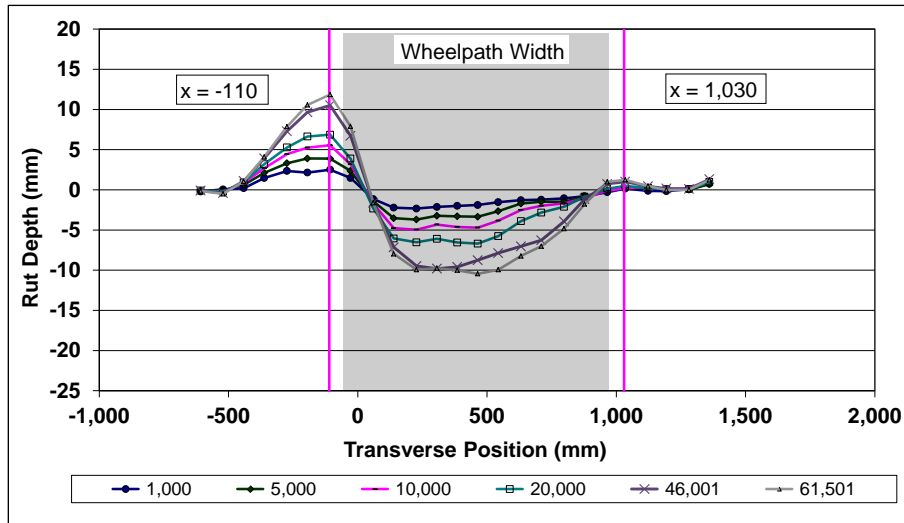


Figure 5.66: 675HC: Profiler cross section at various load repetitions.

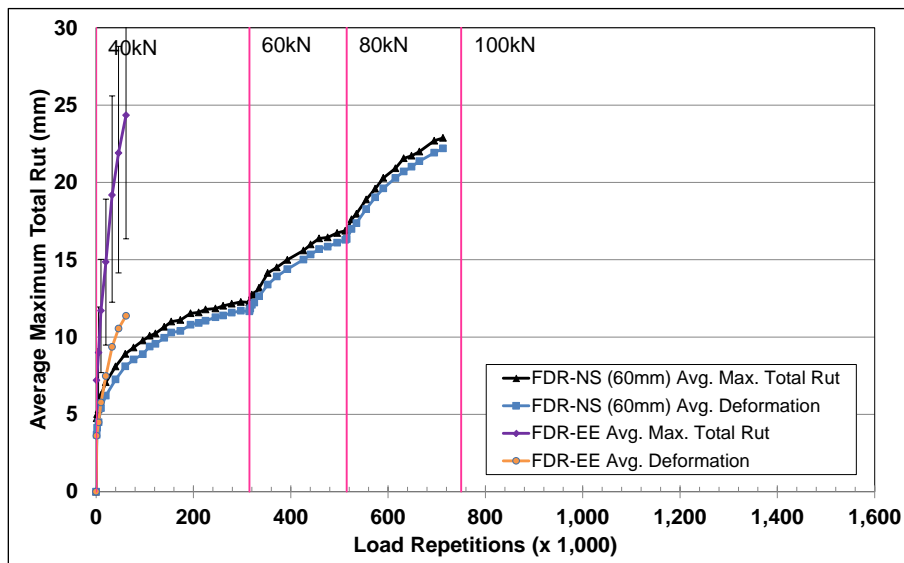


Figure 5.67: 675HC: Average maximum total rut and average deformation.

Figure 5.68 shows contour plots of the pavement surface at the start and end of the test (61,500 load repetitions). The plot indicates that the deepest rut and area with the most sheared material were between Stations 8 and 16. Terminal rut (12.5 mm [0.5 in.]) was reached after just 14,000 load repetitions.

After completion of trafficking, the average maximum total rut depth and the average deformation were 24.4 mm (0.96 in.) and 11.4 mm (0.45 in.), respectively. The maximum rut depth measured on the section was 44.6 mm (1.76 in.), recorded at Station 13. The maximum height of displaced material was 26.6 mm (1.05 in.), also measured at Station 13.

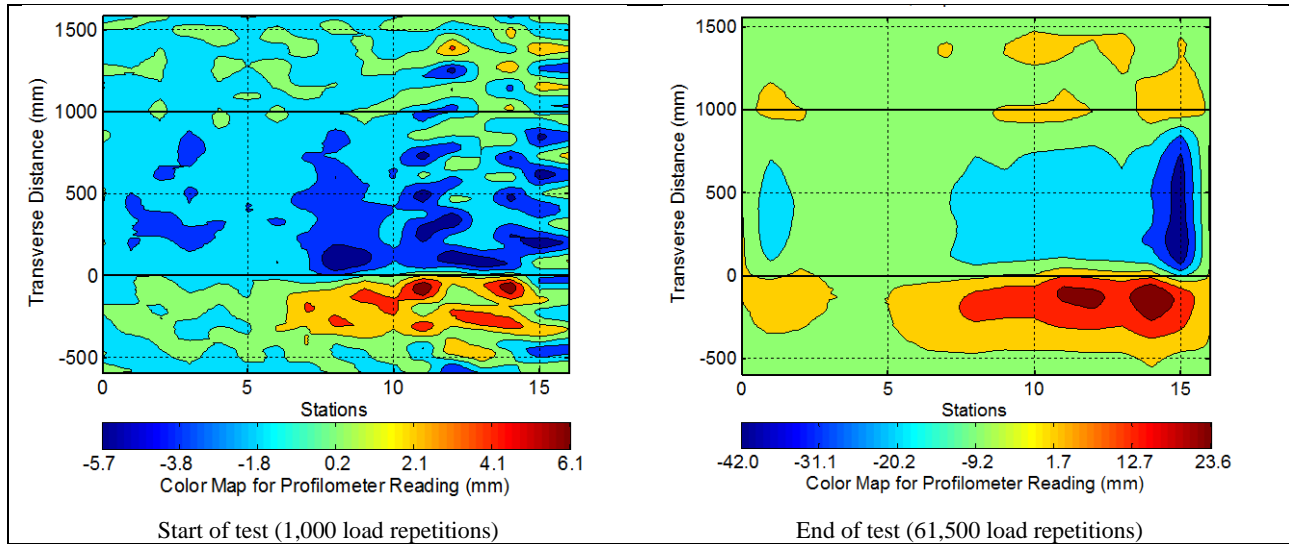


Figure 5.68: 675HC: Contour plots of permanent surface deformation.
 (Note different scales in legends.)

5.7.5 Permanent Deformation in the Underlying Layers

Permanent deformation in the underlying layers, recorded with a multi-depth deflectometer (MDD) at Station 13 and compared to the surface layer laser profilometer measurements is shown in Figure 5.69.

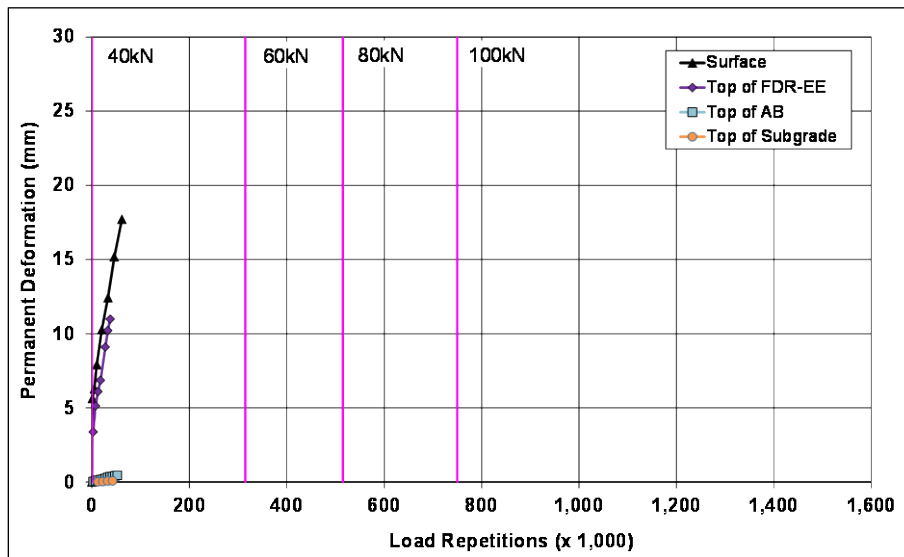


Figure 5.69: 675HC: Permanent deformation in the underlying layers.

The MDD measurements were consistent with the laser profilometer measurements. Deformation in each of the layers is summarized in Table 5.10 (results for the FDR-NS [60 mm] section are included for comparison purposes). After 14,000 load repetitions, when the terminal rut for the test (average maximum total rut [12.5 mm] measured over the full section) was reached, all of the deformation at Station 13 was in

the asphalt concrete surfacing and recycled base. At the end of the test, after 61,500 load repetitions, most of the deformation (10.5 mm [0.41 in.]) was in the recycled base, followed by the asphalt concrete surfacing (7.7 mm [0.3 in.]). Very little permanent deformation was recorded in the existing aggregate base and subgrade. A forensic investigation will be undertaken on completion of the Phase 2 HVS testing to validate these measurements.

Table 5.10: 675HC: Deformation in Each Layer

Layer	Layer Thickness		675HC		675HC		672HB	
			Deformation at Terminal Rut ¹		Deformation at End of Test ²		Deformation at Terminal Rut ¹	
	(mm)	(in.)	(mm)	(in.)	(mm)	(in.)	(mm)	(in.)
Surface	60	2.4	4.6	0.18	7.7	0.30	4.2	0.17
Recycled	250	10.0	5.0	0.20	10.5	0.41	8.5	0.33
Aggregate Base	320	12.6	0.1	0.00	0.4	0.02	2.3	0.09
Subgrade	-	-	0.0	0.00	0.1	0.00	0.4	0.02
Total MDD Measured Deformation			9.7	0.38	17.7	0.70	15.4	0.61
Laser Measured Deformation at Station 13			9.7	0.38	17.7	0.70	15.4	0.61

¹ Terminal rut for test section ² 61,500 load repetitions (~ 61,500 ESALs)

5.7.6 Tensile Strain at the Bottom of the Asphalt Concrete Layer

Figure 5.70 shows the peak traffic-induced tensile strain at the bottom of the asphalt concrete layer. Transverse strain measurements from the FDR-NS (60 mm) section are included in the figure for comparison. Strains increased significantly from the start of the test and were consistent with the early severe deformation that was measured on the section and which is discussed in Sections 5.7.4 and 5.7.5. These problems were attributed to the construction issues discussed in Section 3.5.2.

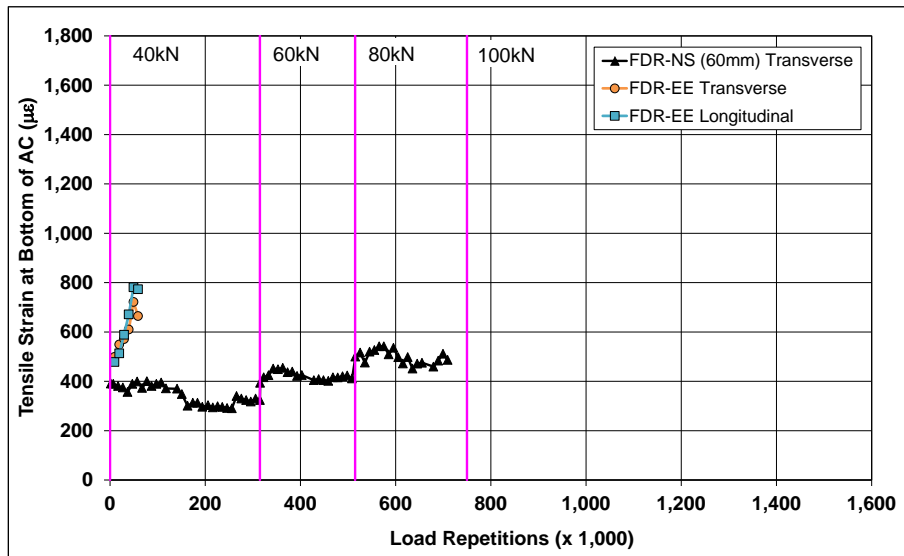


Figure 5.70: 675HC: Tensile strain at the bottom of the asphalt concrete layer.

5.7.7 Vertical Pressure at the Top of the Recycled Layer

Figure 5.71 shows the comparison of traffic-induced vertical pressure at the top of the recycled base layer for the FDR-NS (60 mm) and FDR-EE sections. Pressure readings increased significantly from the start of the test on the FDR-EE section and were consistent with readings from the other instruments and with the surface deformation observed. This performance was attributed to the construction problems discussed in Section 3.5.2.

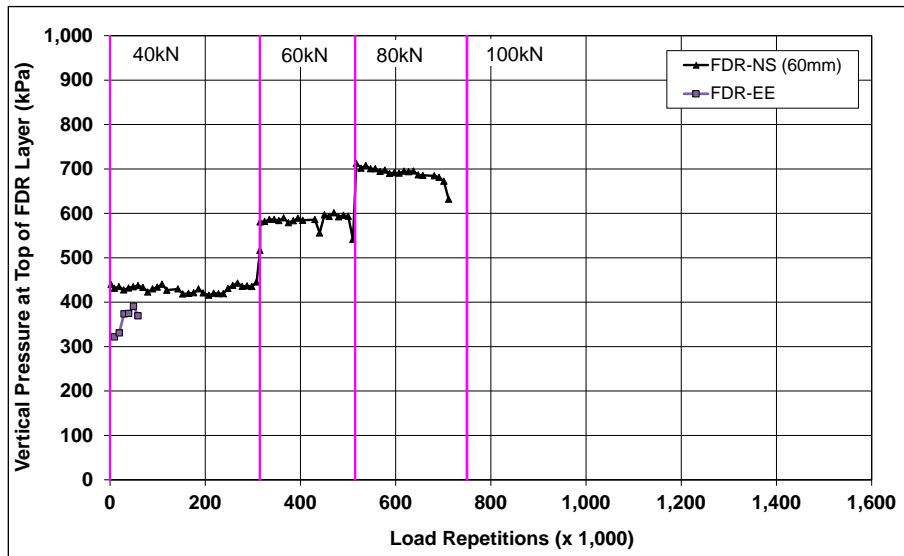


Figure 5.71: 675HC: Vertical pressure at the top of the recycled layer.

5.7.8 Deflection on the Surface (Road Surface Deflectometer)

Figure 5.72 compares elastic surface deflections measured with an RSD on the FDR-EE and FDR-NS (60 mm) sections under a 40 kN half-axle load. Deflections were significantly higher on the FDR-EE section, as expected, this being attributed to the lower stiffness associated with the construction problems discussed in Section 3.5.2.

5.7.9 Deflection in the Underlying Layers (Multi-Depth Deflectometer)

Figure 5.73 shows the history of in-depth elastic deflections measured by the LVDTs in the multi-depth deflectometer in the FDR-EE section. The high deflections recorded are consistent with other measurements on this section, as expected, this being attributed to the lower stiffness associated with the construction problems discussed in Section 3.5.2.

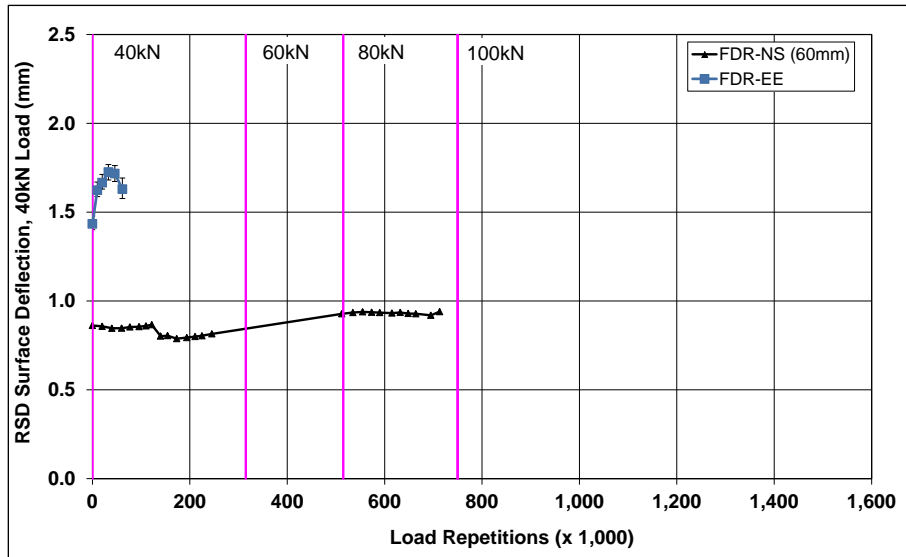


Figure 5.72: 675HC: Surface deflection (RSD).

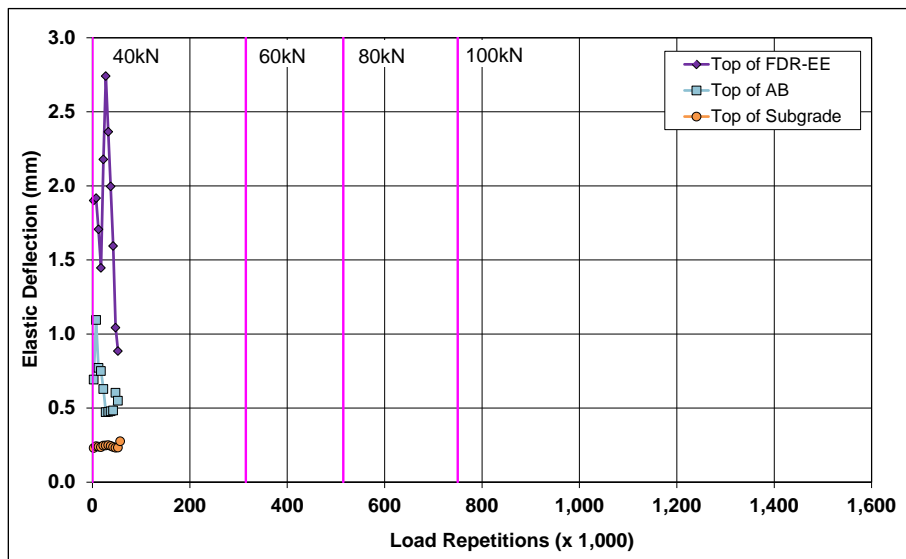


Figure 5.73: 675HC: Elastic deflection in the underlying layers.

5.7.10 Deflection in the Pavement Structure (Falling Weight Deflectometer)

Surface deflection measured with an FWD is summarized in Figure 5.74. Results from the FDR-NS (60 mm) test section are included for comparison. The results were generally consistent with the RSD measurements discussed above, with the section exhibiting high surface deflections (comparable to the FDR-NS [60 mm] section), as expected, attributable to the construction problems discussed in Section 3.5.2.

The recycled layer stiffness was backcalculated from the deflection measurements using the *CalBack* software package. Results are summarized in Figure 5.75. The stiffness of the asphalt emulsion stabilized layer did not change during HVS testing and was similar to that measured on the FDR-NS (60 mm) section.

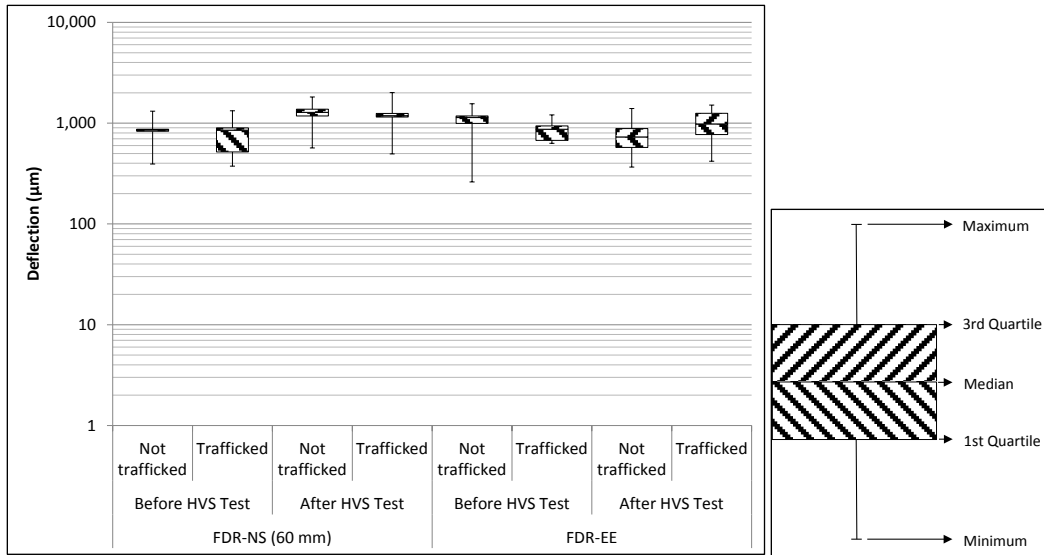


Figure 5.74: 675HC: Surface deflection (FWD).

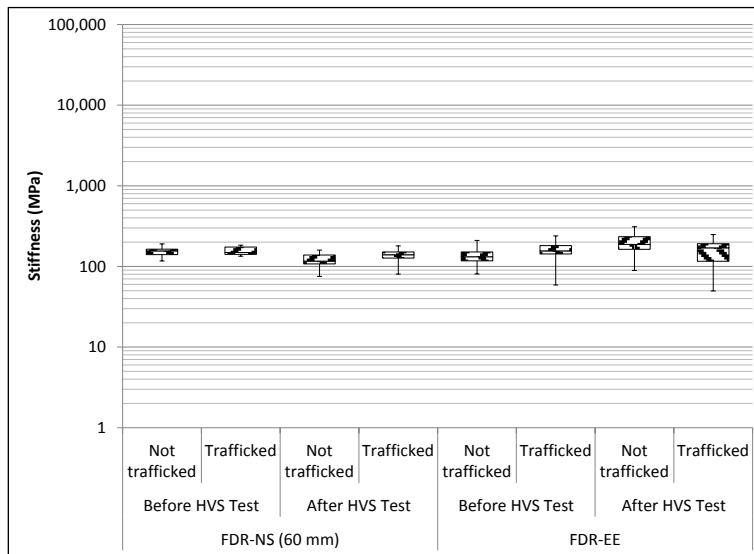


Figure 5.75: 675HC: Backcalculated stiffness of recycled layer (FWD).

5.7.11 Visual Assessment

Both rutting and fatigue cracking were recorded on the section. Severe alligator cracking was present between Station 7 and Station 16, with variation attributed to the construction problems discussed in

Section 3.5.2. The total length of the cracks was 63.2 m (207.4 ft), which equates to an average crack density of 7.9 m/m² (2.4 ft/ft²) on the test section at the end of the test, an amount considerably higher than the failure criterion of 2.5 m/m² (0.75 ft/ft²) set for the study. The total length of the cracks between Station 7 and Station 16 was 53.2 m (174.5 ft), which equates to a crack density of 11.8 m/m² (3.6 ft/ft²). The location of the cracks and the crack pattern are shown in Figure 5.76.

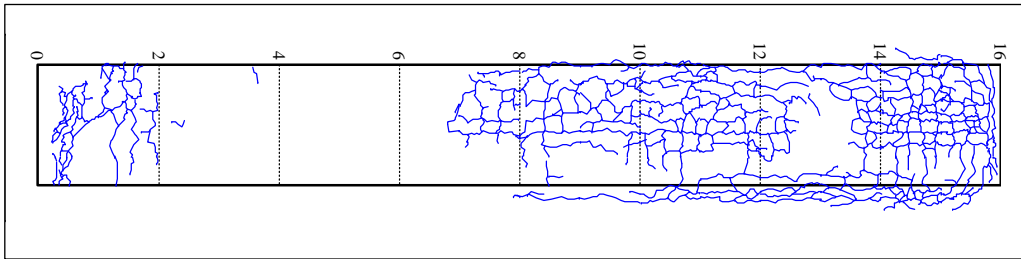


Figure 5.76: 675HC: Crack location and pattern.

Photographs of the test section after HVS testing are shown in Figure 5.78 and Figure 5.78.

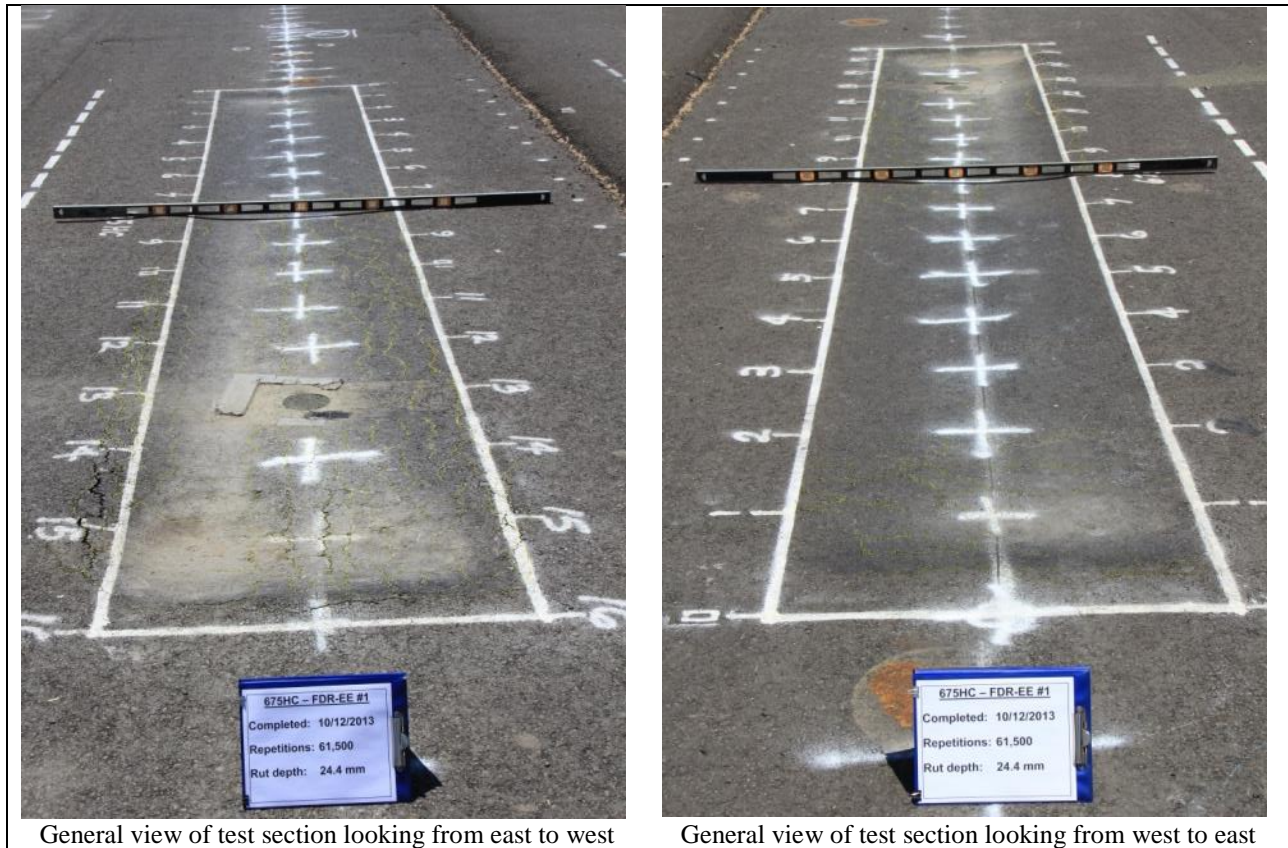
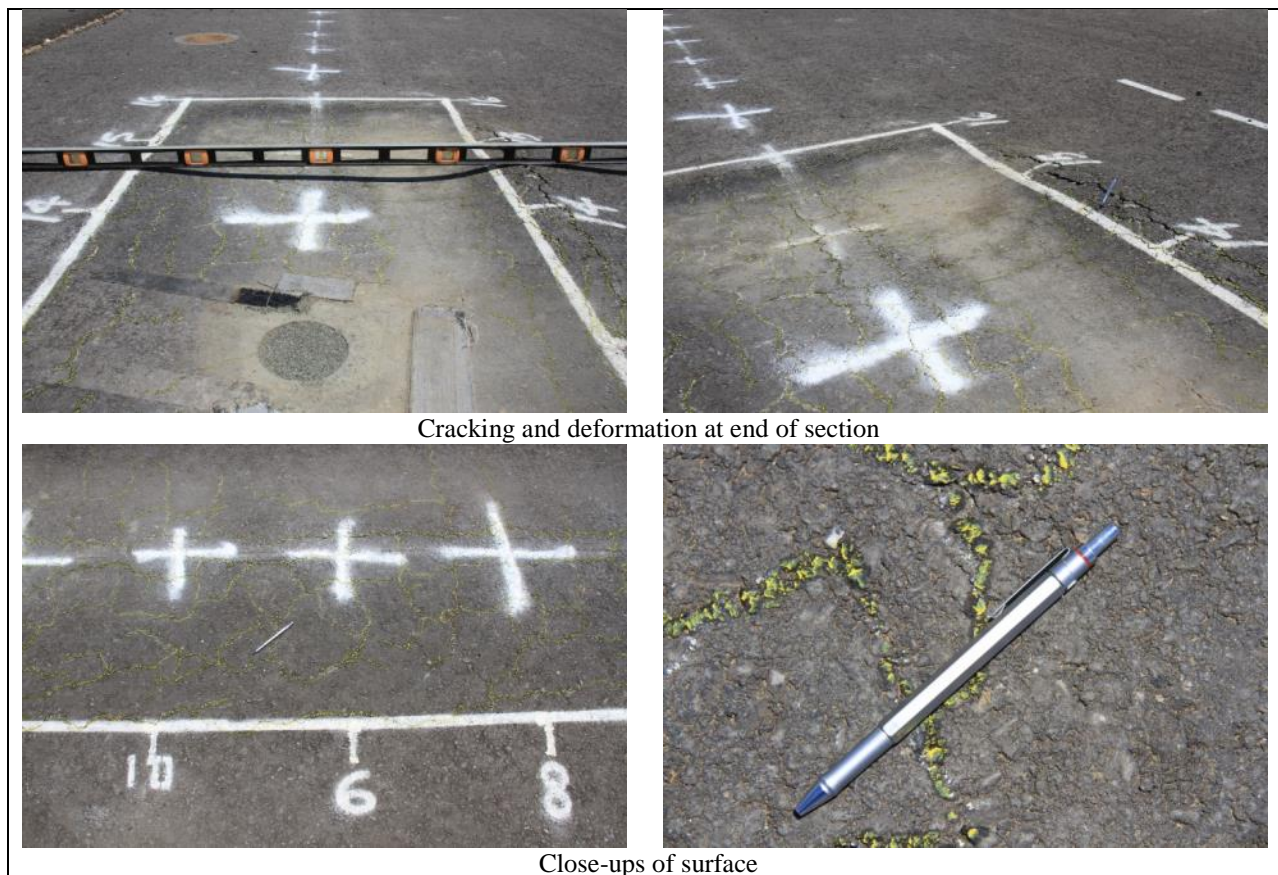


Figure 5.77: 675HC: Test section photographs.



Cracking and deformation at end of section

Close-ups of surface

Figure 5.78: 675HC: Test section photographs (continued).

5.8 Section 676HC: Engineered Emulsion (FDR-EE #2)

Given the poor performance on the first engineered emulsion section, which was attributed to the construction problems discussed in Section 3.5.2, a second section was tested to confirm the results.

5.8.1 Test Summary

Loading commenced with a 40 kN (9,000 lb) half-axle load on October 30, 2013, and ended on November 7, 2013. A total of 120,000 load repetitions were applied and 10 datasets were collected. Load was not increased. No breakdowns occurred during testing on this section. The HVS loading history for Section 675HC is shown in Figure 5.79.

At the start of testing, moisture contents in the recycled layer, original aggregate base, and subgrade were 4.0, 3.9, and 14.6 percent of the dry weight of the materials, respectively.

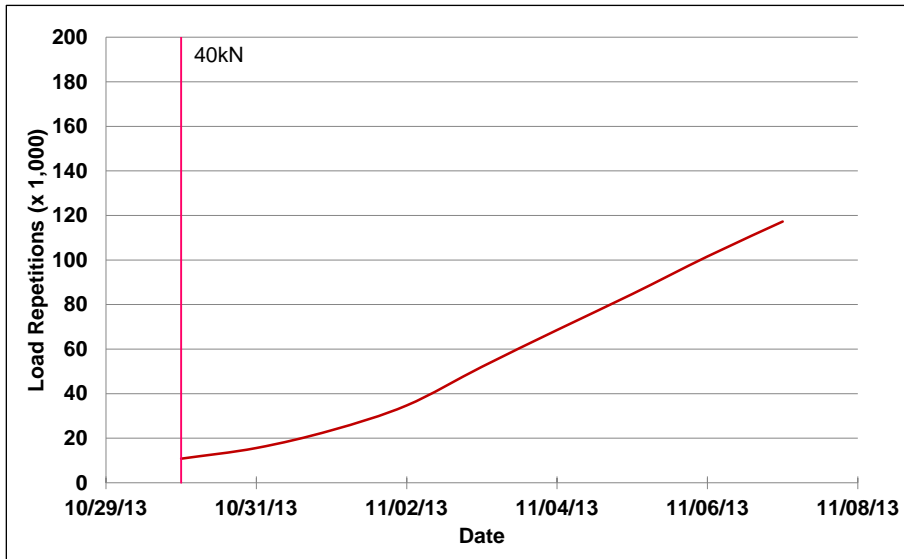


Figure 5.79: 676HC: HVS loading history.

5.8.2 Air Temperatures

Outside Air Temperatures

Daily average outside air temperatures are summarized in Figure 5.80. Vertical error bars on each point on the graph show the daily temperature range. Temperatures ranged from 4°C to 27°C (39°F to 81°F) during the course of HVS testing, with a daily average of 15°C (59°F), an average minimum of 7°C (45°F), and an average maximum of 25°C (77°F).

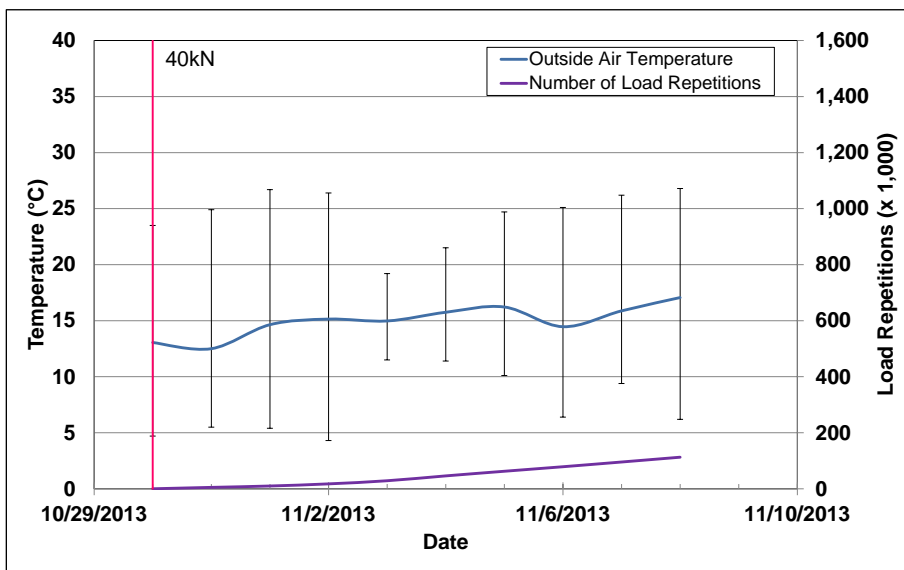


Figure 5.80: 676HC: Daily average air temperatures outside the environmental chamber.

Air Temperatures in the Environmental Chamber

During the test, air temperatures inside the temperature control chamber ranged from 17°C to 38°C (63°F to 100°F) with an average of 27°C (81°F) and a standard deviation of 1.7°C (3.1°F). Air temperature was adjusted to maintain a pavement temperature of 30°C±4°C (86°F±7°F) at a pavement depth of 50 mm (2.0 in.). The recorded pavement temperatures discussed in Section 5.8.3 indicate that the inside air temperatures were adjusted appropriately to maintain the required pavement temperature. The daily average air temperatures recorded in the environmental chamber, calculated from the hourly temperatures recorded during HVS operation, are shown in Figure 5.81. Vertical error bars on each point on the graph show the daily temperature range.

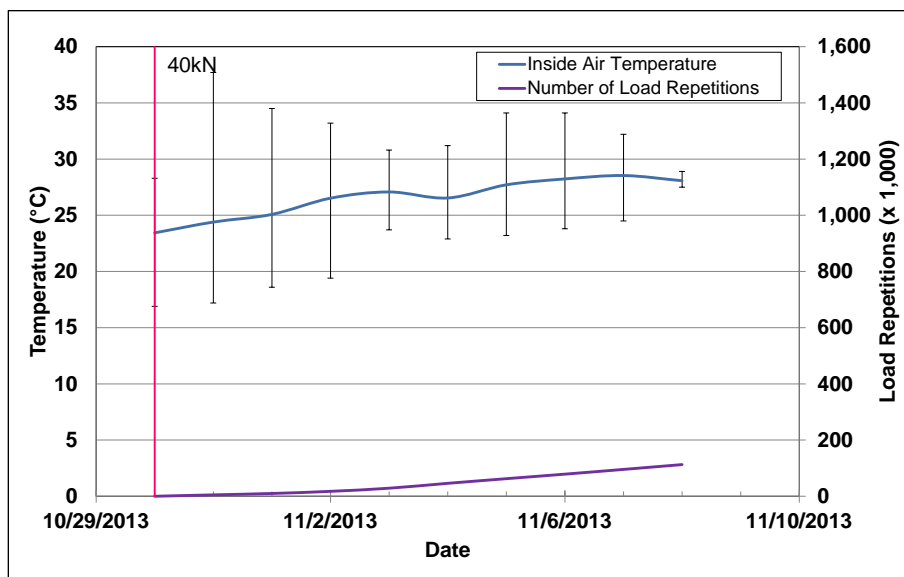


Figure 5.81: 676HC: Daily average air temperatures inside the environmental chamber.

5.8.3 Pavement Temperatures

Daily averages of the surface and in-depth temperatures of the asphalt concrete and recycled layers are listed in Table 5.11 and shown in Figure 5.82. Pavement temperatures increased slightly with increasing depth in the asphalt concrete. Temperatures were consistent throughout the measured depth of the pavement.

Table 5.11: 676HC: Temperature Summary for Air and Pavement

Temperature	Layer	Average (°C)	Std. Dev. (°C)	Average (°F)	Std. Dev. (°F)
Outside air	-	15	1.4	59	2.5
Inside air	-	27	1.7	81	3.1
Pavement surface	AC	28	0.8	82	1.4
- 25 mm below surface	AC	29	0.6	84	1.1
- 50 mm below surface	AC	29	0.7	84	1.3
- 90 mm below surface	FDR	29	0.8	84	1.4
- 120 mm below surface	FDR	29	0.7	84	1.3

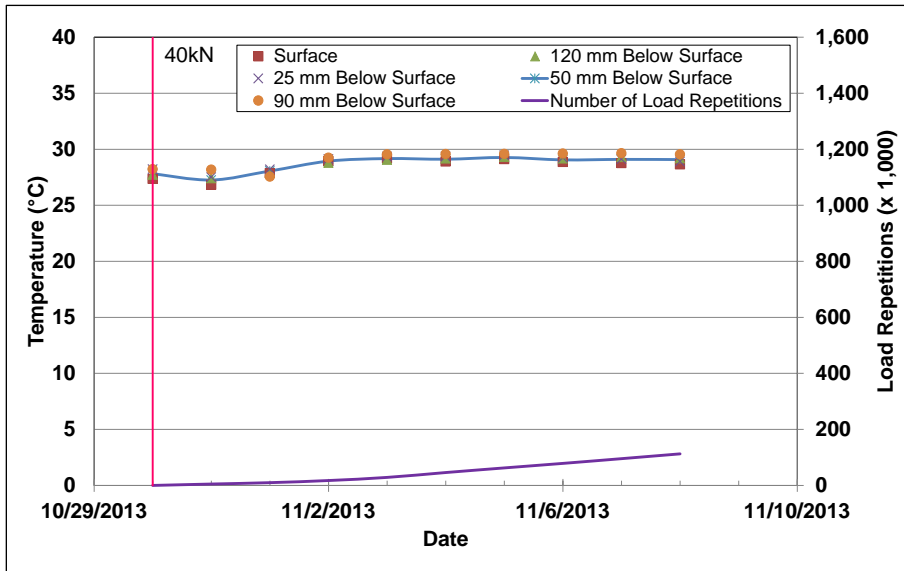


Figure 5.82: 676HC: Daily average pavement temperatures.

5.8.4 Permanent Deformation on the Surface (Rutting)

Figure 5.83 shows the average transverse cross section measured with the laser profilometer at various stages of the test and illustrates similar performance to Section 675HC (FDR-EE#1). Figure 5.84 shows the development of permanent deformation (average maximum rut and average deformation) with load repetitions for the test section. The results for the FDR-NS (60 mm) section are shown for comparison. The two plots show that depression and upward and outward displacement (shear) both contributed to the average maximum total rut depth. The rate of rut depth increase of this test, although slightly slower than that recorded on the FDR-EE#1 section (Section 675HC), was still very high and the test was again terminated before the embedment phase was complete.

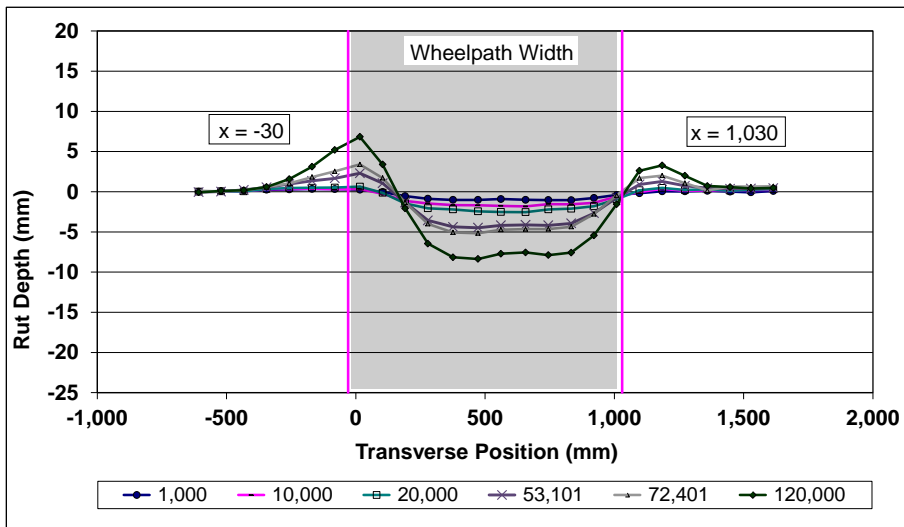


Figure 5.83: 676HC: Profilometer cross section at various load repetitions.

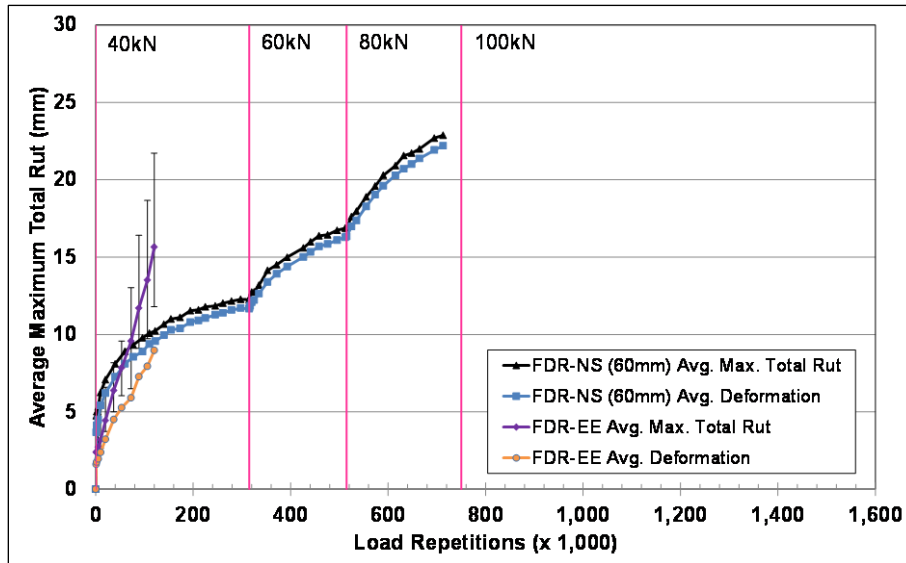


Figure 5.84: 676HC: Average maximum total rut and average deformation.

Figure 5.85 shows contour plots of the pavement surface at the start and end of the test (120,000 load repetitions). The plot indicates that the deepest rut and the area with most sheared material were between Stations 0 and 8, opposite to that recorded on Section 675HC. Terminal rut (12.5 mm [0.5 in.]) was reached after about 80,000 load repetitions.

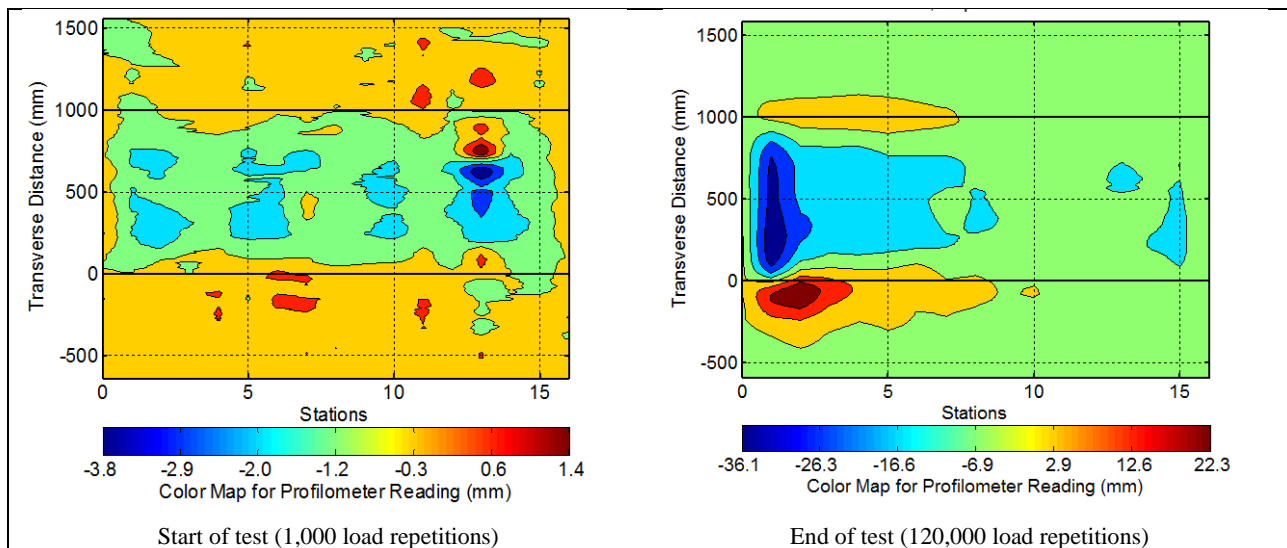


Figure 5.85: 676HC: Contour plots of permanent surface deformation.
(Note different scales in legends.)

After completion of trafficking, the average maximum rut depth and the average deformation were 15.6 mm (0.61 in.) and 9.0 mm (0.35 in.), respectively. The maximum rut depth measured on the section was 24.8 mm (0.98 in.), recorded at Station 13. The maximum height of displaced material was 12.4 mm (0.49 in.) measured at Station 12.

5.8.5 Permanent Deformation in the Underlying Layers

Permanent deformation in the underlying layers, recorded with a multi-depth deflectometer (MDD) at Station 13 and compared to the surface layer laser profilometer measurement is shown in Figure 5.86. The MDD measurements were consistent with the laser profilometer measurements. Deformation in each of the layers is summarized in Table 5.12 (results for the FDR-NS [60 mm] section are included for comparison). After 80,000 load repetitions, when the terminal rut for the test (average maximum total rut [12.5 mm] measured over the full section) was reached, most of the deformation at Station 13 was in the recycled base (5.1 mm [0.2 in.]), followed by the asphalt concrete surfacing (1.7 mm [0.07 in.]). At the end of the test after 120,000 load repetitions, most of the additional deformation had occurred in the asphalt concrete surfacing with only a slight increase recorded in the recycled base. Very little permanent deformation was recorded in the existing aggregate base and subgrade. A forensic investigation will be undertaken on completion of the Phase 2 HVS testing to validate these measurements.

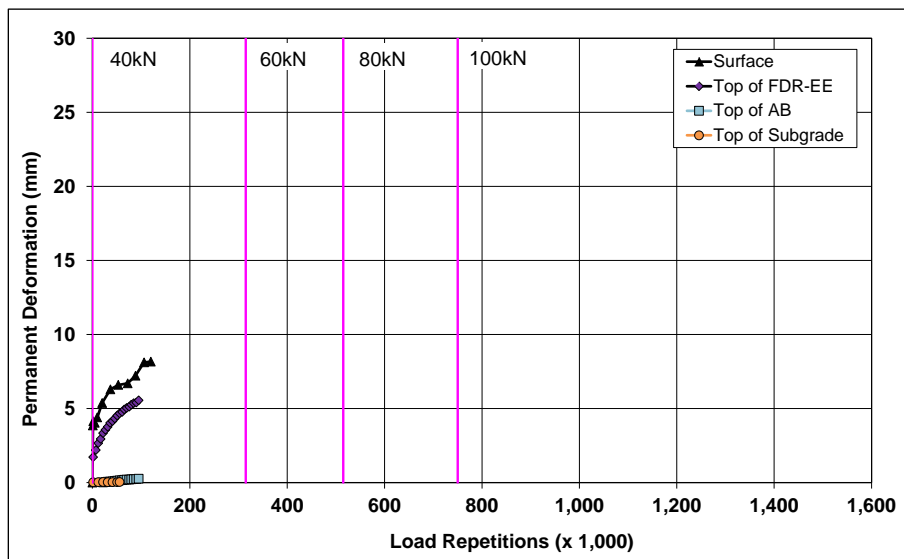


Figure 5.86: 676HC: Permanent deformation in the underlying layers.

Table 5.12: 676HC: Deformation in Each Layer

Layer	Layer Thickness		676HC		676HC		672HB	
			Deformation at Terminal Rut ¹		Deformation at End of Test ²		Deformation at Terminal Rut ¹	
	(mm)	(in.)	(mm)	(in.)	(mm)	(in.)	(mm)	(in.)
Surface	60	2.4	1.7	0.07	2.7	0.11	4.2	0.17
Recycled	250	10.0	5.1	0.20	5.3	0.21	8.5	0.33
Aggregate Base	320	12.6	0.2	0.01	0.2	0.01	2.3	0.09
Subgrade	-	-	0.0	0.00	0.0	0.00	0.4	0.02
Total MDD Measured Deformation			7.0	0.28	8.2	0.32	15.4	0.61
Laser Measured Deformation at Station 13			7.0	0.28	8.2	0.32	15.4	0.61
¹ Terminal rut for test section			² 120,000 load repetitions (~ 120,000 ESALs)					

5.8.6 Tensile Strain at the Bottom of the Asphalt Concrete Layer

Figure 5.87 shows the peak traffic-induced transverse tensile strain at the bottom of the asphalt concrete layer. The strain gauge installed to measure longitudinal strain was damaged during placement of the asphalt concrete surfacing and no data was recorded from this instrument. Transverse strain measurements from the FDR-NS (60 mm) section are included in the figure for comparison. Transverse strains increased significantly from the start of the test and were consistent with the early severe deformation that was measured on the section and attributed to the construction issues discussed in Section 3.5.2. The significant reduction in strain measured in the latter part of the test was attributed to movement of the gauge associated with the depth of rutting in the vicinity of the gauge.

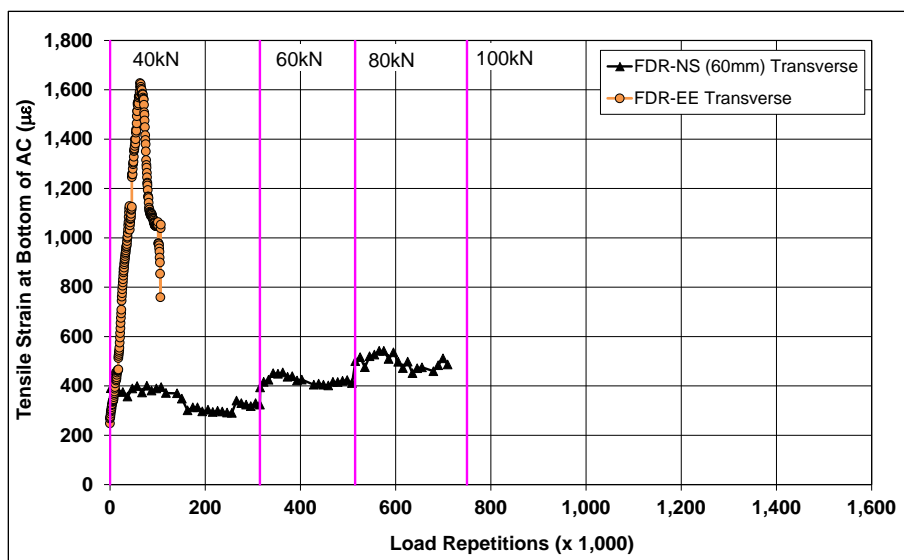


Figure 5.87: 676HC: Tensile strain at the bottom of the asphalt concrete layer.

5.8.7 Vertical Pressure at the Top of the Recycled Layer

Figure 5.88 shows the comparison of traffic-induced vertical pressure at the top of the recycled base layer for the FDR-NS (60 mm) and FDR-EE#2 sections. Pressure readings increased significantly from the start of the test and were consistent with the readings on the FDR-EE#1 (675HC) section.

5.8.8 Deflection on the Surface (Road Surface Deflectometer)

Figure 5.89 compares elastic surface deflections measured with an RSD on the FDR-EE and FDR-NS (60 mm) sections under a 40 kN half-axle load. Deflections were significantly higher on this FDR-EE section, with measurements comparable to those recorded on the FDR-EE#1 section, and were attributed to the lower stiffness associated with the construction problems discussed in Section 3.5.2.

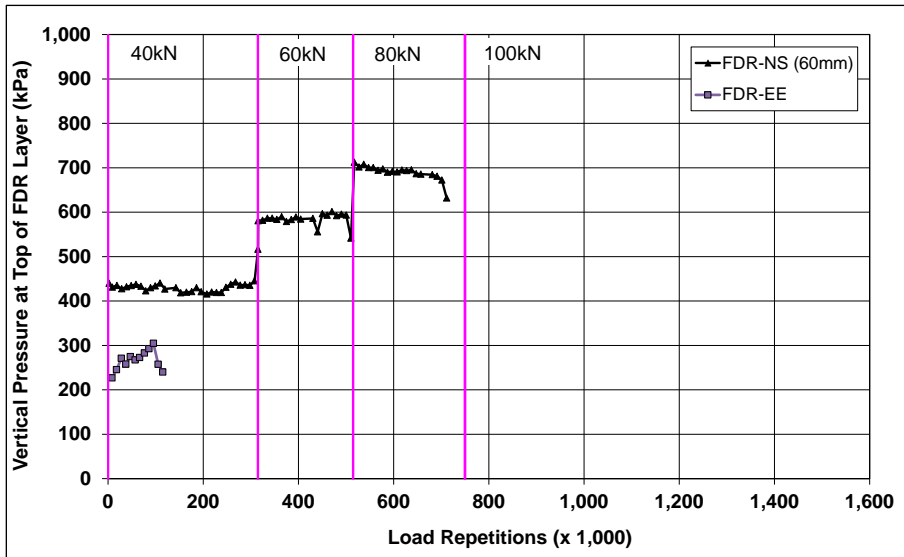


Figure 5.88: 676HC: Vertical pressure at the top of the recycled layer.

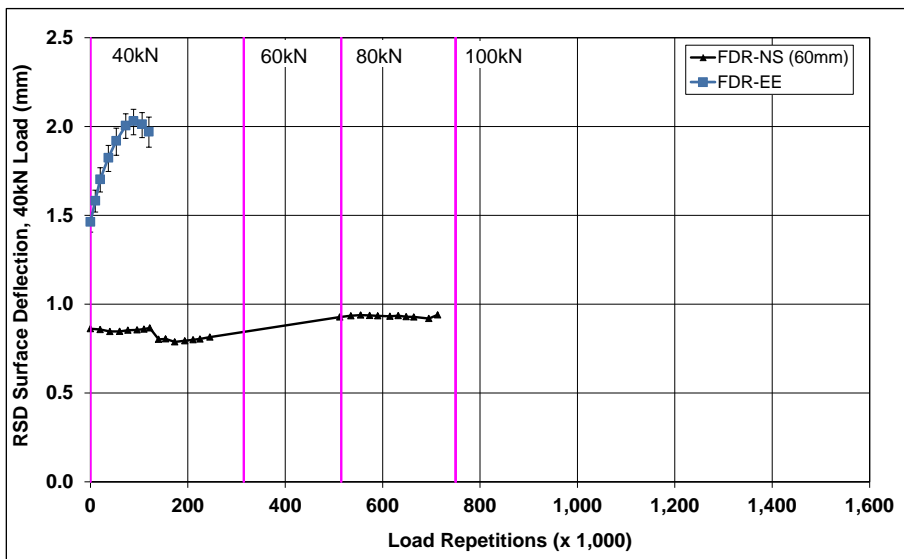


Figure 5.89: 676HC: Surface deflection (RSD).

5.8.9 Deflection in the Underlying Layers (Multi-Depth Deflectometer)

Figure 5.90 shows the history of in-depth elastic deflections, measured by the LVDTs in the multi-depth deflectometer in the FDR-EE#2 section. The high deflections recorded are consistent with other measurements on this section and those measured on the FDR-EE#1 section and are attributable to the lower stiffnesses associated with the construction problems discussed in Section 3.5.2.

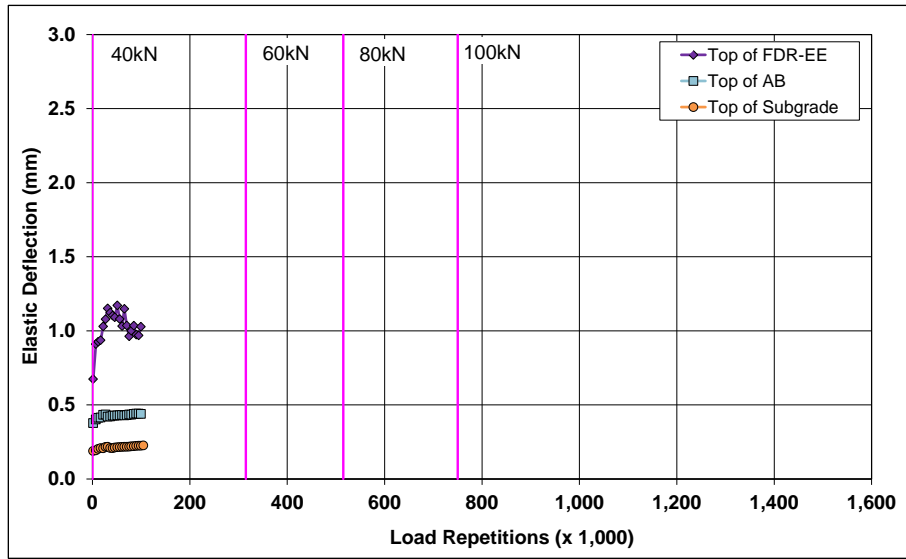


Figure 5.90: 676HC: Elastic deflection in the underlying layers.

5.8.10 Deflection in the Pavement Structure (Falling Weight Deflectometer)

Surface deflection measured with an FWD is summarized in Figure 5.91. Results from the FDR-NS (60 mm) test section are included for comparison. The results were generally consistent with the RSD measurements discussed above and the measurements on the FDR-EE#1 section, with the section exhibiting high surface deflections as expected.

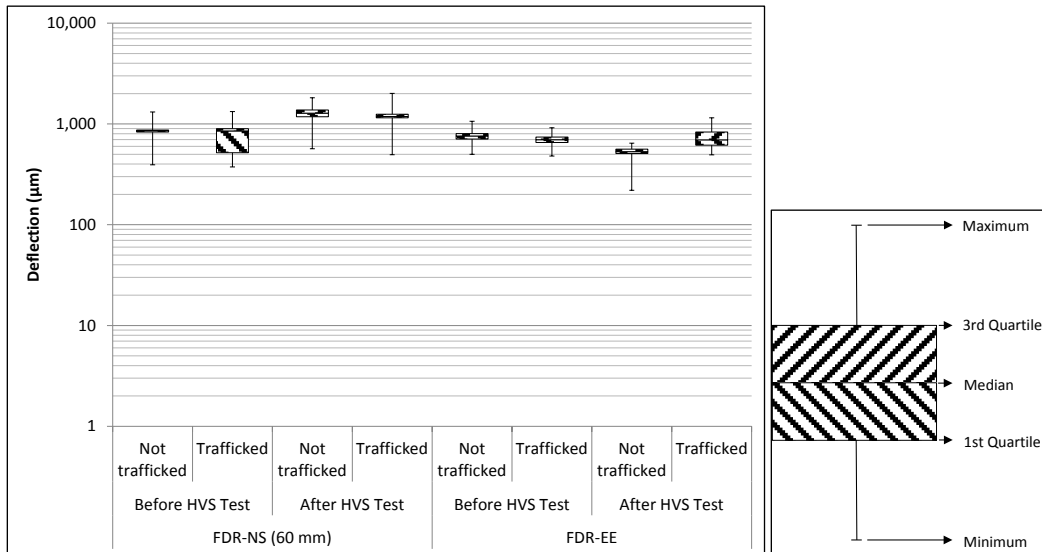


Figure 5.91: 676HC: Surface deflection (FWD).

The recycled layer stiffness was backcalculated from the deflection measurements using the *CalBack* software package, and the results are summarized in Figure 5.92. The stiffness of the asphalt emulsion-

stabilized layer dropped slightly during HVS testing (± 50 MPa) and was similar to that measured on the FDR-NS (60 mm) and FDR-EE#1 sections.

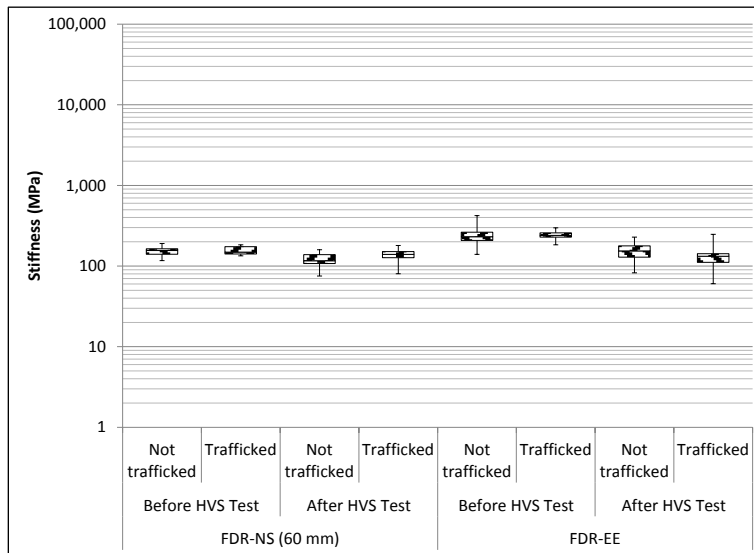


Figure 5.92: 676HC: Backcalculated stiffness of recycled layer (FWD).

5.8.11 Visual Assessment

Both rutting and fatigue cracking were recorded on the section. Severe alligator cracking was present between Station 0 and Station 8, with variation attributed to the construction problems discussed in Section 3.5.2. The total length of the cracks was 64.1 m (210.3 ft), which equates to an average crack density of 8.0 m/m² (2.4 ft/ft²) on the test section at the end of the test, similar to that recorded on the FDR-EE#1 section and considerably higher than the failure criterion of 2.5 m/m² (0.75 ft/ft²) set for the study. Total length of cracks between Station 0 and Station 8 was 55.7 m (182.7 ft), which equates to a crack density of 12.4 m/m² (3.8 ft/ft²). The location of the cracks and the crack pattern are shown in Figure 5.93.

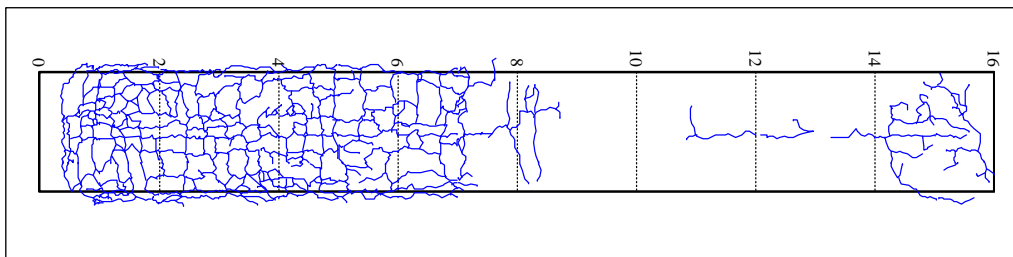
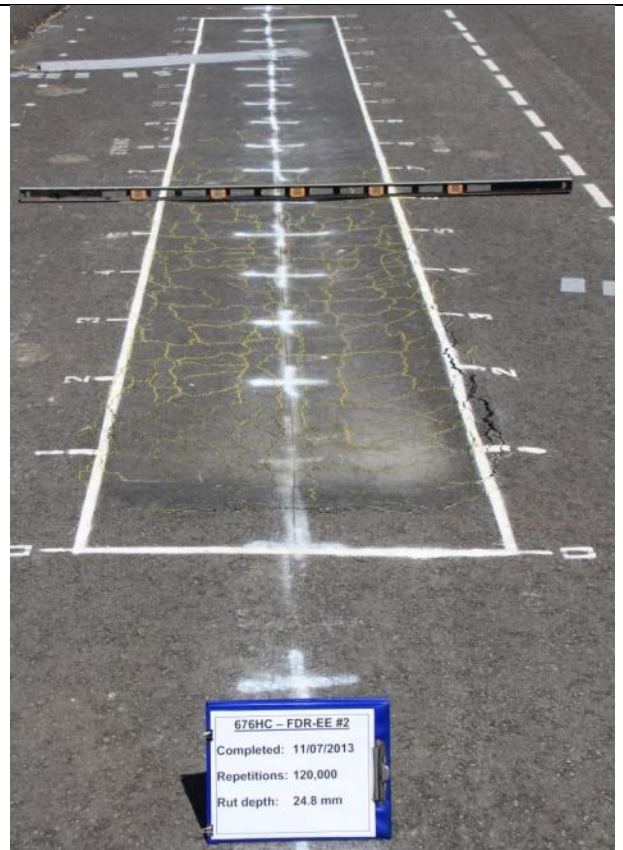


Figure 5.93: 676HC: Crack location and pattern.

Photographs of the test section after HVS testing are shown in Figure 5.94.



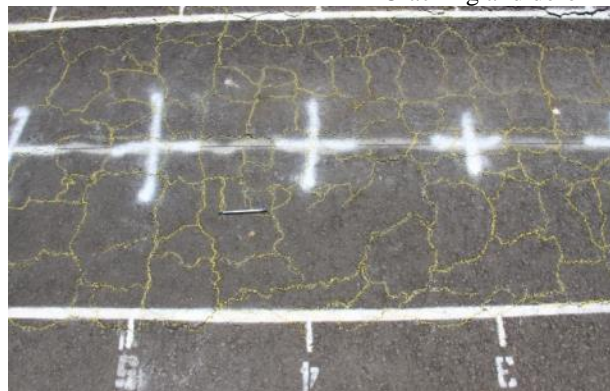
General view of test section looking from east to west



General view of test section looking from west to east



Cracking and deformation at end of test section



Close-ups of surface

Figure 5.94: 676HC: Test section photographs.

5.9 HVS Test Summary

The first phase of testing on the four full-depth reclamation sections started in February 2013 and ended in November of the same year. A range of daily average temperatures was therefore experienced; however, pavement temperatures remained constant throughout HVS trafficking. The FDR-FA and FDR-PC sections performed very well and both tests were terminated long before the terminal rut of 0.5 in. (12.5 mm) or average crack density of 0.8 ft/ft² (2.5 m/m²) was reached (no cracks were observed on either section). The two FDR-NS sections performed acceptably, with the section with the thicker asphalt surfacing outperforming the section with the thinner asphalt surfacing, as expected. Terminal rut was reached on both sections, but no cracking was observed. The FDR-EE sections performed poorly, with terminal rut and terminal cracking both reached after a limited number of load repetitions. This poor performance was attributed to problems associated with construction, and consequently no conclusions can be drawn from the test results regarding this stabilization strategy

Rutting behavior on the FDR-NS, FDR-FA and FDR-PC sections is compared in Figure 5.95. The FDR-EE sections are not included given that the poor performance was construction related and not stabilizer related.

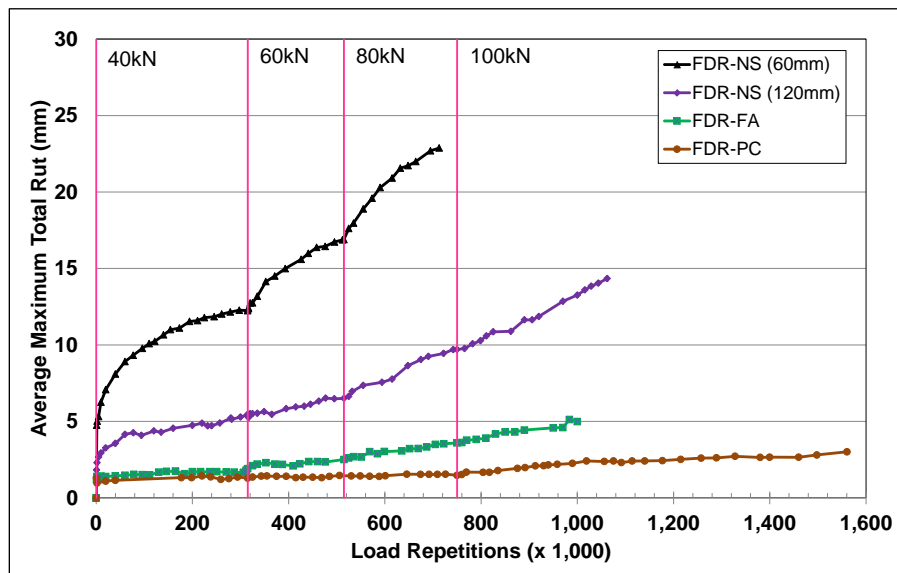


Figure 5.95: Comparison of average maximum rut.

The plot clearly shows the difference in performance between the stabilized and unstabilized sections. Terminal rut depths were recorded on the FDR-NS (60 mm) section after approximately 490,000 equivalent standard axle loads (ESALs) had been applied, and on the FDR-NS (120 mm) section after more than 21.4 million ESALs had been applied. The thicker surfacing layer therefore had a significant

influence on the performance of the structure. On the FDR-FA section, only 4 mm of rutting was measured after more than 17.7 million ESALs, while on the FDR-PC section, only 2.1 mm of rutting was measured after more than 44 million ESALs. Testing was halted on the FDR-FA and FDR-PC sections at these loading points due to time and project funding constraints. Permanent deformation in the recycled layers was consistent with the surface measurements, with considerable deformation recorded in the FDR-NS layers, but very little deformation recorded in the stabilized layers.

Backcalculated stiffnesses determined from falling weight deflectometer measurements on the FDR-NS, FDR-FA and FDR-PC sections are compared in Figure 5.96 (note that the Y-axis is a log scale). The FDR-EE sections are not included. Measured and backcalculated stiffnesses were significantly higher on the FDR-FA and FDR PC sections compared to the two FDR-NS sections, as expected. Although the stiffnesses dropped considerably in the recycled layers on the FDR-FA and FDR-PC sections after trafficking, they were still orders of magnitude higher than those recorded on the FDR NS sections, despite having been subjected to millions more equivalent standard axle loads. The presence of the recycled asphalt concrete material, the presence of rubber in this material, and the fact that the recycled asphalt was relatively unaged, did not appear to affect the stiffness of the layer. Recycled aged asphalt would typically result in slightly high stiffnesses in the recycled layer compared to unaged asphalt.

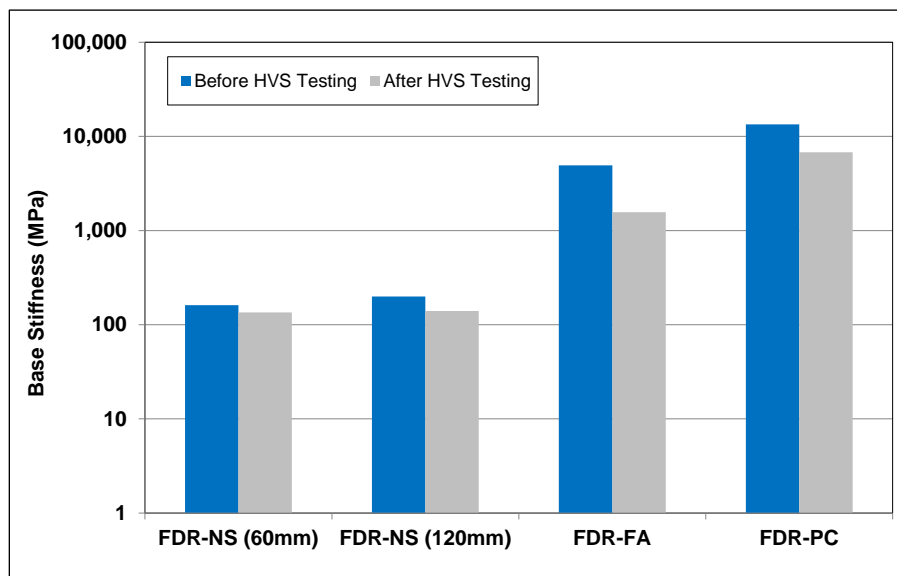


Figure 5.96: Comparison of backcalculated stiffness before and after testing.

Elastic deflection at the bottom of the FDR-FA and FDR-PC layers after completion of testing (17.7 and 44.0 million ESALs, respectively) was approximately the same as that at the bottom of the FDR-NS layers after 490,000 and 21.4 million ESALs, respectively. The rate of change in deflection, was however,

slightly higher on the FDR-FA and FDR-PC sections, which is consistent with stabilized layers containing cement.

The advantages of using foamed asphalt with cement and cement only recycling strategies over recycling strategies with no stabilization are clearly evident from the results.

5.10 Phase 2 HVS Testing

In the Phase 2 study, the base layers on the FDR-NS, FDR-FA, and FDR-PC lanes will be moistened by allowing water to pass through holes drilled through the asphalt outside the demarcated HVS test sections. Wheel loads will be applied with the HVS to compare dry and wet performance. This information is considered important for California, especially in the Central Valley areas where agricultural activities, specifically irrigation, can lead to high moisture contents in the pavement layers. No further HVS testing will be undertaken on the FDR-EE lane.

Blank page

6. PHASE 1 LABORATORY TEST DATA SUMMARY

6.1 Introduction

Laboratory testing in this phase of the study was limited to characterization of the recycled and asphalt concrete materials from the test track, assessment of the mechanistic properties of the asphalt concrete material, and initial assessment of the mechanistic properties of the unstabilized and stabilized recycled base materials. Assessment of the mechanistic properties of the recycled materials will continue in Phase 2 of the study, and is not covered in this report.

6.2 Characterization of Unstabilized Recycled Material and Asphalt Concrete Surfacing

Characterization of the unstabilized recycled material was limited to a grading analysis and determination of the maximum dry density and optimum moisture content, and was undertaken as part of the quality control assessment during construction. Characterization of the asphalt concrete surfacing materials was also undertaken as part of quality control during construction and followed Caltrans specification requirements. Test results for the recycled materials and asphalt concrete surfacing materials are discussed in Section 3.5.5 and Section 3.6.4, respectively.

6.3 Mechanistic Properties of the Asphalt Concrete Surfacing

6.3.1 Experiment Design

Characterization of the mechanistic properties of the asphalt concrete surfacing included shear properties (permanent deformation [rutting]), fatigue cracking properties (fatigue life), and stiffness (fatigue frequency sweep). Tests on these mix properties were carried out on cores and beams cut from the test track after construction (see Section 3.7). Typical experimental designs used in previous studies were adopted for this study to facilitate comparison of results. Tests were not conducted with the Asphalt Mix Performance Test (AMPT) apparatus due to the limited thickness of the asphalt concrete surfacing. The surface thickness on five of the six test sections was 60 mm (0.2 ft) and 120 mm (0.4 ft) on the remaining section. The AMPT requires specimens that are 150 mm [6.0 in.] thick.

Shear Testing for Rutting Performance

The AASHTO T 320 Permanent Shear Strain and Stiffness Test was used for shear testing in this study. In the standard test methodology, cylindrical test specimens 150 mm (6.0 in.) in diameter and 50 mm (2.0 in.) thick are subjected to repeated loading in shear using a 0.1 second haversine waveform followed by a 0.6 second rest period. Three different shear stresses are applied while the permanent (unrecoverable)

and recoverable shear strains are measured. The permanent shear strain versus applied repetitions is normally recorded up to a value of five percent although 5,000 repetitions are called for in the AASHTO procedure. Constant temperatures (45°C or 55°C) are maintained during the test (termed the *critical temperature*), representative of the high temperature that causes rutting in the local environment. In this study, specimens were cored from the test track and then trimmed to size.

A total of 36 shear tests were carried out as follows:

- Two lifts of asphalt (FDR-NS [60 mm] and top lift of FDR-NS [120 mm])
- Two temperatures (45°C and 55°C [113°F and 131°F])
- Three stresses (70 kPa, 100 kPa, and 130 kPa [10.2, 14.5, and 18.9 psi])
- Three replicates

Flexural Beam Testing for Fatigue Performance

The AASHTO T 321 Flexural Controlled-Deformation Fatigue Test method was followed. In this test, three replicate beam test specimens, 50 mm (2.0 in.) thick by 63 mm (2.5 in.) wide by 380 mm (15 in.) long, which were sawn from the test track, were subjected to four-point bending using a haversine waveform at a loading frequency of 10 Hz. Testing was performed at two different strain levels at three different temperatures. Flexural Controlled-deformation Frequency Sweep Tests were used to establish the relationship between complex modulus and load frequency. The same sinusoidal waveform was used in a controlled deformation mode and at frequencies of 15, 10, 5, 2, 1, 0.5, 0.2, 0.1, 0.05, 0.02, and 0.01 Hz. The upper limit of 15 Hz is a constraint imposed by the capabilities of the test machine. To ensure that the specimen was tested in a nondestructive manner, the frequency sweep test was conducted at a small strain amplitude level, proceeding from the highest frequency to the lowest in the sequence noted above.

A total of 12 beam fatigue tests and 18 flexural fatigue frequency sweep tests were carried out on each mix as follows:

- Flexural fatigue test:
 - + Two lifts of asphalt concrete (FDR-NS [60 mm] and top lift of FDR-NS [120 mm])
 - + One temperature (20°C [68°F])
 - + Two strains (200 microstrain and 400 microstrain)
 - + Three replicates
- Frequency sweep test:
 - + Three lifts of asphalt (FDR-NS [60 mm] and top and bottoms lifts of FDR-NS [120 mm])
 - + Three temperatures (10°C, 20°C, and 30°C [50°F, 68°F, and 86°F])
 - + One strain (100 microstrain)
 - + Two replicates

6.3.2 Shear Testing Results

Shear test results are summarized in Table 6.1. The results are typical of mixes produced with this aggregate and binder combination. Variation in the results between replicates tested under the same temperature and stress level was in most instances attributed to differences in air-void content, with higher air-void contents generally resulting in lower permanent shear strains. The results showed sensitivity to the higher temperatures and higher stress levels, as expected.

Table 6.1: Shear Test Results

Specimen Location	Test Parameters	Specimen Number	Air-Void Content (%)	Test Temp. (°C)	Stress Level (kPa)	Initial Resilient Shear Modulus (kPa)	Permanent Shear Strain at 5,000 Cycles (%)
FDR-NS (60 mm)	70 kPa 45°C	sl-10-7045b	6.9	44.84	68.31	592	0.28
		sl-16-7045	5.1	44.81	68.28	412	0.71
		sl-19-7045	5.3	44.77	69.00	525	0.83
	100 kPa 45°C	sl-2-10045	3.2	45.22	97.65	564	0.59
		sl-3-10045	4.7	45.13	97.81	448	0.63
		sl-5-10045	5.9	45.13	97.61	520	0.67
	130 kPa 45°C	sl-13-13045	2.7	45.38	126.42	394	1.07
		sl-18-13045	6.0	45.11	125.46	403	1.33
		sl-22-13045	3.6	45.13	124.35	445	0.98
	70 kPa 55°C	sl-9-7055	7.2	54.81	69.81	142	1.46
		sl-21-7055	3.5	54.94	67.84	163	1.74
		sl-6-7055	6.1	55.03	69.91	154	1.25
100 kPa 55°C	sl-14-10055	3.5	55.04	100.60	181	2.42	
	sl-15-10055	3.6	55.08	100.51	139	2.66	
	sl-11-10055	5.4	54.99	100.91	156	2.19	
130 kPa 55°C	sl-7-13055	6.2	55.00	127.36	121	2.81	
	sl-12-13055	7.4	54.78	129.15	132	3.73	
	sl-24-13055	3.0	55.05	123.94	192	2.42	
FDR-NS (120 mm) Top Lift	70 kPa 45°C	dl-3t-7045	4.7	44.91	68.60	331	0.48
		dl-9t-7045	5.4	44.86	69.19	285	0.36
		dl-21t-7045	5.7	44.79	69.02	254	0.91
	100 kPa 45°C	dl-1t-10045	4.4	45.02	97.52	238	0.93
		dl-20t-10045	4.8	44.99	97.48	324	1.00
		dl-17t-10045	5.4	44.72	99.01	275	1.05
	130 kPa 45°C	dl-7t-13045	5.1	45.02	124.29	248	1.61
		dl-22t-13045	5.1	44.95	125.06	286	1.88
		dl-11t-13045	6.0	44.93	123.49	299	1.32
	70 kPa 55°C	dl-16t-7055	5.6	55.06	70.06	66	2.89
		dl-8t-7055	5.0	55.05	69.43	74	1.72
		dl-14t-7055	5.5	54.96	70.69	95	2.98
100 kPa 55°C	dl-4t-10055	4.6	55.02	100.43	103	3.37	
	dl-10t-10055	4.7	54.97	99.55	102	4.61	
	dl-13t-10055	4.7	55.14	101.57	82	4.80	
130 kPa 55°C	dl-5t-13055	6.3	54.92	126.73	80	n/a	
	dl-19t-13055	5.6	55.04	126.26	82	n/a	
	dl-6t-13055	5.1	55.03	126.72	87	n/a	

6.3.3 Fatigue Cracking Test Results

Fatigue cracking test results are summarized in Table 6.2. The results are typical of mixes produced with this aggregate and binder combination. Variation in the results between replicates tested under the same strain level was in most instances attributed to differences in air-void content, with higher air-void contents generally resulting in lower initial stiffnesses, as expected.

Table 6.2: Fatigue Cracking Test Results

Specimen Location	Test Parameter	Specimen Number	Air-Void Content (%)	Test Temp. (°C)	Test Strain Level (strain)	Phase Angle (°)	Initial Stiffness (MPa)
FDR-NS (60 mm)	200 μ strain 20°C	sl-13	3.1	20.2	0.000198	17.49	9,598
		sl-22	2.1	20.0	0.000186	18.90	10,013
		sl-28	6.4	19.9	0.000195	19.52	8,449
	400 μ strain 20°C	sl-15	4.1	20.1	0.000403	20.19	8,278
		sl-23	2.6	20.2	0.000380	20.20	8,864
		sl-25	3.6	19.9	0.000360	16.34	9,700
FDR-NS (120 mm) Top Lift	200 μ strain 20°C	dlt-14	4.2	20.3	0.000192	22.28	5,353
		dlt-18	3.8	19.7	0.000201	21.51	6,789
		dlt-22	3.4	20.2	0.000198	23.24	6,799
	400 μ strain 20°C	dlt-13	4.3	19.9	0.000409	23.50	5,069
		dlt-26	3.9	20.2	0.000407	24.74	5,285
		dlt-27	4.3	19.9	0.000414	23.38	5,109

6.4 Frequency Sweep Test Results

Frequency sweep test results are summarized in Table 6.3. The results are typical of mixes produced with this aggregate and binder combination.

Table 6.3: Frequency Sweep Test Results

Specimen Location	Test Parameter	Specimen Number	Air-Void Content (%)	Test Temp. (°C)	Phase Angle (°)	Initial Stiffness (MPa)
FDR-NS (60 mm)	10°C	sl-12	2.6	9.7	10.76	14,015
		sl-16	6.3	9.9	10.71	11,620
	20°C	sl-21	1.9	19.9	17.21	10,375
		sl-24	2.9	19.7	18.76	9,695
	30°C	sl-18	7.3	30.0	34.70	3,337
		sl-27	5.3	29.6	33.43	4,224
FDR-NS (120 mm) Top Lift	10°C	dlt-15	3.5	9.8	12.76	11,315
		dlt-28	3.8	9.7	12.69	10,002
	20°C	dlt-24	2.9	19.7	19.46	7,440
		dlt-25	3.6	19.8	19.61	6,592
	30°C	dlt-16	3.6	29.9	35.89	2,799
		dlt-23	3.6	29.7	40.95	3,148
FDR-NS (120 mm) Bottom Lift	10°C	dlb-11-2	3.6	9.8	12.43	12,776
		dlb-21	4.0	10.1	12.12	12,227
	20°C	dlb-12	3.9	19.7	18.50	8,512
		dlb-24	6.2	19.7	18.98	7,154
	30°C	dlb-13	4.7	29.7	34.27	3,206
		dlb-23	4.8	30.1	33.52	3,185

Variation in the results between replicates tested under the same temperature was in most instances attributed to differences in air-void content, with higher air voids generally resulting in lower initial stiffnesses, as expected. The master curve developed from these test results is shown in Figure 6.1.

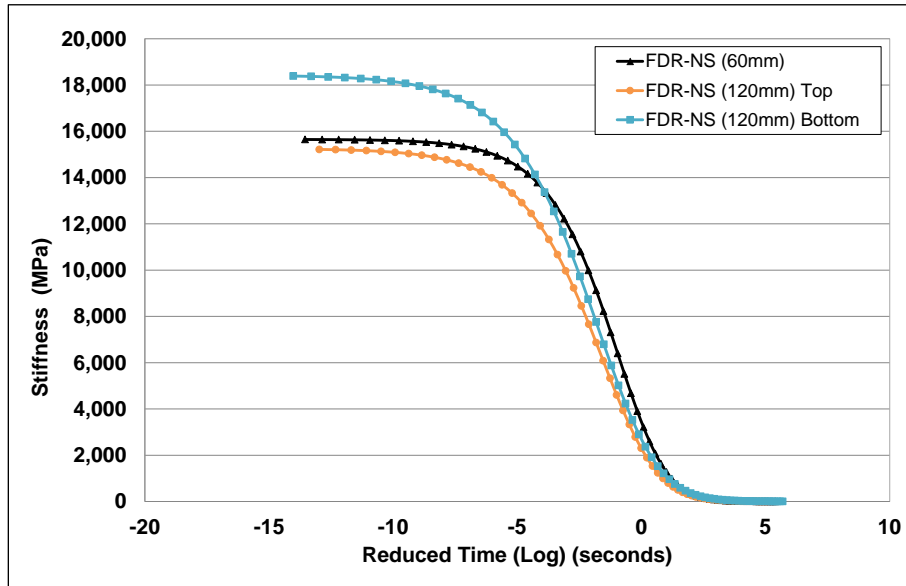


Figure 6.1: Master curve.

6.5 Phase 2 Laboratory Testing

The Phase 2 laboratory testing will focus on quantifying mechanistic properties of the recycled layers using repeated load triaxial tests. Specimens removed from the test track as well specimens prepared in the laboratory will be assessed.

Blank page

7. MECHANISTIC ANALYSIS

Accelerated Pavement Testing (APT) provides performance data from full-scale pavements damaged under controlled full-scale loading and/or environmental conditions in a relatively short period of time. Although immediate performance observations and comparisons are obtained from the results of each APT experiment, the usefulness of the data can be significantly increased at relatively little cost through intensive second-level data analysis and by combining results from different experiments to provide inputs for mechanistic-empirical (M-E) design.

On completion of the Phase 2 accelerated load and laboratory tests, M-E analysis will be used to develop insights into the pavement mechanics and damage mechanisms of full-depth recycled pavements and to validate and calibrate models that can be used to design pavements that include an in-place recycled layer. This analysis will include the following two elements:

- The calibration of damage models of various FDR materials for predicting rutting and fatigue cracking in pavements. This calibration will allow the establishment of correlations between laboratory test data and full-scale performance observations under accelerated loading.
- Validation of these calibrated models using data collected from pilot studies on in-service roads and from other accelerated loading tests that were not included in the model calibration.

Once the models are reasonably well-validated, they will be used to assess additional materials and structures similar to those used in the accelerated load experiments. The models will also be used to “re-run” the APT test sections through simulation with the same underlying conditions, temperature, water content, etc. Because there are inevitable differences in conditions that are supposed to be equal between accelerated load test sections, this simulation will be useful for confirming that the results of the initial empirical comparisons of performance do not change significantly under absolutely uniform conditions. The findings of this analysis will also be used to verify the appropriateness of current gravel factors for the various FDR stabilization strategies.

Blank page

8. CONCLUSIONS AND INTERIM RECOMMENDATIONS

8.1 Summary and Conclusions

This first-level report describes the first phase of a study that compares the performance of four different full-depth pavement reclamation strategies, namely, pulverization with no stabilization (FDR-NS), stabilization with foamed asphalt and portland cement (FDR-FA), stabilization with portland cement only (FDR-PC), and stabilization with engineered asphalt emulsion (FDR-EE). A literature review, the test track layout and design, the stabilization and asphalt concrete mix designs, and the test track construction are discussed, as are the results of Heavy Vehicle Simulator (HVS) and preliminary laboratory testing.

A comprehensive literature review found that although considerable research has been undertaken on full- and partial-depth reclamation, both in the laboratory and in full-scale field experiments, most of the findings and conclusions published are either project-specific or very general in detail. Limited guidance on how to select and design partial-depth reclamation (PDR) and full-depth reclamation (FDR) projects using the different stabilization strategies has been published, and no work appears to have been published on the development of parameters for the mechanistic-empirical rehabilitation design of highways using partial- or full-depth reclamation strategies.

Observations during construction of the test track include the following:

- Based on the results of testing of rubberized warm-mix asphalt in a previous study on the UCPRC North Track, it was concluded that preparation of the subgrade and construction of the original base during that study resulted in a generally consistent subgrade and base platform for the FDR study.
- Recycling of the test track was completed with mixed success:
 - + Conventional FDR construction procedures were followed on the FDR-NS lane. Recycling depth was well controlled and the pulverized material had a consistent grading and uniform moisture content. No problems were observed with recycling the relatively new asphalt concrete surface (i.e., limited aging), although some smoke was observed as the cutting teeth milled through the rubberized layer. Satisfactory compaction and a satisfactory surface finish were achieved on the recycled layer.
 - + Numerous problems were encountered during construction of the FDR-EE lane, including the addition of too much water and blocked nozzles that led to uneven and under- or over-application of asphalt emulsion, all of which resulted in uneven compaction.
 - + Construction of the FDR-FA section followed conventional procedures and no problems were observed. The cement was evenly distributed at the correct application rate and good mixing of the foamed asphalt and cement was achieved. The recycled material had a consistent grading and uniform moisture content. Satisfactory compaction and a satisfactory surface finish were achieved.

- + The spread rate of the cement on the FDR-PC section was not well controlled, and this led to excess cement being applied. Problems with mixing resulted from this excess cement. Only part of one lane was considered suitable for HVS testing.
- + Gradations for the pulverized material on all four lanes were well within the specified limits.
- + Densities after compaction met or exceeded the specification on the FDR-NS and FDR-FA lanes, but were slightly lower than specification on the FDR-PC and FDR-EE lanes. The lower than specification densities were attributed to the construction problems on both lanes and, on the FDR-PC lane, to the generalization of the laboratory reference density, given that reference densities were not determined for the range of cement contents actually applied on the day of construction.
- Placement of the hot-mix asphalt followed conventional procedures. Thickness and compaction appeared to be consistent across the test track.
- The FDR-NS and FDR-FA lanes and one section of the FDR-PC lane (5 percent measured cement content) were considered satisfactorily uniform for the purposes of accelerated pavement testing. The FDR-EE and the remainder of the FDR-PC sections were not considered representative of typical FDR construction with these stabilization strategies. However, HVS testing on the FDR-EE section was undertaken to quantify the effects of these construction issues on performance of the pavement structure and to justify any recommendations with regard to construction specification language for FDR-EE projects.

Key findings from the study include the following:

- The FDR-FA and FDR-PC sections performed very well and testing on both was terminated long before the terminal rut of 0.5 in. (12.5 mm) or average crack density of 0.8 ft/ft² (2.5 m/m²) was reached (no cracks were observed on either section). The two FDR-NS sections performed acceptably, with the section with the thicker asphalt surfacing (120 mm) outperforming the section with the thinner asphalt surfacing (60 mm), as expected. Terminal rut was reached on both of these sections, but no cracking was observed. The FDR-EE sections performed poorly, with terminal rut and terminal cracking both reached after a limited number of load repetitions. This poor performance was attributed to problems associated with construction, and consequently no conclusions can be drawn from the test results regarding this stabilization strategy.
- Key observations from the HVS testing include these:
 - + Terminal rut depths were recorded on the thinner FDR-NS (60 mm) section after approximately 490,000 equivalent standard axle loads (ESALs) had been applied, and on the thicker FDR-NS (120 mm) section after more than 21.4 million ESALs had been applied. The thicker surfacing layer therefore had a significant influence on the performance of the structure.
 - + On the FDR-FA section, only 4 mm of rutting was measured after more than 17.7 million ESALs, while on the FDR-PC section, only 2.1 mm of rutting was measured after more than 44 million ESALs. Testing was halted on the FDR-FA and FDR-PC sections at these loading points due to time and project-funding constraints. Permanent deformation in the recycled layers was consistent with the surface measurements, with considerable deformation recorded in the FDR-NS layers, but very little deformation recorded in the stabilized layers.
 - + Measured and backcalculated stiffnesses were significantly higher on the FDR-FA and FDR-PC sections compared to the two FDR-NS sections, as expected. Although the stiffnesses dropped

considerably in the recycled layers on the FDR-FA and FDR-PC sections after trafficking, they were still orders of magnitude higher than those recorded on the FDR-NS sections, despite their having been subjected to millions more equivalent standard axle loads. The presence of the recycled asphalt concrete material, the presence of rubber in this material, and the fact that the recycled asphalt was relatively unaged, did not appear to affect the stiffness of the layer. Recycled aged asphalt would typically result in slightly higher stiffnesses in the recycled layer compared to recycled unaged asphalt.

- + Elastic deflection at the bottom of the FDR-FA and FDR-PC layers after completion of testing (17.7 and 44.0 million ESALs, respectively) was approximately the same as that at the bottom of the FDR-NS layers after 490,000 and 21.4 million ESALs, respectively. The rate of change in deflection was, however, slightly higher on the FDR-FA and FDR-PC sections, which is consistent with stabilized layers containing cement.
- The advantages of using foamed asphalt with cement and cement only recycling strategies over recycling strategies with no stabilization are clearly evident from the results.

8.2 Recommendations

Although a second phase of accelerated pavement testing, full-scale field testing, and additional laboratory testing still needs to be undertaken to collect sufficient data for the development of mechanistic-empirical design criteria (and revised gravel factors) for full-depth reclaimed pavements, there is sufficient evidence to show that pavements that are rehabilitated using full-depth reclamation strategies will satisfactorily withstand design traffic levels common in California. Rehabilitation using this approach is quick, has minimal disruption to traffic, reuses all materials, does not require removal of material from the site, and effectively replaces weak base layers, thus preventing the reflective cracking that is common in more traditional overlay projects.

Based on the above conclusions, it is recommended that full-depth reclamation be promoted as an appropriate rehabilitation strategy in California. Although partial-depth reclamation was not investigated in this study, future research on partial- and full-depth reclamation should be coordinated to facilitate consistent design and specification documentation, and to facilitate the preparation of a comprehensive guide covering all forms of pavement recycling.

Blank page

REFERENCES

1. JONES, D., Fu, P. and Harvey, J.T. 2009. **Full-Depth Reclamation with Foamed Asphalt in California: Guidelines for Project Selection, Design, and Construction.** Davis and Berkeley, CA: University of California Pavement Research Center. (UCPRC-GL-2008-01).
2. JONES, D., Fu, P. and Harvey, J.T. 2008. **Full-Depth Reclamation with Foamed Asphalt in California: Final Report.** Davis and Berkeley, CA: University of California Pavement Research Center. (UCPRC-RR-2008-07).
3. **Wirtgen Cold Recycling Technology Manual.** 2012. Windhagen, Germany: Wirtgen GmbH.
4. **Basic Asphalt Recycling Manual.** 2001. Annapolis, MD: Asphalt Recycling and Reclaiming Association.
5. ANDHAL, P.S. and Mallick, R.B. 1997. **Pavement Recycling Guidelines for State and Local Governments - Participant's Reference Book.** Washington D.C.: Federal Highway Administration.
6. CROSS, S.A. 1999. Experimental Cold In-Place Recycling with Hydrated Lime. **Transportation Research Record: Journal of the Transportation Research Board, No.1684.** (pp.186-193).
7. CROVETTI, J.A. 2000. Construction and Performance of Fly Ash–Stabilized Cold In-Place Recycled Asphalt Pavement in Wisconsin. **Transportation Research Record: Journal of the Transportation Research Board, No.1730.** (pp. 161-166).
8. GERBRANDT, R., Makahoniuk, T., Borbely, C. and Berthelot, C. 2000. Effect of Cold In-Place Recycling on the Heavyweight Trucking Industry. **Proceedings 6th International Conference on Heavy Vehicle Weights and Dimensions.** Saskatoon, Canada.
9. SALOMON, A. and Newcomb, D.E. 2000. **Cold In-Place Recycling Literature Review and Preliminary Mixture Design Procedure.** Minneapolis, MN: Minnesota Department of Transportation.
10. THOMAS, T., Kadrmas, A. and Huffman, J. 2000. Cold In-Place Recycling on US-283 in Kansas. **Transportation Research Record: Journal of the Transportation Research Board, No.1723.** (pp. 53-56).
11. NATAATMADJA, A. 2001. Some Characteristics of Foamed Bitumen Mixes. **Transportation Research Record: Journal of the Transportation Research Board. No.1767.** (pp. 120-125).
12. BERTHELOT, C. and Gerbrandt, R. 2002. Cold In-Place Recycling and Full-Depth Strengthening of Clay-Till Subgrade Soils Results with Cementitious Waste Products in Northern Climates. **Transportation Research Record: Journal of the Transportation Research Board, No.1787.** (pp. 3-12).

13. FORSBERG, A., Lukanen, E. and Thomas, T. 2002. Engineered Cold In-Place Recycling Project: Blue Earth County State Aid Highway 20, Minnesota. **Transportation Research Record: Journal of the Transportation Research Board, No.1813.** (pp. 111-123).
14. SULEIMAN, N. 2002. **A State-of-the-Art Review of Cold in-Place Recycling of Asphalt Pavements in the Northern Plains Region.** Bismarck, ND: University of North Dakota, Department of Civil Engineering.
15. THOMAS, T. and Kadrmas, A. 2002. Performance-Related Tests and Specifications for Cold In-Place Recycling: Laboratory and Field Experience. **Proceedings Transportation Research Board 81st Annual Meeting.** Washington, DC. (pp. 2-5).
16. LEE, H. and Kim, Y. 2003. **Development of a New Mix Design Process for Cold-In-Place Rehabilitation Using Foamed Asphalt.** Ames, Iowa: Iowa Department Transportation.
17. LEE, W.K., Braynton, T.E. and Harrington, J. 2003. New Mix-Design Procedure of Cold In-Place Recycling for Pavement Rehabilitation. **Proceedings Transportation Research Board 82nd Annual Meeting.** Washington DC. (pp. 1000-1010).
18. ROMANOSCHI, S.A., Hossain, M., Heitzman, M. and Gisi, A.J. 2003. Foamed Asphalt Stabilized Reclaimed Asphalt Pavement: A Promising Technology for Mid-Western Roads. **Proceedings 2003 Mid-Continent Transportation Research Symposium.** Ames, IA.
19. MORIAN, D.A., Oswald, J. and Deodhar, A. 2004. Experience with Cold In-Place Recycling as a Reflective Crack Control Technique: Twenty Years Later. **Transportation Research Record: Journal of the Transportation Research Board. No.1869.** (pp. 47-55).
20. SEBAALY, P.E., Bazi, G., Hitti, E., Weitzel, D. and Bemanian, S. 2004. Performance of Cold In-Place Recycling in Nevada. **Transportation Research Record: Journal of the Transportation Research Board. No.1896.** (pp.162-169).
21. **Cold In-Place Asphalt Recycling Application Checklist.** 2005. Washington, D.C.: Federal Highway Administration.
22. MALLELA, J., Von Quintus, H.L. and Smith, K.L. 2006. **Performance Evaluation of Cold In-Place Recycling Projects in Arizona.** Phoenix, AZ: Arizona Department of Transportation.
23. CHEN, D. and Jahren, C. 2007. **Evaluation of Long-Term Field Performance of Cold In-Place Recycled Roads: Field and Laboratory Testing.** Ames, IA: Iowa State University. Center for Transportation Research and Education.
24. CROSS, S.A. and Jakatimath, Y. 2007. **Evaluation of Cold In-Place Recycling for Rehabilitation of Transverse Cracking on US 412.** Oklahoma City, OK: Oklahoma Department of Transportation.

25. KIM, Y., Lee, H. and Heitzman, M. 2007. Experiences of Developing and Validating a New Mix Design Procedure for Cold In-Place Recycling Using Foamed Asphalt. **Proceedings 2007 Mid-Continent Transportation Research Symposium**. Ames, IA: Iowa State University. (pp. 1-13).
26. MURPHY, D.T. and Emery, J.J. 2007. Modified Cold In-Place Asphalt Recycling. **Transportation Research Record: Journal of the Transportation Research Board. No.1545**. (pp. 143-150).
27. DAI, S., Skok, G., Westover, T., Labuz, J. and Lukanen, E. 2008. **Pavement Rehabilitation Selection**. Minneapolis, MN: Minnesota Department of Transportation.
28. SMITH, C.R., Lewis, D.E., Turner, J. and Jared, D.M. 2008. Georgia's Use of Lime in Full-Depth Reclamation. **Transportation Research Record: Journal of the Transportation Research Board, No.2059**. (pp. 89-94).
29. HENAULT, J.W. and Kilpatrick, D.J. 2009. **Evaluation of Cold In-Place Recycled Rehabilitation Treatment**. Newington, CT: Connecticut Department of Transportation.
30. THOMPSON, M.R., Garcia, L. and Carpenter, S.H. 2009. **Cold In-Place Recycling and Full Depth Recycling with Asphalt Products**. Urbana-Champaign, IL: Illinois Center for Transportation University of Illinois.
31. CARTER, A., Feisthauer, B., Lacroix, D. and Perraton, D. 2010. Comparison of Cold In-place Recycling and Full-Depth Reclamation Materials. **Proceedings Transportation Research Board 89th Annual Meeting**. Washington, DC.
32. CHESNER, W.H., Stein, C.W., Justus, H.G., Kearney, E.R. and Cross, S.A. 2011. Evaluation of Factors Affecting Long-Term Performance of Cold In-Place Recycled Pavements in New York State. **Transportation Research Record: Journal of the Transportation Research Board, No.2227**. (pp. 13-22).
33. MILLER, H., Amatrudo, M., Kestler, M.A., and Guthrie, W.S. 2011. Mechanistic Analysis of Reconstructed Roadways Incorporating Recycled Base Layers. **Proceedings Transportation Research Board 90th Annual Meeting**. Washington, DC.
34. MILLER, H.J., Kestler, M.A., Amatrudo, M., Eaton, R. and Hall, A. 2011. Comparison of Test Sections of Low-Volume Roadways Reconstructed with Conventional Techniques and Full-Depth Reclamation. **Transportation Research Record: Journal of the Transportation Research Board, No.2204**. (pp. 215-220).
35. NANTUNG, T.E., Ji, Y. and Shields, T. 2011. Pavement Structural Evaluation and Design of Full-Depth Reclamation (FDR) Pavement. **Proceedings Transportation Research Board 90th Annual Meeting**. Washington, DC.
36. STROUP-GARDINER, M. 2011. **Recycling and Reclamation of Asphalt Pavements Using In-Place Methods**. Washington D.C.: Transportation Research Board. (NCHRP Synthesis 421).

37. WILSON, B.T. Guthrie, W.S. 2011. Strength and Deformation Characteristics of a Cement-Treated Reclaimed Pavement with a Chip Seal. **Transportation Research Record: Journal of the Transportation Research Board, No.2212.** (pp. 100-109).
38. YUAN, D., Nazarian, S., Hoyos, L.R. and Puppala, A.J. 2011. Evaluation and Mix Design of Cement-Treated Base Materials with High Content of Reclaimed Asphalt Pavement. **Transportation Research Record: Journal of the Transportation Research Board, No.2212.** (pp. 110-119).
39. CROSS, S.A., Chesner, W.H., Justus, H.G. and Kearney, E.R. 2012. Comparative Performance Analysis of Cold In-Place Recycling in New York State. **Proceedings Transportation Research Board 91st Annual Meeting.** Washington, DC.
40. DIEFENDERFER, B.K., Apeageyi, A.K., Gallo, A.A., Dougald, L.E. and Weaver, C.B. 2012. In-Place Pavement Recycling on I-81 in Virginia. **Transportation Research Record: Journal of the Transportation Research Board, No.2306.** (pp. 45-51).
41. DIXON, P.A., Guthrie, W.S. and Eggett, D.L. 2012. Factors Affecting Strength of Road Base Stabilized with Cement Slurry or Dry Cement in Conjunction with Full-Depth Reclamation. **Transportation Research Record: Journal of the Transportation Research Board, No.2310.** (pp. 113-120).
42. ESTAKHRI, C.K., Scullion, T. and Sebesta, S. 2012. Test to Measure the Bond of Surface Treatments to Reclaimed Stabilized Bases. **Proceedings Transportation Research Board 91st Annual Meeting.** Washington, DC.
43. LANE, B. and Kazmierowski, T. 2012. Ten-Year Performance of Full-Depth Reclamation with Expanded Asphalt Stabilization on Trans-Canada Highway, Ontario, Canada. **Transportation Research Record: Journal of the Transportation Research Board, No.2306.** (pp. 21-27).
44. STROUP-GARDINER, M. 2012. Selection Guidelines for In-Place Recycling Projects. **Transportation Research Record: Journal of the Transportation Research Board, No.2306.** (pp. 3-10).
45. JOHANNECK, L. and Dai, S. 2013. Responses and Performance of Stabilized Full-Depth Reclaimed Pavements at the Minnesota Road Research Facility. **Transportation Research Record: Journal of the Transportation Research Board, No.2368.** (pp. 114-125).
46. NAZARIAN, S., Yuan, D., Franco, S. and Moss, S. 2013. Design and Constructability of Emulsion-Stabilized Bases for Full-Depth Reclamation. **Proceedings Transportation Research Board 92nd Annual Meeting.** Washington, DC.
47. JONES, D., Wu, R., Tsai, B. and Harvey, J. 2011. **Warm-Mix Asphalt Study: Test Track Construction and First-Level Analysis of Phase 3a HVS and Laboratory Testing (Rubberized Asphalt,**

- Mix Design #1).** Davis and Berkeley, CA: University of California Pavement Research Center. (UCPRC-RR-2011-02).
48. JONES, D., Wu, R., Tsai, B. and Harvey, J. 2011. **Warm-Mix Asphalt Study: Test Track Construction and First-Level Analysis of Phase 3b HVS and Laboratory Testing (Rubberized Asphalt, Mix Design #2).** Davis and Berkeley, CA: University of California Pavement Research Center. (UCPRC-RR-2011-03).
49. PAIGE-GREEN, P. and du Plessis, L. 2009. **The Use and Interpretation of the Dynamic Cone Penetrometer (DCP) Test.** Pretoria, South Africa: Council for Scientific and Industrial Research.
50. **Maintenance Technical Advisory Guide.** 2013. Sacramento, CA: Caltrans Division of Maintenance. (Chapter 14, Full depth Reclamation using Cement).
51. JONES, D. 2005. **Quality Management System for Site Establishment, Daily Operations, Instrumentation, Data Collection and Data Storage for APT Experiments.** Pretoria, South Africa: CSIR Transportek. (Contract Report CR-2004/67-v2.)

